NISTIR 89-4051

Technical Activities 1986-1988 Molecular Spectroscopy Division

A. Weber, Chief

U.S. DEPARTMENT OF COMMERCE
National Institute of Standards and Technology
(Formerly National Bureau of Standards)
National Measurement Laboratory
Center for Atomic, Molecular, and Optical Physics
Molecular Spectroscopy Division
Gaithersburg, MD 20899

November 1988

Issued March 1989

Prepared for
U.S. DEPARTMENT OF COMMERCE
National Institute of Standards and Technology
Gaithersburg, MD 20899

NISTIR 89-4051

Technical Activities 1986-1988
Molecular Spectroscopy Division

A. Weber, Chief

U.S. DEPARTMENT OF COMMERCE
National Institute of Standards and Technology
(Formerly National Bureau of Standards)
National Measurement Laboratory
Center for Atomic, Molecular, and Optical Physics
Molecular Spectroscopy Division
Gaithersburg, MD 20899

November 1988

Issued March 1989

National Bureau of Standards became the National Institute of Standards and Technology on August 23, 1988, when the Omnibus Trade and Competitiveness Act was signed. NIST retains all NBS functions. Its new programs will encourage improved use of technology by U.S. industry.

Prepared for
U.S. DEPARTMENT OF COMMERCE
National Institute of Standards and Technology
Gaithersburg, MD 20899

U.S. DEPARTMENT OF COMMERCE
Robert A. Mosbacher, Secretary
Ernest Ambler, Acting Under Secretary for Technology
NATIONAL INSTITUTE OF STANDARDS AND TECHNOLOGY
Raymond G. Kammer, Acting Director

ABSTRACT

This report summarizes the technical activities of the NIST Molecular Spectroscopy Division for the Fiscal Years 1987 and 1988. The activities span experimental and theoretical research in high resolution molecular spectroscopy, quantum chemistry, and laser photochemistry, and include the development of frequency standards, critically evaluated spectral data, applications of spectroscopy to important scientific and technological problems, and the advancement of spectroscopy measurement methods and techniques. A listing is given of publications and talks by the Division staff.

FOREWORD

* The National Institute of Standards and Technology (NIST) is the new name of the Commerce Department's National Bureau of Standards (NBS). NIST was created by the Omnibus Trade and Competitiveness Act signed by President Reagan on August 23, 1988.

* NBS was originally established in 1901 as the government's science and engineering laboratory for measurement technology and research on standards. Over the years it evolved to become the sole federal laboratory directly concerned with aiding industry and commerce.

* The name National Institute of Standards and Technology reflects the broadened role and new responsibilities assigned to the agency which will include the traditional functions of providing the measurements, calibrations, data, and quality assurance support which are vital to U.S. commerce and industry, together with several new programs to support the aggressive use of new technologies in American industry.

This report is a summary of the technical activities of the NBS Molecular Spectroscopy Division for the two year period of October 1, 1986 to September 30, 1988. It was prepared as part of the Annual Report of the

Center for Atomic, Molecular, and Optical Physics within the National Measurement Laboratory of NIST. The Molecular Spectroscopy Division is organized into three working groups comprised of permanent staff, post doctoral fellows, guest scientists, and support personnel. An organizational chart of the Division is given at the end of this Foreword.

The goals and activities of the Division and the general nature of its technical programs are described in the Introduction, Section 1. Sections 2-4 present the descriptions of technical work done by the High Resolution Spectroscopy, Laser Photochemistry, and Quantum Chemistry Groups. Each group report gives project objectives, details of results obtained during the past year, and plans for future work. A mini-table of contents precedes each group report to afford a quick overview of the group's activities.

The technical descriptions are followed by Sections 5 and 6 which list the publications and talks given during the past year, while Section 7 lists the seminars hosted by the Division. The Division has had a number of visiting scientists during the past year; these are identified in Section 8.

Further information on the activities of the Division can be obtained by contacting the scientists identified in each project report, or by writing to Dr. Alfons Weber, Chief, Molecular Spectroscopy Division, Physics Building, B268, National Institute of Standards and Technology, Gaithersburg, MD 20899.

MOLECULAR SPECTROSCOPY DIVISION

A. Weber, Chief
A. Kuehl, Secretary
C. V. Kurtz, Division Technician

HIGH RESOLUTION

A. Weber, Group Leader
L. Coudert*
G. Fraser
C. Gillies*
J. Hougen
M. Jacox
I. Kleiner*
W. Lafferty
F. Lovas
A. Maki
K. Matsumura*
S. Novick*
W. Olson
K. Peterson*
A. Pine
G. Rotter
R. Suenram
W. Thompson*
J. Zozom*

QUANTUM CHEMISTRY

M. Krauss, Group Leader
H. Basch*
D. Garmer+
N. Goldgaber
P. Julienne
F. Mies
K. Miller++
S. Pan*
W. Stevens
L. Vahala*

MOLECULAR DYNAMICS

J. Stephenson, Group Leader
M. Casassa
L. Elwell
B. Foy+
E. Heilweil
D. King

* Guest Scientist
\+ Postdoctoral Research Associate
++ Contractor

TABLE OF CONTENTS

Abstract i

Foreword iii

Staff v

1. Introduction 1

   A. Goal 1

   B. Organization 1

   C. Division Programs 2

   D. Collaborations 4

   E. Other Agency Support 4

2. High Resolution Spectroscopy Group 5

   A. Introduction 5

   B. Calibration and Data Center Activities 9

   C. Spectroscopy for Environmental Studies 14

   D. Spectroscopy of Hydrogen-bonded and van der Waals Complexes 21

   E. Rare Gas-Molecule Complexes 41

   F. Matrix Isolation Spectra 45

   G. General Spectroscopy and Theory 51

3. Molecular Dynamics Group 63

   A. Condensed Phase Energy Transfer 64

   B. Decomposition of Molecules from Metastable Vibrational States 67

   C. Molecular Desorption from Surfaces 70

4. Quantum Chemistry Group. 75

A. Introduction 77

B. Electronic Structure 77

C. Scattering Program 86

5. Publications 105

6. Talks. 117

7. Molecular Spectroscopy Division Seminars 123

8. Visiting Scientists. 125

MOLECULAR SPECTROSCOPY DIVISION

A. Weber, Chief

SUMMARY OF ACTIVITIES

1. INTRODUCTION

A. Goal

This Division is a discipline oriented unit and its goal is to be at the forefront of modern theoretical and experimental molecular spectroscopy in order to:

Advance spectroscopic measurement methods and techniques.

Develop models, theoretical concepts and quantum theoretical methods for predicting molecular properties and energetics of molecules and clusters.

Obtain reliable reference spectroscopic data for NIST, government, research community and industrial needs.

Understand and model fundamental chemical processes.

Provide state-of-the-art frequency standards.

Transfer forefront spectroscopic expertise to other NIST Divisions, other government agencies, industry and the research community.

Within the framework of these general goals the Division also follows several specific objectives which have been part of the overall program of the Center for Atomic, Molecular and Optical Physics (CAMOP) - Properties of Weakly Bonded Systems, Biotechnology, and Energy Transfer. Properties of weakly bonded systems are obtained for small atomic and molecular complexes held together by van der Waals and hydrogen bond forces in order to determine the structure, conformation, thermodynamics, and reactivity of such systems. The objective of the biotechnology quantum mechanical effort is the development of an ab initio reaction field program for studies of complex systems such as clusters, proteins, and surfaces. In the third area the major effort involves the study of vibrational energy transfer in the spectroscopy and kinetics of molecules.

This report contains descriptions of these activities and other related studies of each of the three groups.

B. Organization

The Molecular Spectroscopy Division is organized into three working groups: High Resolution Spectroscopy (HRS), Molecular Dynamics Group (MD), and Quantum Chemistry (QC). The permanent Division staff is augmented by that of postdoctoral fellows and guest scientists. During the past year we have had ten guest scientists and one post doctoral fellow engaged in

Division projects. In addition four members of the Surface Science Division participated in the work of the MD group. A list of the guest scientists, their permanent affiliations, and their activities is given in Section 10 of this report.

C. Division Programs

To be able to respond to the present and projected needs of NIST, the Center for Atomic, Molecular and Optical Physics (CAMOP), and the user community, a significant fraction of the Division's effort is directed toward achieving and maintaining the expertise of its staff in their discipline oriented fields, and into maintaining its experimental facilities at the state-of-the-art level. We must remain at this level of expertise in spectroscopic measurements, theory, and interpretation in order to respond quickly to provide standards, serve national technical needs, and to insure adequate response to future problems. Remote sensing for industrial and atmospheric monitoring, laser chemistry and physics and combustion diagnostics are a few of the many important high technology areas that depend on modern spectroscopic techniques. These applications also provide much of the direction and motivation for our efforts.

As described in Section 2, the work of the HR group involves experimental and theoretical applications of molecular spectroscopy for characterizing gas phase molecules, primarily in the infrared (rotation-vibrational) and microwave (rotational) spectral regions, the development of frequency standards for the infrared, and the development and application of new experimental techniques for high resolution spectroscopy. The emphasis of these studies is on the applications of our expertise to problems in structural chemistry, atmospheric chemistry, chemical analysis, radio astronomy and the properties of weakly bound molecular species.

The environmental problem posed by the pollutants of the earth's atmosphere, especially the role played by trace constituents in the chemistry of the upper atmopshere, are of major concern and a portion of the group's activities is devoted to providing critically needed data to help solve some of these problems. In this effort our activities are guided by the needs of the environmental research community, and are conducted with the support of NASA. These efforts will continue to play an important role in the work of the HR group during the coming years.

Weakly bound molecular complexes, i.e., van der Waals and hydrogen bonded molecules have received considerable attention in our laboratory with major progress in characterizing large amplitude tunneling effects and structural information on trimeric complexes. The Division is in a unique position of having available personnel and instrumentation that permits such studies to be performed using any and all of the facilities from the microwave to the near infrared region of the spectrum in a concerted attack on the problems posed by these weakly bound systems. These experimental efforts are augmented by the analytical and computational theoretical expertise available in the Division.

The Division is the home of the Molecular Spectra Data Center. This Center, supported by the Office of Standard Reference Data and staffed by

members of the HR group provides evaluated data on molecular rotational spectra in the microwave region with special emphasis on spectra of interstellar species. A more recent effort is the development of evaluated vibrational frequency and electronic band center data for transient molecules. Closely related to these activities is the measurement and evaluation of infrared spectra to be used as standards in calibrating diode lasers and infrared laser spectrometers. The work on infrared standards is a response to requests from the instrumentation industry, industrial research laboratories, applied technological user groups, government agencies and laboratories. Improvements in the stability of diode lasers have emphasized the need for accurate calibration standards. New absorption frequencies of N_2O, CS_2, and OCS have been obtained by heterodyne methods to produce tables of accurate frequencies in spectral regions not covered previously. This work has been made possible through the joining of the unique facilities of the Time and Frequency Division of NIST/Boulder with our spectroscopic expertise. Other collaborations, with non-U.S. research groups exist as well in an effort to develop the most extensive and accurate set of frequency calibration data. Section 2.B of the HR group report describes these activities in greater detail.

The MD group primarily does quantum-state specific studies of molecular dynamics. A common factor in the research of this group is the role of energy transfer in the spectroscopy and kinetics of molecules. Three major activities are pursued: Condensed Phase Energy Transfer, Laser Diagnostics of Surface Dynamics, and Dynamics of van der Waals Molecules. As described in Section 3.A, in the first of these, the direction taken is the study of condensed phase vibrational energy transfer from vibrationally excited chemical bonds in liquids, solids, and on molecules bound to surfaces or small clusters.

Time resolved spectroscopic measurements at the picosecond level have been employed in thorough studies of vibrational predissociation of weakly bound molecular clusters and overtone photodissociation of the HN_3 molecule. Since the measurements are performed in the time domain, a direct measure of the lifetimes of the predissociating states is obtained. These studies are described in Section 3.B of the MD group report.

In the third major activity the goal is to obtain an understanding of the energy transfer and chemical dynamics occurring at metal surfaces at a fundamental level. This work is done in close collaboration with staff members of the Surface Science Division. This collaboration has resulted in the ability to perform state-resolved studies of thermally and laser desorbed molecular processes at well characterized surfaces. Details about recent accomplishments are presented in Section 3.C.

Several of these studies are supported by AFOSR and DOE as indicated in the report.

Quantum Chemistry group continues to develop and extend the range of reliable and useful calculations to complex polyatomic systems. The stabilities, conformations spectroscopy and reactivity of complex molecules, clusters, ions, radicals, and transition states, among others, are successfully investigated by the Quantum Chemistry group.

Electronic structure calculations are described in Section 4.B. The first version of an ab initio reaction field computer program has been developed and tested on a variety of hydrogen bonded complexes and further tests are in progress on larger more complex systems such as proteins. Several ab initio SCF calculations have been performed on molecular complexes, which have been experimentally investigated in the HR group, to obtain a more detailed interpretation of their structures, binding energies and electronic properties.

A second major effort in the QC group is in the area of scattering theory with the goal of understanding the spectroscopy of colliding molecular fragments. Two approaches are employed: (1) numerical state-to-state close coupled quantum scattering methods and (2) analytic tools based on the generalized form of the multichannel quantum defect theory (MCQDT). The application of this theory to molecular photodissociative effects, generalized MCQDT applications and ultracold atomic collision phenomena are described in Section 4.C. The problems which may be treated arise in a variety of areas of molecular physics, e.g., laser spectroscopy, laser development, chemistry of planetary atmospheres and ultracold collision phenomena.

D. Collaborations

The Division staff conducts its research in collaboration with postdoctoral associates, members of the Surface Science and Time and Frequency Divisions as well as with many visiting scientists. Some of these use the facilities of the Division and are appointed guest scientists at NIST. Section 10 of this report lists the names, affiliations, and activities of the guest scientists who collaborated with us during the past year. Further collaborations exist with other scientists associated with universities from the U.S. and abroad whose names are given in the various project descriptions and appear as co-authors of many of the publications and talks listed in Sections 5 and 6 of this report.

E. Other Agency Support

Among the several goals of the Division are the services provided to various agencies of the government which in turn support some of the work done in the Division. The various agencies of the Department of Defense (USARO, AFOSR, Hanscom AFB), NASA, DOE are among those that sponsored some of the research done during the past year.

In the remainder of this Annual Report are the individual group reports (Sections 2, 3, 4), the listings of publications and talks (Sections 5 and 6), Division seminars (Section 7), outside professional activities by the staff (Section 8), professional interactions and consultations by the Division staff (Section 9), and visiting scientists (Section 10).

2. HIGH RESOLUTION SPECTROSCOPY GROUP

T. Blake, G. T. Fraser, C. W. Gillies, J. (Zozom) Gillies, J. T. Hougen, M. E. Jacox, W. J. Lafferty, F. J. Lovas, A. G. Maki, K. Matsumura, S. E. Novick, W. B. Olson, M. Onda, A. S. Pine, J. Rice, G. Rotter, W. Stahl, R. D. Suenram, W. A. Thompson, and A. Weber

A. Introduction

B. Calibration and Data Center Activities

1. Heterodyne Frequency Measurements on CS_2 to Cover the 1460 to 1550 cm^{-1} Region

2. New Heterodyne Frequency Measurements on OCS

3. New Heterodyne Measurements of N_2O

4. Microwave Spectral Tables-III. Hydrocarbons CH to $C_{10}H_{10}$

5. Vibrational and Electronic Energy Levels of Transient Molecules

6. Compilation of Bond Distances of Molecules in the Gas Phase

7. Future Plans.

C. Spectroscopy for Environmental Studies

1. Absorption Bands of Nitric Acid Below 1250 cm^{-1}

2. The Low Frequency Bands of Sulfur Dioxide

3. High Resolution Measurements on the Two Low Frequency Fundamentals of Sulfur Trioxide

4. Analysis of the Infrared Spectrum of Chlorine Dioxide (OCℓO)

5. Line Coupling Studies in the Spectrum of CO_2 in the ν_2 Region

6. Doppler-Limited Spectra of the C-H Bending Overtone of Fluoroform

7. Molecular Beam Spectrum of the Highly Perturbed C-H Stretching Region of Fluoroform

8. N_2 and Air Broadening in the Fundamental Bands of HF and HCl

9. Q-branch Line Mixing in N_2O: Effects of ℓ-type Doubling

10. Future Plans.

D. Spectroscopy of Hydrogen-Bonded and van der Waals Complexes

1. Pulsed Fourier Transform Microwave Spectrometer - Improvements

2. New Measurements of Microwave Transitions in the Water Dimer

3. Tunneling Splittings in the Water Dimer: Further Development of the Theory

4. The Torsional-Rotational Spectrum and Structure of the Formaldehyde Dimer

5. Infrared and Microwave Investigations of Interconversion Tunneling in the Acetylene Dimer

6. Vibrational, Rotational, and Tunneling Dependence of Vibrational Predissociation in the HF Dimer

7. Vibrational Exchange Upon Interconversion Tunneling in $(HF)_2$ and $(HCCH)_2$

8. Ammonia Dimer: Further Structural Studies

9. Microwave Spectrum and Molecular Structure of the N_2-H_2O Complex

10. Rotational Spectra and Structures of the H_2S-H_2O and $(H_2S)_2$ Complexes

11. Microwave Spectrum of the Ozone-Water Complex

12. The Structure of the CO_2-CO_2-H_2O van der Waals Complex Determined by Microwave Spectroscopy

13. Structural Study of the H_2O-H_2O-CO_2 Trimer

14. Microwave Spectrum of the CH_3OH-NH_3 Complex

15. Determination of the Structure of OCS-CO_2

16. Microwave Spectrum and Structure of H_2CO-CO_2

17. Structure and Vibrational Dynamics of the CO_2 Dimer from the Sub-Doppler Infrared Spectrum of the 2.7μm Fermi Diad

18. Sub-Doppler Infrared Spectrum of the Carbon Dioxide Trimer

19. Vibrational Predissociation in the CO_2 Dimer and Trimer and Rare Gas-CO_2 Complexes

20. Rotational Spectrum and Structure of H_2CO-HCl

21. Electric Dipole Moments of HCl- and HCN-Hydrocarbon Complexes

22. Isotope Effects in the High-Resolution Infrared Spectrum of OC-HF

23. Infrared and Microwave Spectra of OCO-HF and SCO-HF

24. Pulsed Beam Rotational Study of the CH_2CH_2-O_3 van der Waals Complex

25. Future Plans.

E. Rare Gas-Molecule Complexes

1. Optothermal-Infrared and Pulsed Nozzle Fourier-Transform Microwave Spectroscopy of Rare Gas-CO_2 Complexes

2. Rotational-Tunneling Spectrum of Ar-H_2O and Ar-H_2S

3. Determination of the Structure of Ar-H_2CO

4. Rotational Spectra and Structure of Ar-CH_3OH and Kr-CH_3OH

5. Microwave Spectrum, Structure and Electric Dipole Moment of the Ar-Formamide van der Waals Complex

6. Rotational Spectrum and Structure of Ar-CH_2CHCl

F. Matrix Isolation Spectra

1. Free Radical Stabilization and Spectra

2. Molecular Ion Stabilization and Spectra

3. Spectroscopy of Reaction Intermediates in Nitramine Decomposition and Combustion

4. Future Plans.

G. General Spectroscopy and Theory

1. The Ozonolysis of Ethylene. Microwave Spectrum, Molecular Structure, and Dipole Moment of Ethylene Primary Ozonide (1,2,3-Trioxolane)

2. Molecular Beam Studies of Larger Organic Species

3. Microwave Spectrum and ^{14}N Quadrupole Coupling Constants of Indole

4. Microwave Spectrum and ^{14}N Quadrupole Coupling Constants of Carbazole

5. Quadrupole Hyperfine Splitting in the $J = 1 \leftarrow 0$ Rotational Transition of CCl_3F

6. Millimeter- and Submillimeter-wave Surveys of Orion A Emission Lines in the Ranges 200.7-202.3, 203.7-205.3 and 330-360 GHz

7. Instrumental Studies for the BOMEM FTS

8. Analysis of the 3-μm Bands of Benzene

9. Influence of AC Stark Effect on Multiphoton Transitions

10. Far Infrared Spectrum of Methylamine. Assignment and Analysis of the First Torsional State

11. Effect of Tunneling Motions on the Hyperfine Structure of Hydrazine

12. A Two Tunneling Path IAM-Like Treatment of the Microwave Spectrum of Divinyl Ether

13. WKB Potential Well Ground States Without Matching?

14. Measuring Transition Moments by Means of the Herman-Wallis Effect

15. The Vibrational Dependence of the Transition Moment

16. An FTS Measurement of the Rotational Spectrum of LiH and LiD

17. High Temperature FTS Measurements

18. Analysis of the Infrared Spectrum of the BO_2 Radical

19. Doppler Broadening of Raman Lines

20. High Resolution Spectroscopic Studies of CH_2F_2: The ν_8 Band at 1435 cm^{-1}.

A. Introduction

The work of this group spans a variety of spectroscopic topics, many of which are part of programmatic efforts. Accordingly the activity reports are grouped into six separate sections: Calibration and Data Center Activities, Spectroscopy for Environmental Studies, Spectroscopy of Hydrogen-bonded and van der Waals Complexes, Rare Gas-Molecular Complexes, Matrix Isolation Spectroscopy, as well as General Spectroscopy and Theory. Each section is concluded with a brief statement of work planned for the coming year. The descriptions list the scientists active on the projects. These include NBS staff, guest scientists, as well as outside collaborators.

B. Calibration and Data Center Activities

We collect under this heading the work of the group connected most closely with the core mission of NBS, namely the production and dissemination of compilations of accurately measured frequencies or wavenumbers for use as secondary standards, and of critically evaluated molecular constants for use in other disciplines. Occasionally, spectral fitting programs, for use in reducing data by investigators in other laboratories, are also provided. The group devotes a significant portion of its effort each year to this program, and frequently collaborates with workers in other laboratories. Outputs of the program serve needs spanning the microwave to the ultraviolet spectral regions.

1. Heterodyne Frequency Measurements on CS_2 to Cover the 1460 to 1550 cm^{-1} Region

(A. G. Maki, J. S. Wells, and M. Schneider)

In order to provide frequency calibration benchmarks in the 1460 to 1550 cm^{-1} region, we have made heterodyne frequency measurements on 15 absorption lines for the 00^01-00^00 band of $^{12}CS_2$ and $^{13}CS_2$. Since these absorption lines are very strong, the data on $^{13}CS_2$ are quite useful even if isotopically enriched samples are not used. This is part of a continuing collaboration between the NIST-Boulder and the NIST-Gaithersburg laboratories to provide frequency calibration benchmarks based on heterodyne frequency measurements throughout the infrared region. These measurements were combined with other data to get improved rotational constants which were used to produce tables of accurate transition frequencies (or wavenumbers) such as Table I.

Table I. Wavenumbers (in cm^{-1}) Calculated for the ν_3 Band of $^{13}CS_2$

P-BRANCH	J"	R-BRANCH	P-BRANCH	J"	R-BRANCH
---	0	1485.54812(09)	1471.00438(10)	56	1495.49568(13)
1484.89334(09)[a]	2	1485.97778(09)	1470.41377(10)	58	1495.77074(13)
1484.44997(09)	4	1486.40194(09)	1469.81773(10)	60	1496.04025(14)
1484.00111(09)	6	1486.82062(09)	1469.21627(10)	62	1496.30421(14)
1483.54677(09)	8	1487.23380(09)	1468.60940(11)	64	1496.56261(15)
1483.08696(09)	10	1487.64148(09)	1467.99711(11)	66	1496.81545(15)
1482.62166(09)	12	1488.04366(09)	1467.37940(11)	68	1497.06272(15)
1482.15090(09)	14	1488.44034(08)	1466.75629(11)	70	1497.30443(15)
1481.67466(09)	16	1488.83152(08)	1466.12777(11)	72	1497.54058(15)
1481.19295(08)	18	1489.21719(08)	1465.49384(11)	74	1497.77115(15)
1480.70578(08)	20	1489.59735(08)	1464.85451(11)	76	1497.99615(15)
1480.21314(08)	22	1489.97200(08)	1464.20978(11)	78	1498.21558(15)
1479.71504(08)	24	1490.34113(08)	1463.55965(12)	80	1498.42943(15)
1479.21148(08)	26	1490.70475(08)	1462.90412(12)	82	1498.63770(15)
1478.70246(08)	28	1491.06286(08)	1462.24320(12)	84	1498.84039(14)
1478.18799(08)	30	1491.41544(08)	1461.57688(13)	86	1499.03750(14)
1477.66806(07)	32	1491.76250(08)	1460.90518(14)	88	1499.22903(14)
1477.14268(07)	34	1492.10404(08)	1460.22808(15)	90	1499.41496(13)
1476.61185(08)	36	1492.44005(08)	---	92	1499.59531(13)
1476.07558(08)	38	1492.77053(09)	---	94	1499.77006(13)
1475.53386(08)	40	1493.09548(09)	---	96	1499.93922(14)
1474.98670(08)	42	1493.41489(10)	---	98	1500.10278(14)
1474.43410(08)	44	1493.72877(10)	---	100	1500.26075(16)
1473.87606(08)	46	1494.03711(10)	---	102	1500.41311(17)
1473.31259(09)	48	1494.33992(11)	---	104	1500.55987(19)
1472.74368(09)	50	1494.63718(11)	---	106	1500.70103(22)
1472.16934(09)	52	1494.92889(12)	---	108	1500.83657(25)
1471.58957(09)	54	1495.21506(12)	---	110	1500.96651(29)

a) The uncertainty (twice the estimated standard error) in the last digits is given in parentheses. In spite of the small uncertainty given by the statistics of the fits, the absolute frequency uncertainty should not be less than ±0.0001 cm^{-1} (3 MHz).

2. New Heterodyne Frequency Measurements on OCS
(A. G. Maki, W. B. Olson, and J. S. Wells)

At this time we can not make accurate heterodyne frequency measurements on absorption features located in arbitrary regions of the infrared spectrum. We therefore have been engaged in a program to accurately measure the lower energy levels of the OCS molecule so that we may calculate accurate frequencies for transitions where direct measurements are not possible. One of the levels that has, until now, been missing from our measurements is the ν_2, or 01^10, level. By using a long-path absorption cell, Joe Wells (NIST-Boulder) has now been able to measure the 01^11-00^00 and 02^01-01^0 bands near 1375 cm^{-1}. When these heterodyne measurements are combined with heterodyne measurements on the 01^11-01^10 and 02^01-00^00 bands, we have two different paths for evaluating the 01^10 energy

levels. Furthermore, these measurements will enable us to accurately calculate the transition frequencies for the $01^10\text{-}00^00$ band of OCS near 520 cm^{-1}.

In a similar fashion we have measured a number of hot band transitions in the region from 1866 to 1919 cm^{-1} in order to determine accurate frequencies for energy levels that can be used to provide calibration tables for the region from 2700 to 3000 cm^{-1}. These heterodyne measurements were supplemented with new FTS measurements which we made to help determine some of the effects of centrifugal distortion and ℓ-type resonance.

3. New Heterodyne Measurements of N_2O
(A. G. Maki, J. S. Wells, and L. R. Zink)

In another part of our collaboration with NIST-Boulder, we have continued to make heterodyne measurements of transitions of N_2O that will help to locate accurately the energy levels of N_2O that are involved in transitions useful for calibration. Heterodyne measurements have been made on the $10^00\text{-}02^00$ band near 1060 cm^{-1} and the $10^00\text{-}01^10$ band near 1635 cm^{-1}. These measurements allowed us to prepare calibration tables for the $02^00\text{-}00^00$ band near 1168 cm^{-1}, the $01^10\text{-}00^00$ band near 589 cm^{-1}, and the $02^01\text{-}00^00$ band near 2462 cm^{-1}.

4. Microwave Spectral Tables - III. Hydrocarbons, CH to $C_{10}H_{10}$
(F. J. Lovas and R. D. Suenram)

All of the rotational spectral lines observed and reported in the open literacture for 91 hydrocarbon molecules have been tabulated. The isotopic molecular species, assigned quantum numbers, observed frequency, estimated measurements uncertainty and reference are given for each transition reported. In addition to correcting a number of misprints and errors in the literature cited, the spectral lines for many normal isotopic species have been refit to produce a comprehensive and consistent analysis of all the data extracted from various literature sources. The derived molecular properties, such as rotational and centrifugal distortion constants, hyperfine structure constants, electric dipole moments, and rotational g-factors are listed (see J. Phys. Chem. Ref. Data, in press).

5. Vibrational and Electronic Energy Levels of Transient Molecules
(M. E. Jacox)

With partial support from the Office of Standard Reference Data, a compilation of the electronic energy levels of polyatomic transient molecules with from three to six atoms has been prepared and published. This major work represents a critical evaluation of optical and photoelectron spectral data for approximately 500 free radicals, molecular ions, and other highly reactive molecules. While most of the data were obtained from gas-phase studies, spectral observations in rare-gas and nitrogen matrices, for which matrix interactions are relatively weak, were also included. Radiative lifetimes, vibrational energy levels, and the principal rotational constants were tabulated. Because new observations are accumulating rapidly and because ground-state vibrational data were

included, this new publication updates an important subset of the ground-state vibrational data complitation for small polyatomic transient molecules which was published four years ago (M. E. Jacox, J. Phys. Chem. Ref. Data 13, 945 (1984)).

In April 1988, support was received from the Office of Standard Reference Data for the preparation of computer-accessible versions of these spectral tables. The first stage of this project, conversion of the tables to ASCII files suitable for distribution on floppy disks or to network transmission to users, has recently been completed. With help from a summer worker, work is well along on the preparation of the data on band origins and vibrational energy levels for conversion to a pair of dBase III+ files, TDATA and VDATA, which can be used for range searches. When this conversion has been completed, compiled dBase files will be prepared, removing the need for the user to possess the dBase III+ software package.

The vibrational and electronic spectral data are constantly being updated. Preparation of a supplement to the earlier ground-state vibrational data tables is in progress. These new tables, which will be submitted for publication in the Journal of Physical and Chemical Reference Data, will include new spectral data for transient molecules with from 7 to 16 atoms, as well as for transient molecules with from 3 to 6 atoms for which no electronic spectral data have been reported. The forthcoming publication will also include a master index, to facilitate location of spectral data for a given molecule in the three compilations.

6. Compilation of Bond Distances of Molecules in the Gas Phase
(W. J. Lafferty)

This project has the goal of compiling the best molecular structural parameters reported in the literature. It is part of a long standing collaboration with J. H. Callomon (University College, London), K. Kuchitsu (University of Tokyo), and E. Hirota (Institute for Molecular Science, Japan) under the auspices of Landolt-Börnstein and includes gas phase structural studies determined by electron diffraction methods, visible spectroscopy, microwave spectroscopy as well as infrared techniques. Evaluation of structures determined by IR techniques is done at NIST. The first publication of this effort was in 1976 (Landolt-Börnstein, New Series, Group II, Volume 7). A supplement to update the original work was completed in 1986 and should appear in print this year. Since a flood of new studies on ions, van der Waals complexes, and hydrogen bonded molecules has appeared since the completion of the last literature search in 1985, it has been decided to issue an additional supplement. The cut-off date for the literature search will be at the end of 1988 and the manuscript will be submitted by June 1989.

7. Future Plans

a. Calibration Efforts
(A. G. Maki)

In our efforts to use heterodyne techniques to measure all the lower energy levels of OCS we would like to locate the 10^00 level to within a few MHz. Several possible schemes for doing that are under consideration. One

would be to make a direct measurement of the 10^00-00^00 band using doubled CO_2 laser transitions as the frequency standard. Since we have no strong local oscillator lasers at 2060 cm^{-1}, this would require measuring the beat frequency between the diode laser and the doubled CO_2 laser. This has been done successfully before for the region around 1900 cm^{-1} in the NIST-Boulder lab., but success for the scheme proposed here is not guaranteed.

Other possibilities would be to measure the 10^00-02^00 band at 1020 cm^{-1} or the 10^00-01^10 band at 1540 cm^{-1}. These are weak bands that occur in regions where there are a great many stronger lines either from OCS or, in the case of the 1540 cm^{-1} region, from CS_2 which is present as an impurity in most OCS samples.

The N_2O band 11^10-00^00 at 2800 cm^{-1} and the 10^01-00^00 band at 3480 cm^{-1} are strong enough to use for calibration if we could measure the 11^10 and the 10^01 levels. With the long-path absorption cell it may be possible to measure the 11^10-01^11 transition at 940 cm^{-1} and the 10^01-10^00 transition near 1260 cm^{-1}.

There is a particular need for calibration data in the 3000 to 4000 cm^{-1} region. Since Joe Wells' laboratory at NIST-Boulder is not equipped to make direct heterodyne measurements on transitions in that region, it is necessary to attempt to measure energy levels appropriate to transitions in that region. In addition to the N_2O 10^01 level mentioned above, the 12^00 level of N_2O and the 10^01 and 12^00 levels of OCS would be good candidates if the heterodyne measurements can be made. It may also be possible to make some heterodyne measurements on CO_2 which will be useful for filling gaps in our calibration tables.

b. Molecular Spectra Data Center
(F. J. Lovas)

The first revision of the paper originally entitled "Recommended Rest Frequencies for Observed Interstellar Molecular Microwave Transitions - 1985 Revision" was published in the January 1986 issue of J. Phys. Chem. Ref. Data.

Work has begun on the next revision of this paper, and completion is planned for 1989. The literature search of radio astronomy papers and data evaluation of new microwave studies of these species will continue throughout this period. Since the last revision was published, 15 new interstellar species have been identified, bringing the number of identified molecules to 74. Many new transitions of the previously known species have also been reported, which represents about a 15 increase in the observational data.

During FY88 we started work on Part IV of the Microwave Spectral Tables which will treat organic species containing oxygen. Our reprint collection currently contains 157 species in this class with empirical formulas CHO through $C_7H_{12}O$. Spectral data for the first 25 species (130 isotpic forms) have been coded for spectral fitting and table generating programs. This review is projected to be completed in the fall of 1990.

c. Vibrational and Electronic Energy Levels of Transient Molecules (M. E. Jacox)

During FY89 it is planned to complete the conversion of the vibrational frequency and electronic band center data to compiled dBase III+ files. The electronic spectral tables will continue to be updated, and a supplement to the 1984 ground-state vibrational energy level tables will be prepared for publication.

C. Spectroscopy for Environmental Studies

Many small molecules play a significant role in the chemistry of the earth's atmosphere. As such, they are of significant interest to agencies like NASA, DOD and the CMA (Chemical Manufacturer's Association). The interest of these agencies generally focusses on molecular spectroscopy as a remote sensing tool and for the determination of concentration profiles. Consequently, the emphasis in this section is on band analyses as well as the important information on line intensities, line widths, line shapes, and the effect of pressure on these quantities. As in all branches of spectroscopy, the very narrow band width of infrared laser sources now permits quite reliable studies of phenomena involved in spectroscopic concentration determinations.

1. Absorption Bands of Nitric Acid Below 1250 cm^{-1}
(A. G. Maki, W. B. Olson, R. Escribano, A. Goldman, J. Burkholder, and C. J. Howard)

All of the infrared absorption bands of nitric acid (HNO_3) below 1250 cm^{-1} have been measured and analyzed in our continuing study of the spectrum of this important atmospheric molecule. The lowest frequency band, the ν_9 band at 458 cm^{-1}, has been studied in collaboration with three other laboratories, A. Goldman at the University of Denver, J. Burkholder and C. J. Howard at NOAA in Boulder, Colorado, and R. Escribano at the Instituto de Estructura de la Materia, Madrid, Spain. This is the strongest low frequency band of HNO_3 but four other weaker bands have been studied in our laboratory, ν_6, ν_7, ν_8, and $\nu_8 + \nu_9$, because they also are observed in atmospheric spectra.

Relative intensity measurements were also made to compare the intensity of the ν_7 band to that of the ν_6 band for which we have a value for the absolute intensity. Our measurements also provide information on the direction of the transition moment with respect to the rotational axes of the molecule for all the observed bands.

The goal of this work is to provide constants that allow one to accurately calculate the spectrum of nitric acid under different conditions of temperature and pressure in order to quantitatively account for the observed atmospheric spectrum. In Fig. 2.1 the comparison of the observed and calculated spectrum of the central part of the ν_6 band is presented. For the low frequency bands of nitric acid the agreement between the observed and calculated spectrum is very good.

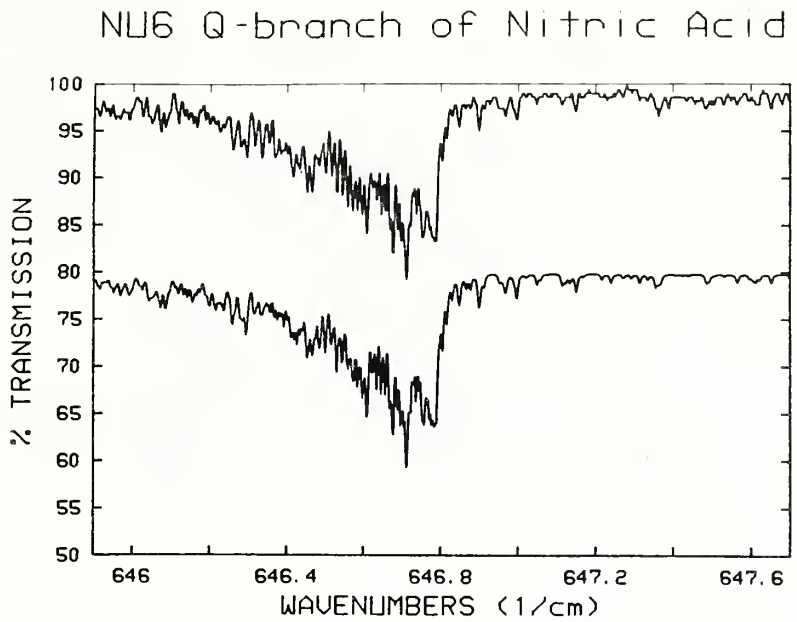

Fig. 2.1 Spectrum of the central part of the ν_6 band of HNO_3. The upper curve is the observed spectrum and the lower curve is the calculated spectrum. The calculated spectrum is displaced for greater clarity.

The ν_8 band is shown in Fig. 2.2. This band has an intensity anomaly that results in weaker than expected absorption in the low frequency part of the band (the P-branch) and stronger than expected intensity in the high frequency part (the R-branch). By making relative intensity measurements we are able to obtain two empirical parameters that account for this intensity anomaly.

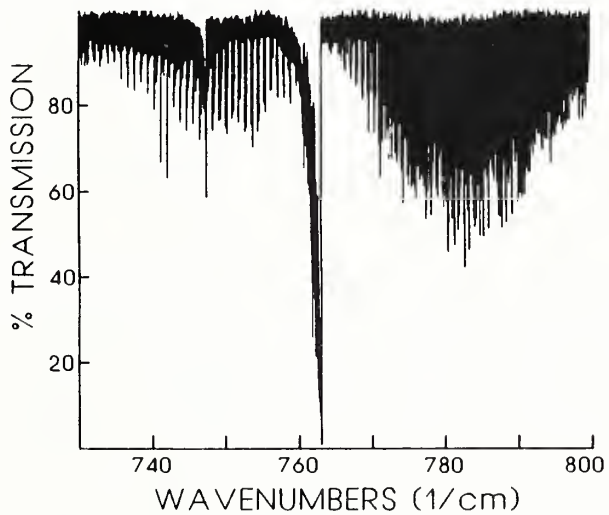

Fig. 2.2 A compressed view of the entire ν_8 band of HNO_3 showing the difference in intensity of the P-branch and R-branch transitions. Note the hot band Q-branch at 747.5 cm^{-1}.

The band at 1205 cm^{-1} was of particular interest because it occurs in an important part of the atmospheric spectrum and the exact vibrational assignment was uncertain. From our analysis of the ν_6, ν_7, ν_8, and ν_9 bands we have shown that the 1205 cm^{-1} band must be due to the combination $\nu_8 + \nu_9$. Knowing the correct assignment was helpful in assigning the fine structure for this band and we now have most of the lines assigned.

Fig. 2.3 shows the observed spectrum of $\nu_8 + \nu_9$ and the spectrum calculated assuming it can be described by simply combining the constants for the ν_8 and ν_9 bands (and shifting the center to allow for an anharmonic vibrational term). An alternative assignment is $\nu_6 + \nu_7$ and the expected spectrum for that possibility is also given in Fig. 2.3.

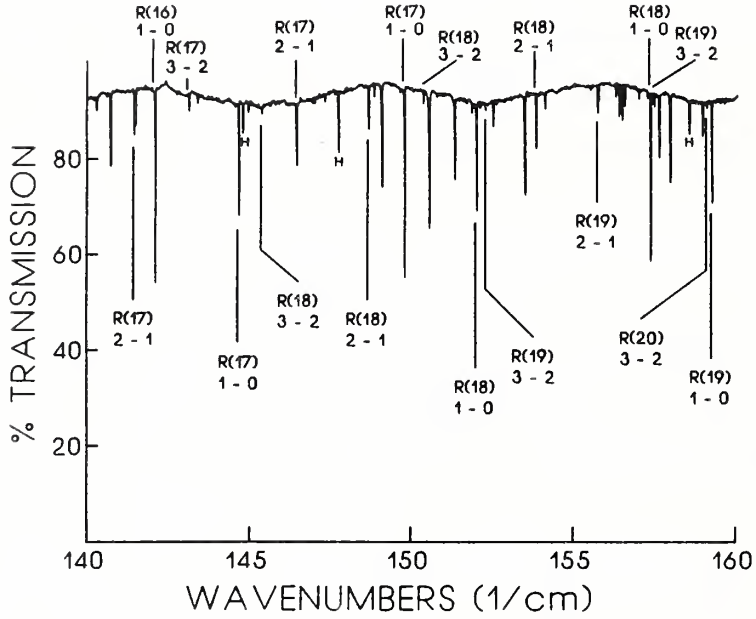

Fig. 2.3 Spectrum of the Q-branch region of the 1205 cm^{-1} band of HNO_3. The upper curve is the observed spectrum. The middle curve is calculated from the constants for ν_8 and ν_9. The lower curve is calculated from the constants for ν_6 and ν_7. The curves are displaced for clarity.

The results of this work have been transmitted to various laboratories that are involved in measuring and analyzing atmospheric spectra.

2. The Low Frequency Band of Sulfur Dioxide
(A. G. Maki, W. B. Olson, and L. Coudert)

One of the important gases involved in the chemistry of acid rain is, of course, sulfur dioxide (SO_2). Most of the sulfur in the atmosphere that comes from industrial processes is originally in the form of SO_2. Prior to this work the lowest frequency fundamental band of SO_2 had not been studied with high resolution.

To understand all the observed features of the high resolution spectrum of SO_2 it is necessary to remember that several different states and isotopic species are normally present. At room temperature a normal sample of SO_2 has the following population distribution:

000 state (ground state) of $^{32}S^{16}O_2$	86.5%
000 state (ground state) of $^{34}S^{16}O_2$	3.8%
010 state of $^{32}S^{16}O_2$	7.0%.

The remaining 2.7% of the molecules are other isotopic species and/or other vibrationally excited states. The intensity of the first hot band, $2\nu_2-\nu_2$, has an additional factor of 2 that comes from the transition moment so the intensity ratio of the ground state transitions to those of the first hot band is only 86.5/2x7.0 = 6.2 at room temperature.

We have measured and analyzed the ν_2 fundamental band and the $2\nu_2-\nu_2$ hot band for $^{32}SO_2$ and $^{34}SO_2$. In the analysis we have combined the FTS infrared measurements with microwave measurements given in the literature to obtain band centers and rotational constants. These constants can be used to produce a synthetic spectrum which accounts for all the observeable features in the spectrum of SO_2 between 400 and 600 cm^{-1}.

3. High Resolution Measurements on the Two Low Frequency Fundamentals of Sulfur Trioxide
(A. G. Maki, W. B. Olson, and R. Escribano)

The spectrum of sulfur trioxide (SO_3) is also of interest because it is a possible intermediate in the conversion of SO_2 to H_2SO_4. In a collaboration with Rafael Escribano of the Instituto de Estructura de la Materia, Madrid, Spain, we have measured and analyzed the two fundamental bands of SO_3 between 400 and 600 cm^{-1}. These two bands are coupled by a Coriolis resonance which complicates the analysis and makes it necessary to analyze both bands at the same time. In order to fit the spectrum a special computer program was developed that would use all the necessary elements in the Hamiltonian. Similar analyses had already been made in both the Madrid laboratory and at NIST so the assignment and analysis of the spectrum was fairly easy for us. Our measurements also allowed us to improve the rotational constants for the ground state of SO_3. This project is part of a program for scientific cooperation between the U.S. and Spain sponsored by the U.S. State Department.

4. Analysis of the Infrared Spectrum of Chlorine Dioxide (OCℓO)
(A. G. Maki, J. Burkholder, C. J. Howard, and R. Escribano)

A new endeavor in our collaboration with R. Escribano of the Instituto de Estructura de la Materia, Madrid, Spain, is the analysis of all the fundamental bands of OCℓO. This molecule is an intermediate in the chlorine chemistry that relates to the ozone composition in the atmosphere. At the present time only two papers have described moderately high resolution measurements on OCℓO in the infrared and much better measurements and a better analysis are required before one can claim to understand the complete infrared spectrum.

There are two complicating features of the COℓO spectrum. One is the existence of two chlorine isotopes. At present only one isotopic species has been studied. The other complication is caused by the unpaired spin of the odd electron on the chlorine atom. This spin couples with the angular momentum of the molecule to give rise to a doublet structure for which the spacing varies from 0.0 to 0.2 cm^{-1}, depending on the transition involved.

To analyze the spectrum it is necessary to take into account the spin-splitting by either an approximation calculation, or by an exact calculation. For many transitions the approximation formulae are not

adequate so a complete analysis requires that we use a computer program that fits the spectrum to a Hamiltonian with the appropriate spin coupling matrix elements. Such a program has been developed by Escribano for the analysis of the three fundamental bands. The spectra that we are using were measured by Burkholder and Howard in the NOAA laboratory in Boulder, Colorado.

5. Line Coupling Studies in the Spectrum of CO_2 in the ν_2 Region (W. J. Lafferty and W. B. Olson)

The spectra of several Q-branches of the CO_2 molecule have been used for some time in atmospheric temperature sounding studies. Recently, it has been determined that shapes of Q-branch envelopes in a pressure broadened spectrum can not be simply accounted for by using sums of simple Lorentzian line shapes. This is due to the fact that molecules in states of appropriate symmetry can be collisionally mixed if the resulting transitions overlap (1,2). The effect on the spectrum is to make the Q-branch envelopes appear to be sharper than expected from the simple model so frequently this effect is referred to as collisional narrowing. Using perturbation theory, the shape of a given line can be expressed as:

$$S_J = 1/\pi \sum_k d_k^2 \rho_k \left[\frac{P w_{kk}}{(\nu - \nu_k^\circ)^2 + (P w_{kk})^2} + \frac{P (\nu - \nu_k^\circ) Y_k}{(\nu - \nu_k^\circ)^2 + (P w_{kk})^2} \right]$$

where d_k is the line intensity, P is the pressure, ν_k° is the transition frequency, ρ_k is the Boltzmann factor and

$$Y_k = \sum_{j \neq k} (d_j/d_k) w_{jk}/(\nu_k - \nu_j)$$

where w_{jk} is the collisional rate matrix. The first term is the conventional Lorentz expression; the second term is due to collisional mixing.

In collaboration with M. L. Hoke and S. A. Clough of the AF Geophysical Lab., we are studying collisional narrowing effects in the N_2 broadened CO_2 spectrum in the ν_2 region around 650 cm^{-1} with the ultimate goal being the determination of the temperature dependence of the Y_k coefficients. About 30 spectra have been obtained with our BOMEM FT-spectrometer with the total pressure varying from 250 Torr to one atmosphere. In order to obtain reliable intensity data from the BOMEM interferometer, it was necessary to make a number of modifications to the instrument including placing a secondary aperture in the He-cooled detector Dewar to remove spurious modulated radiation. In order to check the intensity accuracy of the instrument, line strengths and pressure broadening measurements have been made on 150 P- and R-branch transitions of the fundamental as well as a number of "hot band" transitions. Work is currently in progress to determine the Y_k coefficients not only for the fundamental band but for the $2\nu_2^0 - \nu_2^1$ and $\nu_1 - \nu_2^1$ bands as well. An illustration of the effect of collisional narrowing is shown in Fig. 2.4. Work on the spectra of cold samples will begin shortly.

1. G. J. Rosasco, W. Lempert, W. S. Hurst, and A. Fein, Chem. Phys. Letters 97, 436 (1982).

2. L. L. Strow and B. M. Gentry, J. Chem. Phys. 84, 1149 (1986).

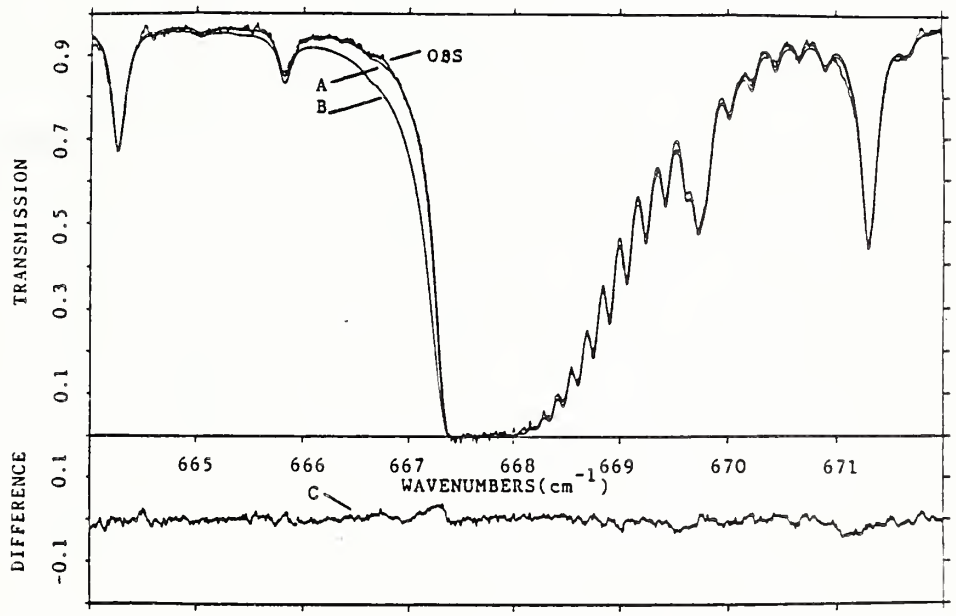

Fig. 2.4 Observed, calculated and difference spectra of the Q-branch of the fundamental $\nu_2{}^1$ band of CO_2. The spectra were taken in a 10 cm cell with 6.2 Torr of CO_2 and 641 Torr of N_2 at a temperature of 296 K and a resolution of 0.006 cm^{-1}. Curve B is a spectrum calculated without line broadening while Curve A is calculated with line broadening effects included. Curve C is the difference between the observed spectrum and Curve A.

6. Doppler-Limited Spectra of the C-H Bending Overtone of Fluoroform (A. S. Pine and J. M. Pliva)

The parallel (A_1) and perpendicular (E) bands of the C-H bending overtone, $2\nu_4$, of CHF_3 have been recorded at Doppler-limited resolution at room temperature using a difference-frequency laser spectrometer. The ℓ=0 component, $2\nu_4{}^0$ (A_1), and the ℓ=+2 component, $2\nu_4{}^{+2}$(E), (accessed by ΔK=-1 transitions) are only weakly perturbed by a mutual ℓ-type resonance near the K'=31 and 33 levels respectively; they can be fit to $\leq$0.0002 cm^{-1}, approaching the experimental precision. The $2\nu_4{}^{-2}$ (E) component (accessed by ΔK=+1 transitions) is strongly perturbed, principally by anharmonic and Coriolis resonances with $2\nu_3+\nu_4{}^{\pm1}$ (E). This perturbing state, though not observed directly, can be well specified by its influence on $2\nu_4{}^{-2}$. Additional localized resonances, arising from a multitude of possible combinations of lower frequency vibrations, are also observed in the high K levels of $2\nu_4{}^{-2}$. These increase the rms deviation of the fit to the ΔK=+1 transitions, but a reliable set of deperturbed constants can be obtained by judicious selection of the data.

7. Molecular Beam Spectrum of the Highly Perturbed C-H Stretching Region of Fluoroform
(A. S. Pine, G. T. Fraser, and J. M. Pliva)

Assignments of the C-H stretching fundamental of fluoroform, CHF_3, have been obtained from a spectrum recorded near 3035 cm^{-1} at sub-Doppler resolution (~10 MHz FWHM) and low effective temperature (~4 K) in an adiabatically-cooled molecular beam using bolometric detection of molecules excited by a color-center laser. This fundamental band is highly perturbed and has resisted analysis at higher temperatures, even at Doppler-limited resolution, whereas its overtones have been the subject of several studies of intramolecular vibrational relaxation. Under molecular beam conditions, the central Q-branch, which dominates the spectrum at room temperature, almost vanishes, while the bulk of the intensity is equally shared by two "sidebands" with Q-branches symmetrically displaced by ~±5 cm^{-1} from the suppressed central Q-branch. This peculiar structure is due to a close anharmonic and Coriolis resonance between the fundamental ν_1 (species A_1) and the combinations $\nu_4^{\pm} + \nu_5^{\pm} + \nu_6^{\pm}$ ($A_1 + A_2$) located only 1.40 cm^{-1} above ν_1, whose origin is at 3033.55 cm^{-1}. The coupling constant of the resonance is $\kappa_{1456}/2\sqrt{2} = 3.68$ cm^{-1}. Additional severe perturbations by the E components of $\nu_4 + \nu_5 + \nu_6$ as well as by $\nu_2 + \nu_4 + \nu_6$ have been identified in the spectrum.

8. N_2 and Air Broadening in the Fundamental Bands of HF and HCl
(A. S. Pine and J. P. Looney)

There have been many measurements reported of N_2, O_2, or air broadening of HF and HCl, but none with sufficient resolution to obtain detailed line profiles near the Doppler limit at pressures below ~1 atm[1] and temperature below ~300 K. We therefore determined the N_2- and air-broadened lineshapes of HF and HCl transitions in the $\nu = 1 \leftarrow 0$ bands measured at T = 295 and 202 K with a high-resolution difference-frequency laser spectrometer. Pressure broadening, shift and collisional narrowing parameters have been extracted by least-squares fitting of several collisional profiles to the spectra. At low pressures, the collisional, or Dicke, narrowing effect causes deviations from the Voigt profile having a Doppler-fixed Gaussian component and yields a measure of the diffusion constants for the hydrogen halides in the buffer gases. At high J, where the pressure shifts are comparable to or larger than the broadenings, a slight asymmetry is observed in the lineshapes which is attributed to statistical correlation between velocity- and state-changing collisions. The ratio of air-to-N_2 broadening is roughly given by the relative quadrupolar contributions of O_2 and N_2, though it varies systematically with rotational level. The temperature variations in the broadening coefficients are also J dependent, deviating significantly from $T^{-½}$ and exhibiting opposite behavior for HF and HCl.

9. Q-branch Line Mixing in N_2O: Effects of ℓ-type Doubling
(A. S. Pine and L. L. Strow)

Rotational collisional narrowing, or line mixing, has been observed in the Q-branch of the $\nu_2 + \nu_3$ Π-Σ band of N_2O near 2798 cm^{-1} using a difference-frequency spectrometer. Self-broadening spectra were recorded at pressures ranging from 20 to 747 Torr. The broadening coefficients,

derived from the lower pressures before the lines significantly overlap, are in close agreement with prior measurements of P- and R-branch widths in Σ-Σ bands. At higher pressures where Q-branch lines are blended, the band contours deviate from purely additive component line shapes, exhibiting stronger peak absorptions and weaker wings characteristic of line mixing. A simple rotational energy gap scaling law is used to model the off-diagonal relaxation matrix elements needed to calcuate the observed collisional narrowing. Spectra calculated using several trial sets of collisional selection rules are presented. We find evidence for a parity conserving collisional selection rule and/or elastic-reorientation collisions.

10. Future Plans

As indicated above, the work on the analysis of the infrared spectrum of OCℓO has just begun and we expect the analysis to take much of the coming year even though the spectra are all in hand. There is still more work to be done on the analysis of the $2\nu_9$ band of HNO_3. Our analysis of the resonance between $2\nu_9$ and ν_5 needs improving. Frank DeLucia of Duke University would like us to help them identify the $2\nu_9$ transitions in their millimeter and sub-millimeter wave spectrum of HNO_3. Aaron Goldman of the University of Denver also needs the best calculation we can give him for the positions and intensities of the absorption lines in the $2\nu_9$ and ν_5 bands.

Another molecule that has been found in the atmosphere and that results from fluorocarbon chemistry is F_2CO. Carl Howard of NOAA has measured a number of infrared bands that do not seem to be too badly affected by perturbations and we hope to find time to analyze some of them.

The optothermal molecular-beam color-center laser spectrometer, built for the investigation of molecular complexes and used for the low temperature, subDoppler resolution study of fluoroform mentioned above, will continue to be applied to the spectra of large or heavy molecules of atmospheric interest with previously unresolved or undeciphered structure. In particular, we will examine the hydrogen stretching vibrations in nitric acid, $HONO_2$, and the two chlorofluorocarbons, CHF_2Cl and $CHFCl_2$.

The high-power single-frequency broadly-tunable color-center laser developed for optothermal spectroscopy is also ideal for precision photoacoustic studies of collisional lineshapes. Photoacoustic spectroscopy has the advantage over transmission measurements because of reduced uncertainties in the zero absorption baseline, since only the power absorbed by the molecules is registered. This method will be applied to the study of differential broadening of the Λ-doublets in NO and to search for collisional interference (line mixing) in the Q branches of CH_4 and NH_3.

D. Spectroscopy of Hydrogen-Bonded and van der Waals Complexes

In the past several years the structures of a large number of dimer and heterodimer van der Waals complexes have been evaluated by high resolution spectroscopic methods. In the microwave spectroscopic work the lowest

energy configuration is generally observed providing structural information; some vibrational information can also be obtained. For example, van der Waals stretching frequencies can be estimated from the centrifugal distortion constants. For some complexes, evidence for internal motions are indicated and analysis of the spectra can lead to information concerning the barriers to those motions. Even more dynamical information is often obtained for those complexes studied by infrared spectroscopy. The result of this research, combined with theoretical studies, is that a better description of intermolecular interactions is being developed.

In this section we report the tunneling-rotation and vibrational spectra for the dimers of water, formaldehyde, acetylene, hydrogen fluoride, ammonia hydrogen sulfide, and carbon dioxide. in addition to these pure dimers, we report spectroscopic studies of mixed species, e.g., N_2-H_2O, H_2S-H_2O, etc.

A complete understanding of intermolecular interactions requires some information concerning the effects of a third body on the interaction between two molecules. If bimolecular interactions alone were important, no further information would be needed to predict the properties of condensed phases. Certainly many body interactions are present but the importance of their contribution needs to quantified. It is possible to make a further step in this direction by experimentally determining the structure of trimeric van der Waals complexes. The effect of a third molecule can then be analyzed by noting structural changes of dimer-type bonding within the larger complex.

Until recently, measuring the microwave spectra of large clusters was hampered by difficulties in obtaining sufficient concentrations in a supersonic expansion these being ultimately due to limited vacuum pumping speeds. The use of a pulsed source, which is naturally included in a Fourier transform microwave spectrometer, has dramatically changed this situation. Stronger expansions and, consequently, lower expansion temperatures can be produced with very little loading of reasonably sized diffusion pumps. This advantage has allowed microwave spectra to be obtained for a growing number of trimeric van der Waals complexes. The list of trimeric complexes which have been studied in the last few years by microwave spectroscopy is so far fairly short and includes Ar_2HF, $Ar_2HC\ell$, $(HCN)_3$ and $(HCN)_2Ar$. The structures for all of these have been determined by Professor H. S. Gutowsky and his coworkers at the University of Illinois. An important observation that is evident in their work is that the trimers are composed of sets of dimer-type structures. That is, the concept of pairwise additivity in the interaction of molecules seems to be reasonable. This is shown by the fact that the bond length of the dimers are about the same as the relevant bond lengths within the trimers. For example, in the Ar_2HF trimer, the Ar-F bond distance is only 0.04 A longer than in ArHF. On the other hand, the angular orientations are somewhat different; the HF is pointed toward the Ar in ArHF but is pointed between the Ar atoms in Ar_2HF.

Our studies of dimeric complexes in the CO_2/H_2O systems has led us to pursue an investigation of trimeric van der Waals complexes which incorporate these two molecules. Three trimers have been observed, $(CO_2)_3$

in the infrared, and $CO_2(H_2O)_2$ and $H_2O(CO_2)_2$ in the microwave regions. These studies are described below.

Complexes formed by rare gas-atoms and molecules are also held together by van der Waals forces and could be described here. Since, however, they do compose a separate category, our work with these systems is presented in Section E. The program of study of hydrogen-bonded and van der Waals complexes initiated several years ago now represents a significant fraction of the group's total effort. Continuing studies using a difference frequency laser spectrometer in the 3 micron region, the optothermal beam spectrometer and the pulsed beam Fourier transform microwave spectrometer are reported. The major efforts during the past two years deal with structural determinations of weakly bound dimers and trimers from microwave spectra and potentials derived from extensive infrared spectra. This program has benefitted greatly this past year from collaborations with guest scientists. We certainly plan to continue work in this direction for the forseeable future.

1. Pulsed FT Microwave Spectrometer - Improvements
   (R. D. Suenram and F. J. Lovas)

A major improvement in the design of the pulsed FT microwave spectrometer has been made. The innovation greatly improves the scanning speed under manual operation and will make computer automation much simpler. In addition, the amount of equipment necessary for operation has been reduced which results in considerable cost savings over the previous version.

The design change involves the use of a microwave single sideband modulator in lieu of a second microwave source and the associated electronics necessary for phase locking and counting of the second source. The new design is shown in the accompaning block diagram (Fig. 2.5). As

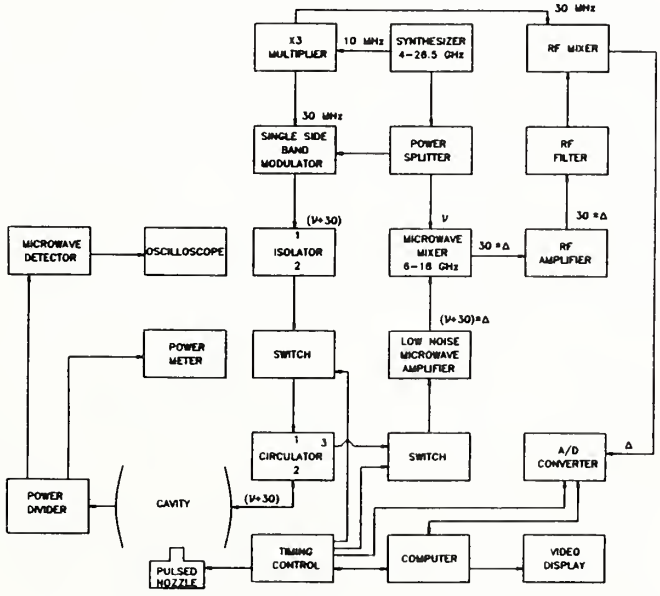

Fig. 2.5 Block diagram of the single sideband Fourier transform microwave spectrometer.

can be seen in the diagram only one synthesized microwave source is necessary. The output of the microwave synthesizer is split by a power divider. Part of the microwave signal is used to bias the LO part of a microwave mixer. The other half of the signal is used to drive the microwave input of a single sideband modulator. A 30 MHz sideband is generated by using the 10 MHz reference crystal output of the synthesizer to drive a X3 multiplier which generates an extremely clean, filtered, and amplified 30 MHz signal which is phase coherent with the microwave output. This 30 MHz signal is used to generate a 30 MHz sideband on the microwave frequency, ν_{syn} in the single sideband. The single sideband modulator output is concentrated in either a ν_{syn} + 30 MHz or ν_{syn}-30 MHz (selectable) sideband with the fundamental frequency ν, and all other related sidebands and higher harmonics being suppressed. This signal (usually ν_{syn} + 30 MHz) is used to pump the molecules in the molecular beam in the cavity. The novel aspect of this is that the microwave cavity further suppress all the unwanted signals since it is tuned to ν_{syn} + 30 MHz also. The molecular signal which emanates from the cavity returns through the circulator and is sent to the RF port of the microwave mixer while the LO port receives the clean ν_{syn} to generate the 1F signal. The IF signal (30 MHz + Δ, the shift in ν caused by the molecular transition frequency) is sent to the RF port of an RF mixer. The LO drive for this mixer is the same ultra clean 30 MHz signal from the X3 multiplier. All the other aspects of the data collection scheme remain unchanged.

2. New Measurements of Microwave Transitions in the Water Dimer (L. H. Coudert, F. J. Lovas, R. D. Suenram, and J. T. Hougen)

New measurements of ten K = 1 lines, including six Q-type and four R-type, were made on the completely protonated species of the water dimer. For some of these lines, as well as for some K = 0 transitions known from the literature, Stark coefficients were determined, and these Stark coefficients provide a confirmation of the assignments. The new K = 1 measurements show that the splitting associated with the $(HF)_2$-like tunneling motion decreases from about 19.5 GHz for K = 0 to about 16.2 GHz for K = 1. To understand the fact that K = 1 lines are populated in our 1 K beam, we must assume, in accordance with the results of beam studies on other molecules, that levels of different nuclear spin modification relax separately. In an attempt to gain information on tunneling splittings other than that caused by the $(HF)_2$-like motion, we have made new measurements on 1-0 and 2-1 transitions with K = 0 for several partially deuterated species, in which the $(HF)_2$-like motion cannot occur. Small splittings ranging from 4 to 145 MHz were observed. Because of the nature of the tunneling motions involved, these new data yeild only the difference of the tunneling splitting in the upper and lower states of the transition.

We have also observed spectra for $(HOD)_2$, two singly substituted ^{18}O species, two singly substituted ^{17}O species and the doubly substituted ^{17}O species. For $(HOD)_2$, the unshifted E-states of $(H_2O)_2$ are absent, leaving only A and B states present. The 1-0 and 2-1 K = 0 transitions have been observed for these levels. The tunneling frequency corresponding to the HF dimer like motion (exchanging of D atoms in the hydrogen bond) for this species is 2643 MHz. A schematic diagram of the energy levels is given in Fig. 2.6.

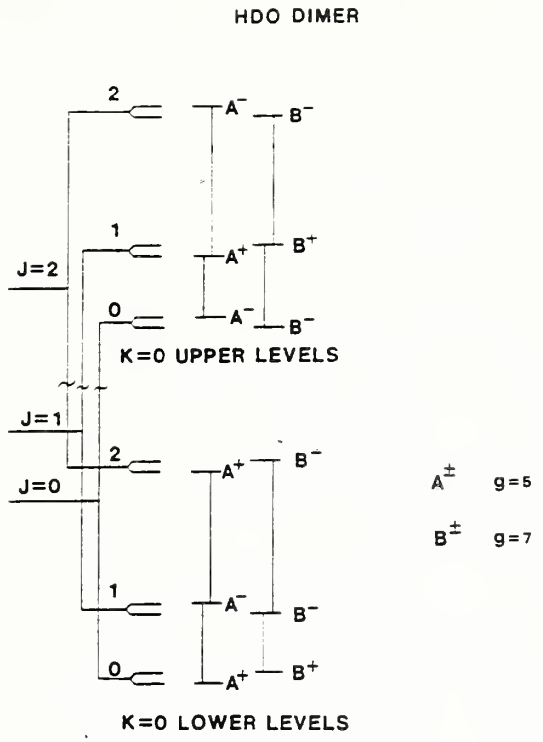

Fig. 2.6 Schematic diagram of the energy levels for $(HDO)_2$. The vertical lines indicate the observed microwave transitions.

The nuclear quadrupole coupling constants for the ^{17}O species have been determined from measurements on the J = 1-0 transitions. The values determined are shown in Fig. 2.7.

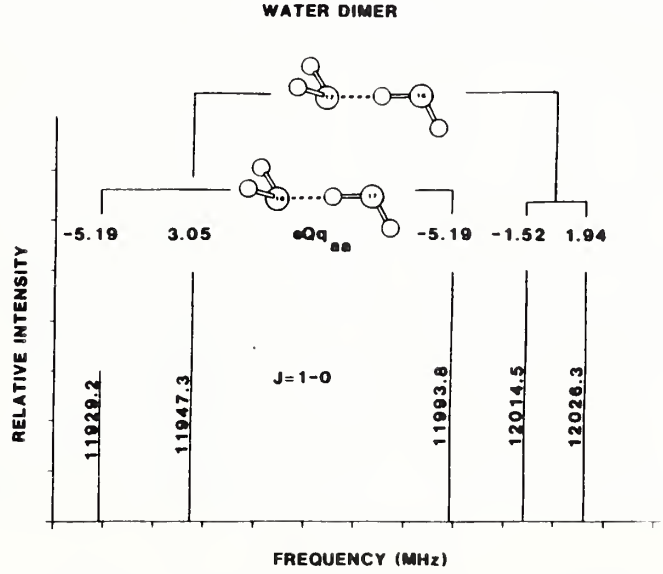

Fig. 2.7 Stick diagram of the observed J=1-0 transitions of H_2O-$H_2{}^{17}O$ and $H_2{}^{17}O$-H_2O. The nuclear electric quadrupole coupling constants of ^{17}O are shown above each transition.

3. Tunneling Splittings in the Water Dimer: Further Development of the Theory
(L. H. Coudert and J. T. Hougen)

Energy level expressions were derived for the hydrogen-bonded water dimer complex and some of its deuterated species, using a previously reported Internal-Axis-Method-like formalism development for high-barrier tunneling problems involving several large amplitude motions. First, the feasibility of various tunneling motions was considered, using a potential surface given by Coker and Watts, and three main tunneling paths for $(H_2O)_2$ were chosen. We assumed that the most feasible path corresponds to a 180° rotation of the acceptor monomer; that the next most feasible path corresponds to a geared-type rotation of the two monomers, leading to an exchange of donor and acceptor monomer roles; and that the third most feasible path corresponds to an exchange of donor hydrogen atoms in the hydrogen bond, accompanied by an umbrella motion of the acceptor monomer. As the second step, the J and K dependence of the purely vibrational tunneling splittings, which arise in the IAM-like formalism because angular momentum is generated during the tunneling motions, was taken into account by computing sets of angles χ, θ, ϕ for Wigner $D^{(J)}(\chi, \theta, \phi)_{K,K'}$ expressions appearing as factors in the vibrational tunneling matrix elements. Symmetry relations determined for the angles χ, θ, ϕ greatly simplify the calculations. Finally, the Hamiltonian matrix was set up and diagonalized to obtain the desired energy level expressions. For the most symmetric species $(H_2O)_2$ and $(D_2O)_2$ we also treated the J and K dependence of the tunneling splittings arising from the presence of rotational terms in the effective Hamiltonian operator.

4. The Torsional-Rotational Spectrum and Structure of the Formaldehyde Dimer
(F. J. Lovas, R. D. Suenram, L. H. Coudert, T. Blake, K. J. Grant, and S. E. Novick)

The microwave spectra of $(H_2CO)_2$ and $(D_2CO)_2$ have been observed with a pulsed beam Fabry-Perot cavity Fourier transform microwave spectrometer. Both species exhibit a-type spectra which are split by internal rotation of each momomer unit and an interchange of donor-acceptor bonding roles analogous to the water dimer. A rotational analysis of each spectrum provides the constants A = 18554. (40) MHz, B = 1887.133(25) MHz, and C = 1384.576(25) MHz for $(H_2CO)_2$ and A = 14862. (4) MHz, B = 1760.607(10) MHz, and C = 1269.629(10) MHz for $(D_2CO)_2$. Stark effect measurements yielded the following components of the electric dipole moments: μ_a = 0.858(4) D and μ_b = 0.027(10) D for $(H_2CO)_2$, and μ_a = 0.908(4) D and μ_b = 0.095(4) D for $(D_2CO)_2$. The geometry obtained from fitting the derived moments-of-inertia, shown in Fig. 2.8, has the planes of the two monomer units perpendicular to one another with a nearly antiparallel orientation of the CO groups and a carbon to oxygen distance of 2.84Å.

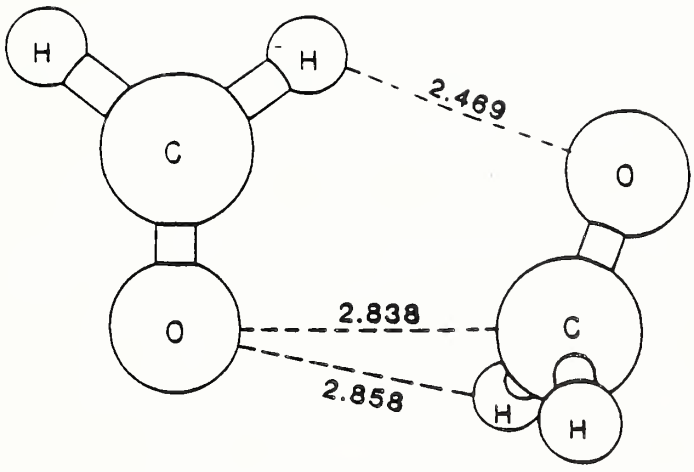

Fig. 2.8 Molecular structure of formaldehyde dimer.

5. Infrared and Microwave Investigations of Interconversion Tunneling in the Acetylene Dimer
(G. T. Fraser, R. D. Suenram, F. J. Lovas, A. S. Pine, J. T. Hougen, W. J. Lafferty, and J. S. Muenter)

A sub-Doppler infrared spectrum of $(HCCH)_2$ has been obtained in the region of the acetylene C-H stretching fundamental using an optothermal molecular-beam color-center laser spectrometer. Microwave spectra were obtained for the ground vibrational state using a pulsed-nozzle Fourier-transform microwave spectrometer. In the infrared spectrum, both a parallel and perpendicular band are observed with the parallel band having been previously assigned to a T-shaped C_{2v} complex by Prichard, Nandi, and Muenter and the perpendicular band to a C_{2h} complex by Bryant, Eggers, and Watts. The parallel band exhibits three K_a=0 and three asymmetry-doubled K_a=1 series. The transitions show a clear intensity alternation with K_c with two of the K_a=0 series missing every other line. In addition, the perpendicular band has the same ground-state combination differences as the parallel band. To explain these apparent anomalies in the spectrum, we invoked a model consisting of a T-shaped complex with interconversion tunneling between four isoenergetic hydrogen-bonded minima as illustrated in Fig. 2.9. In this model, the parallel and perpendicular bands arise from excitation of the acetylene units parallel and perpendicular to the hydrogen bond. The observation of rotation-inversion transitions in the microwave spectrum, in addition to the pure rotation transitions of Prichard, Nandi, and Meunter, verifies the model. The measured microwave splittings yield a tunneling frequency of 2.2 GHz which is consistent with a ~33 cm^{-1} barrier separating the four minima.

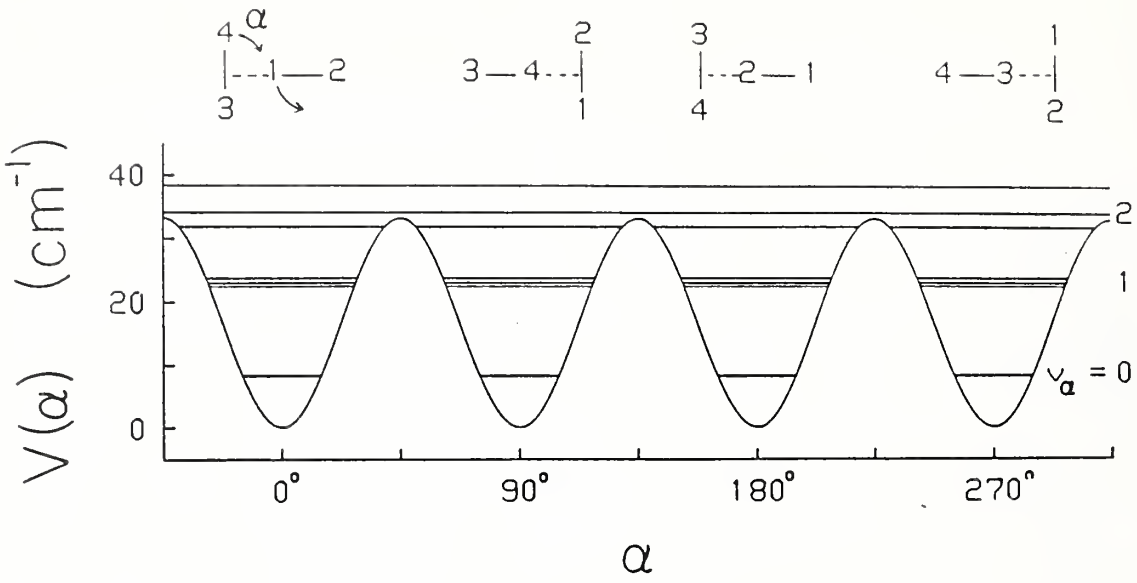

Fig. 2.9 Model potential for the internal-rotation tunneling in the acetylene dimer. The potential energy is taken as $V(\alpha) = V_4(1-\cos 4\alpha)/2$ where $V_4 = 33.2$ cm^{-1} and α is defined in the figure. The $\nu_\alpha = 0$ level is split into A_1^+, E^+, and B_1^+ tunneling sublevels with the B_1^+-A_1^+ splitting determined by microwave spectroscopy to be 2207 MHz (0.07362 cm^{-1}).

6. Vibrational, Rotational, and Tunneling Dependence of Vibrational Predissociation in the HF Dimer
(A. S. Pine and G. T. Fraser)

Vibrational predissociation linewidths have been resolved in the two H-F stretching bands of the HF dimer using an optothermal (bolometer-detector) molecular-beam color-center laser spectrometer. In addition to the strong vibrational mode dependence reported earlier by several groups, we observe a substantial K-rotational and tunneling dependence on the longer-lived mode, ν_1, which is associated with the "free-H" stretching vibration. The predissociation linewidths (FWHM in MHz) for this vibration are 6.4(5) for $K=0^+$, 9.5(5) for $K=0^-$, 10.2(5) for $K=1^+$ and 11.8(5) for $K=1^-$, where the +/- superscripts refer to the symmetric/antisymmetric tunneling states. The J dependence (at low J) is negligible compared to the K dependence. The K=0 levels of the "bound-H" stretch have tunneling-independent widths of 330(30) MHz. Extraneous broadening due to saturation effects was observed and corrected for in these measurements.

7. Vibrational Exchange upon Intercoversion Tunneling in $(HF)_2$ and $(HCCH)_2$
(G. T. Fraser)

Model calculations were undertaken to interpret the large H-F and C-H stretching vibrational dependencies of the interconversion tunneling splitting and the corresponding infrared vibration-tunneling state selection rules in $(HF)_2$ and $(HCCH)_2$. The model consists of two potential curves, $V_a(\rho)$ and $V_b(\rho)$, with $V_a(\rho)=V_b(-\rho)$, where ρ is the tunneling coordinate. For $(HF)_2$, $V_a(\rho)$ and $V_b(\rho)$ correspond to having the vibrational excitation localized in submolecules H_aF_a and H_bF_b, respectively (see Fig. 2.10). The two potential curves are coupled by an interaction term, $V_{ab}(\rho)$, that allows the vibrational excitation to be

exchanged between the two monomer units, permitting tunneling to occur. The interaction term is approximated by resonant infrared transition-dipole coupling. The magnitudes of the calculated vibrational dependencies and the predicted selection rules are in agreement with previous experimental observations.

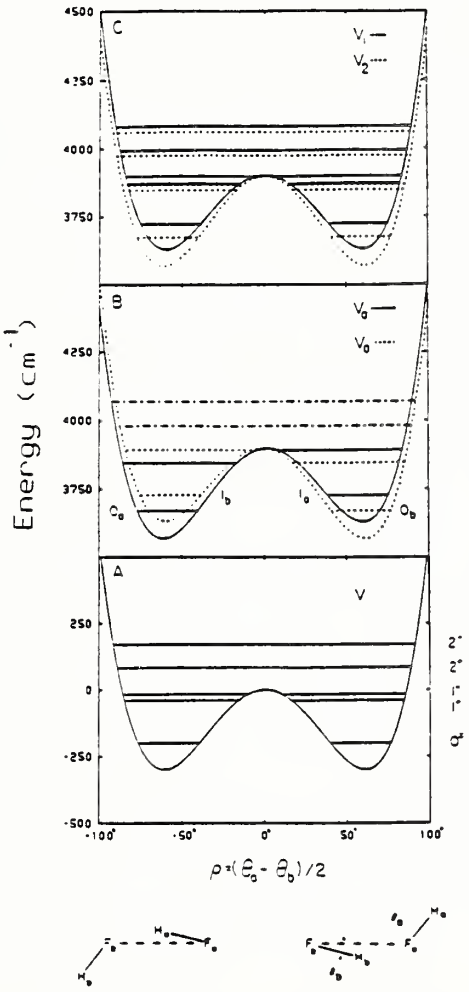

Fig. 2.10 Potential curves and tunneling pathway used to model the vibrational dependence of the interconversion tunneling splittings in $(HF)_2$. Here, ρ is the tunneling coordinate. Figures A-C show the ground-state potential $V(\rho)$, the two excited-state curves $V_a(\rho)$ and $V_b(\rho)$, which correspond to having the HF excitation in H_aF_a and H_bF_b, respectively, and the effective (adiabatic) potentials $V_1(\rho)$ and $V_2(\rho)$ for the ν_1 and ν_2 vibrational states of the dimer. Also shown are vibrational states calculated for these potentials.

8. Ammonia Dimer: Further Structural Studies
(D. D. Nelson, Jr., W. Klemperer, G. T. Fraser, F. J. Lovas, and R. D. Suenram)

New experimental results on the structural and dynamical properties of NH_3 dimer were obtained with the NIST pulsed beam Fourier transform microwave spectrometer. The J = 1-0, K = 0 transitions of $^{14}NH_3$-$^{15}NH_3$,

$^{15}NH_3$-$^{14}NH_3$, ND_3 dimer, and ND_3-ND_2H have been measured at high resolution and ^{14}N electric quadrupole coupling constants determined. The NH_3 subunits comprising the dimer are inequivalent. The quadrupole coupling constant associated with the first ammonia subunit eqQ^1_{aa}, is measured in $^{14}NH_3$-$^{15}NH_3$ [- 627(8) kHz], in the ND_3 dimer [- 531(15) kHz], and in ND_3-ND_2H [- 991(18) kHz]. For the other subunit, eqQ^2_{aa} was found for $^{15}NH_3$-$^{14}NH_3$ [892(8) kHz], the ND_3 dimer [745(13) kHz], and NH_2H [1013 (18) kHz]. These numbers can be used to estimate the vibrationally averaged polar angles of these isotopomers of the NH_3 dimer. The result is (including the primary isotopomer) θ_1 for $^{14}NH_3$-$^{14}NH_3$ is 48.6°, for $^{14}NH_3$-$^{15}NH_3$ is 48.7°, for ND_3 dimer is 49.6° and for ND_3-ND_2H is 45.3°; while θ_2 for $^{14}NH_3$-$^{14}NH_3$ is 64.5°, for $^{15}NH_3$-$^{14}NH_3$ is 64.3°, for ND_3 dimer is 62.6°, and for ND_3-ND_2H is 65.8°. The remarkable invariance of these values rules out the possibility of large vibrational averaging or tunneling averaging in this system and establishes that the angles $\theta_1 = 49°$ and $\theta_2 = 65°$ are near equilibrium. The isotope effect in the component of the electric dipole moment along the a inertial axis μ_a, correlates well with the trend in polar angles given by the quadrupole coupling constants. The absence of interchange tunneling effects in the observed states of the NH_3 dimer implies that these states are asymmetrically excited internal rotor states of the complex. These experimental structural results are in disagreement with all previous theoretically determined structures for the NH_3 dimer except one. A recent electronic structure calculation which incorporates correlation through the coupled pair functional approach (while systematically varying geometry) obtains a compact, asymmetric structure for the dimer; this is in close accord with our observations.

9. Microwave Spectrum and Molecular Structure of the N_2-H_2O Complex (H. O. Leung, M. D. Marshall, R. D. Suenram, and F. J. Lovas)

We observed the a-type, K = 0 microwave spectrum of the N_2-H_2O complex using a pulsed molecular beam Fabry-Perot cavity microwave spectrometer. Seven isotopic species have been studied in the range of 5-23 GHz. The N_2-H_2O complex exhibits tunneling motions similar to the 1 → 2 tunneling motion of the H_2O-DOD complex which gives rise to four components for each rotational transition. The molecular constants obtained for $^{14}N_2$-HOH are (in MHz):

Constant	A_2-State	A_1-State	B_1-State	B_2-State
B	2906.3618(2)	2906.9252(2)	2914.1457(2)	2914.2520(2)
D_J	0.041806(15)	0.043486(15)	0.042625(15)	0.043300(15)
$eQq(^{14}N)$	-4.253(2)		-4.227(3)	

The structure has a nearly linear N-N-HO geometry with a N-H distance of 2.42(4) Å and an OHN angle of 169° (R_{O-N} = 3.37(4) Å). The electric dipole moment along with a principal axis of inertia was determined for the $^{15}N_2$-HOH species with μ_a = 0.833(3) Debye. Unlike the H_2O-D_2O species, all four expected transitions are observed and exhibit the singlet and triplet spin-spin hypderfine structure expected for both $^{15}N_2$-HOH and $^{14}N_2$-HOH.

10. Rotational Spectra and Structures of the H_2S-H_2O and $(H_2S)_2$ Complexes

(F. J. Lovas, R. D. Suenram, and L. H. Coudert)

A pulsed-beam Fabry-Perot cavity microwave spectrometer has been employed in the measurement of rotational spectra of H_2S-H_2O and $(H_2S)_2$. The a-type K = 0 rotational transitions of both species have been observed in the 6-21 GHz range. The spectrum of H_2S-H_2O is expected to be analogous to those of $H_2{}^{18}O$-H_2O and $^{15}N_2$-H_2O (described above) for which two tunneling motions give rise to four components for each transition. For H_2S-H_2O and its ^{34}S and ^{18}O isotopic forms, only 3 of the 4 components have been observed as illustrated in Fig. 2.11. The molecular parameters for H_2S-H_2O are:

State		1	2	3
(B+C)/2	(MHz)	3443.899(1)	3450.712(1)	3450.777(2)
D	(kHz)	28.71(5)	21.20(4)	24.67(4)
μ	(D)	0.551(3)	0.702(3)	0.697(6)

The energy levels of H_2S dimer and its isotopic forms are expected to be similar to those of the water dimer. While hoping to observe a wider range of states than presently known for the water dimer, at present only the K = 0 states for the E levels for $(H_2S)_2$, $(H_2{}^{34}S)$ and $(D_2S)_2$, and the similar levels of the mixed isotopic forms have been observed. For $(H_2S)_2$ the rotational constants are: B (E^+) = 1749.310(1) MHz and B (E^-) = 1748.109(1). The structures of both complexes are shown in Fig. 2.12. The fact that only three of the four expected transitions have been observed remains unexplained, as it is for the deuterated and ^{18}O species of the water dimer.

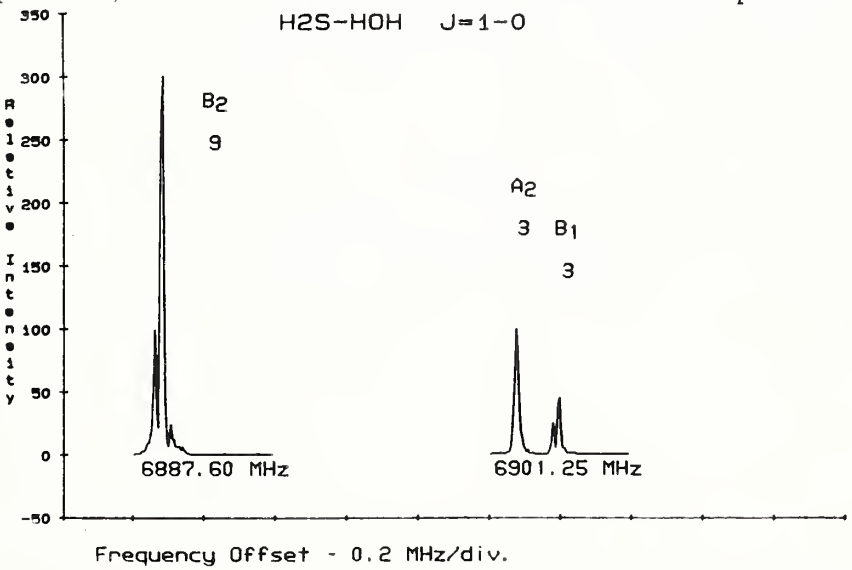

Fig. 2.11 The three observed components for the J=1-0 transition are shown. Two of the transitions have a triplet pattern.

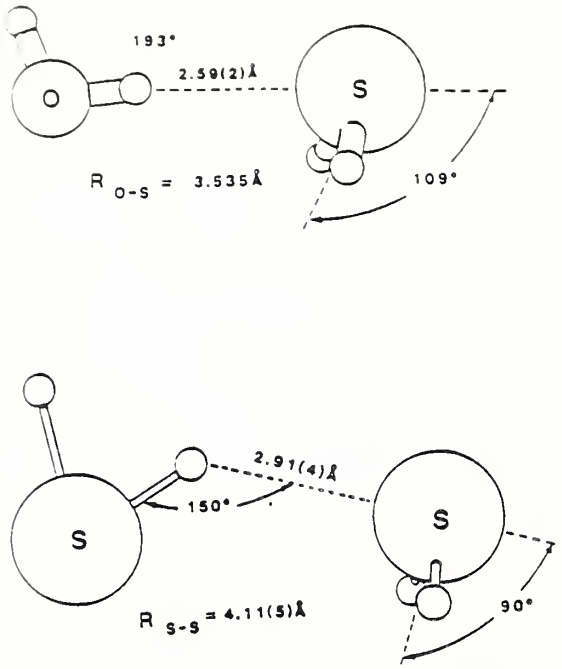

Fig. 2.12 Molecular Structures of H_2O-H_2S and H_2S dimer.

11. Microwave Spectrum of the Ozone-Water Complex
(R. D. Suenram, F. J. Lovas, J. Gillies, and C. W. Gillies)

The microwave spectrum of the ozone-water complex has been observed using a pulsed molecular beam microwave spectrometer. The spectra for the normal species, $H_2{}^{18}O$, and one deuterated species have been assigned. Both a- and c-type transitions have been observed and fit using a centrifugal distortion Hamiltonian. For the O_3-H_2O species the rotational constants are A=11960.584(5), B=4174.036(8) and C=3265.173(8) MHz. The measured components of the dipole moment for the complex are μ_a=1.014(2)D, μ_b=0D, and μ_c=0.52(3)D which gives for the total dipole moment μ_T=1.14(1)D. From the available data several structural conclusions can be drawn, but details of the conformation are, at present, somewhat uncertain. The inertial defect ($\Delta \equiv I_c - I_b - I_a$) is -8.55uÅ^2 which indicates that the complex has a non-planar heavy atom structure. From Ray's asymmetry parameter $\kappa \equiv (2B-A-C)/(A-C)$ ($\kappa \equiv -0.8$) we conclude that the observed conformation must have a sandwich (H_2O and O_3 monomer planes parallel) or T-shaped (H_2O and O_3 monomer planes perpendicular), as opposed to an elongated structure with water bound to one end of the ozone molecule.

The dipole moment of the complex indicates that the two monomer subunits must be arranged such that substantial cancellation of the monomer dipoles occurs since μ_{water} = 1.85D and μ_{ozone} = 0.53D. This is also consistent with a T-shaped structure as shown in Fig. 2.13. Additional work is in progress involving the second deuterated isotope and $H_2{}^{17}O$.

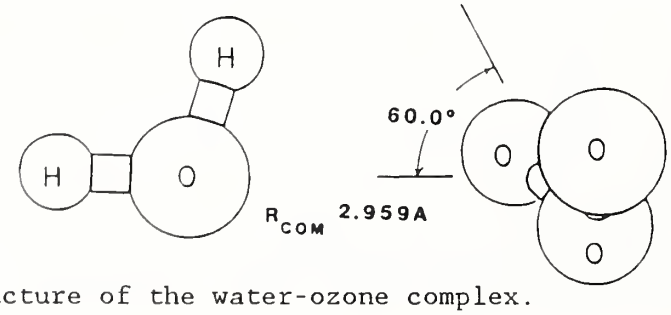

Fig. 2.13 Structure of the water-ozone complex.

12. The Structure of the CO_2-CO_2-H_2O van der Waals Complex Determined by Microwave Spectroscopy
(K. I. Peterson, R. D. Suenram, and F. J. Lovas)

The rotational spectra of CO_2-CO_2-H_2O, CO_2-CO_2-D_2O, $^{13}CO_2$-$^{13}CO_2$-H_2O and CO_2-CO_2-$H_2{}^{18}O$ were measured using a pulsed molecular beam Fabry-Perot Fourier transform microwave spectrometer. The rotational constants of the normal species are A=3313.411(5) MHz, B=1470.548(3) MHz, C=1308.850(3) MHz, Δ_J=0.00341(4) MHz, Δ_{JK}=-0.0016(1) MHz, Δ_K=0.020(5) MHz, δ_J=0.000179(2) MHz, and δ_K=0.0005(7) MHz. The dipole moment, μ_b, is 1.989(2) D. Only b-type transitions are observed and the $J_{K-K+}' - J_{K-K+}'' = J_{eo}'-J_{oe}''$ transitions are three times more intense than the others. This indicates a structure with two-fold symmetry with the C_{2v} axis of the water subunit aligned with the C_2 axis of the complex. The CO_2 subunits lie in a plane perpendicular to the C_2 axis located 2.47 Å below the oxygen atom in the water subunit. The C-C bond distance is 3.41(5) Å. Their orientation is very similar to that observed for the CO_2-CO_2 dimer although the C-C bond length is 0.19 Å shorter in the trimer. The C-O bond distances between the H_2O and two CO_2 subunits are both 3.00(5) Å which is 0.16 Å longer than that found in the CO_2-H_2O dimer. The hydrogens of the H_2O subunit are directed away from the CO_2-CO_2 plane; their angular orientation around the b axis is not well-determined. Two views of the structure are shown in Fig. 2.14.

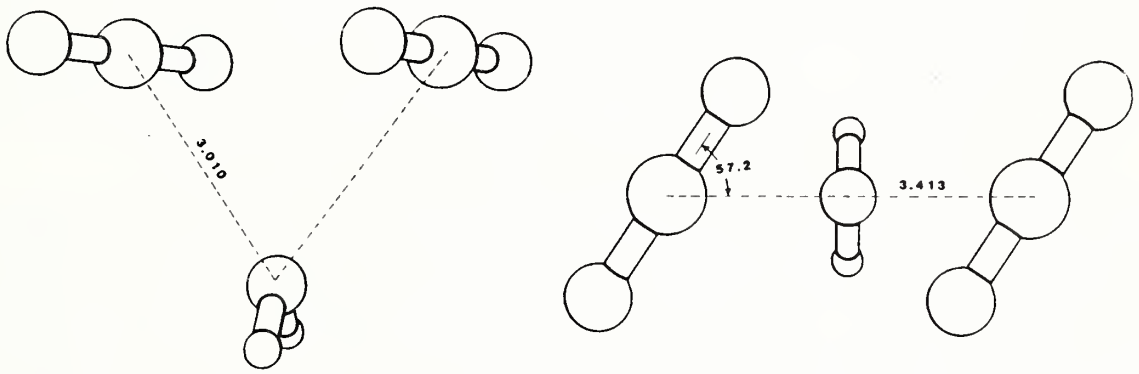

Fig. 2.14 Two views of the molecular structure of $(CO_2)_2H_2O$.

13. Structural Study of the H_2O-H_2O-CO_2 Trimer
(K. I. Peterson, R. D. Suenram, and F. J. Lovas)

The microwave spectrum of the trimeric species H_2O-H_2O-CO_2 was studied in the 7-18 Ghz frequency range using a pulsed molecular beam Fabry-Perot Fourier transform microwave spectrometer. Each transition is doubled because of energy level splitting due to coupling of an internal rotation of one of the H_2O subunits with the overall rotation of the complex. Both states can be fit using a centrifugal distortion Hamiltonian. The rotational constants and inertial defects are:

	Lower State	Upper State
A	6163.576(5) MHz	6164.068(7) MHz
B	2226.156(3) MHz	2226.677(3) MHz
C	1638.972(2) MHz	1638.839(3) MHz
Δ	-0.66197 uÅ^2	-0.57724 uÅ^2

The electric dipole moment has also been measured yielding μ_a=1.57D, μ_b=0.76D and μ_c<0.1D. Several isotopically substituted species have been studied with various ^{13}C, ^{18}O and deuterium substitutions. All except a singly deuterated species exhibit doubled spectra. We conclude that the species has a nearly-planar triangular structure with dimer-type structures evident within the trimer complex (see Fig. 2.15). The oxygen of one of the H_2O subunits is bonded to the CO_2 carbon with a bond length of 2.8Å, within 0.1Å of that found in the H_2O-CO_2 dimer. The other H_2O has its oxygen bonded to one of the hydrogens of the first H_2O; the bond distance is 2.0Å, within 0.1Å of that found in the H_2O-H_2O dimer. This second H_2O is also hydrogen bonded to one of the oxygens in the CO_2 subunit with a bond distance of 2.0Å which is what one would expect for a hydrogen bonded H_2O-CO_2 dimer (this species has not been observed). Evidence suggests that this H_2O subunit is involved in the internal rotation.

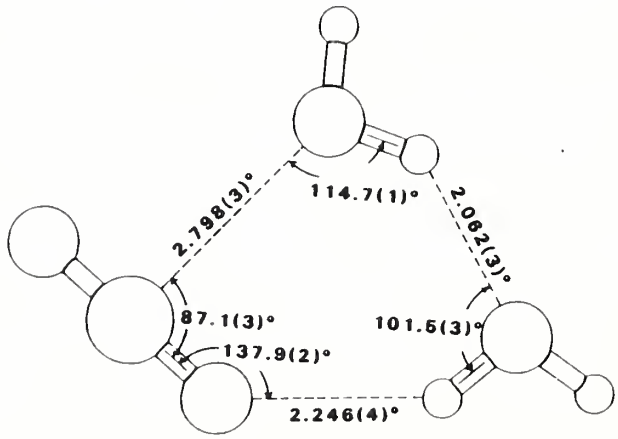

Fig. 2.15 Molecular structure of $(H_2O)_2CO_2$.

14. Microwave Spectrum of the CH_3OH-NH_3 Complex
(G. T. Fraser, R. D. Suenram, F. J. Lovas, and W. J. Stevens)

Microwave spectra of CH_3OH-NH_3 and $^{13}CH_3OH$-NH_3 have been obtained using a pulsed-nozzle Fourier-transform microwave spectrometer. The spectra, which are complicated by the internal rotation of the CH_3 and NH_3 groups, exhibit five K = 0 states at the ≈ 1 K rotational temperature of the expansion. Four of these are metastable, excited internal rotor states and correlate to E states of free CH_3OH or NH_3. For the two states in which the NH_3 top is in its ground internal rotor state, ΔJ=1, K = 0 progressions are observed and fit to linear-molecule-type frequency expressions to obtain effective spectroscopic constants. For CH_3OH-NH_3 these constants are: (B + C)/2=3690.119(2) and 3686.114(2) MHz; eQq_{aa}=-3.184(10) and -3.182(9) MHz; and μ_a=2.854(9) and 2.956(14) D. The complexes are hydrogen bonded with an OH-N bond length of 2.02Å. This bond

length is similar to that found by Herbine and Dyke in the related HOH-NH_3 complex, 1.97Å. Ab initio SCF calculations have also been carried out for the CH_3OH-NH_3 and HOH-NH_3 complexes in order to compare interaction-energy components and origins of the dipole moment enhancements.

15. Determination of the Structure of OCS-CO_2
(S. E. Novick, R. D. Suenram, and F. J. Lovas)

The rotational spectrum of the weakly bound complex OCS-CO_2 has been measured using a pulsed beam Fourier transform microwave spectrometer. The rotational constants of the major isotopomer are A = 4454.606 MHz, B = 1517.7788 MHz, and C = 1129.666 MHz. The molecule is planar with a "slipped near parallel" structure analogous to the structure of the dimer of carbon dioxide. The sulfur atom occupies the "inner" position; this is the obtuse rather than the acute vertex of the O-O-O-S quadrangle. The distance from the center-of-mass (c.m.) of CO_2 to the c.m. of OCS is 3.552Å which is slightly shorter than the C-C distance in CO_2 dimer (3.599Å).

16. Microwave Spectrum and Structure of H_2CO-CO_2
(T. A. Blake, S. E. Novick, R. D. Suenram, and F. J. Lovas)

The rotational spectrum of the H_2CO-CO_2 van der Waals complex has been measured using a pulsed beam Fourier transform microwave spectrometer. Each rotational line is split into a "strong" and "weak" intensity component due to the internal rotation of the formaldehyde moiety about its C_2 axis. The "strong" transitions are assigned to a B symmetry internal rotor state with the rotational constants A = 10.399.1(2) MHz, B = 2678.215(1) MHz, and C = 2128.340(1) MHz. The "weak", or A state lines were assigned with the rotational constants A = 10.400.5(2) MHz, B = 2678.271(1) MHz, and C = 2128.312(1) MHz.

The complex has a planar structure analogous to the "near slipped parallel" structures of $(CO_2)_2$ and CO_2-OCS, with the oxygen of H_2CO interacting with the carbon of CO_2 as illustrated in Fig. 2.16. The structural parameters and dipole moments of both the A and B states are the same within the stated uncertainties. The C-O (formaldehyde)-C (carbon dioxide) angle is 102.90(5)°, the O (formaldehyde)-C-O (carbon dioxide) angle is 83.23(3)°, and the O (formaldehyde)-C (carbon dioxide) distance is 2.980(1) A. The measured dipole moments are μ_a=1.661(2) D, and μ_b=1.671(2) D.

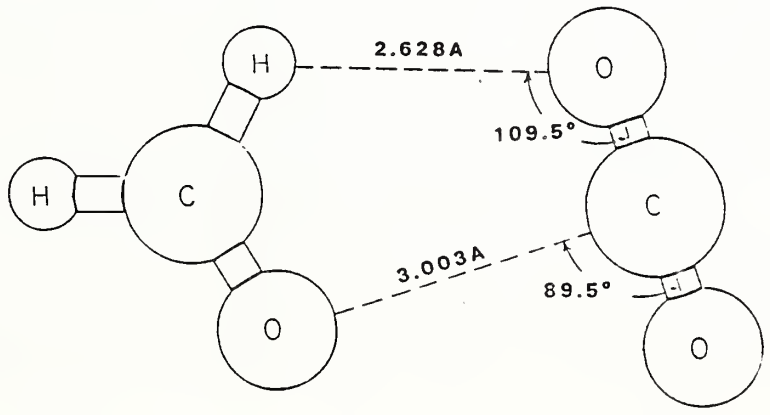

Fig. 2.16 Structure of the Formaldehyde-Carbon Dioxide Complex

17. Structure and Vibrational Dynamics of the CO_2 Dimer from the Sub-Doppler Infrared Spectrum of the 2.7 μm Fermi Diad (K. W. Jucks, Z. S. Huang, R. E. Miller, G. T. Fraser, A. S. Pine, and W. J. Lafferty)

Sub-Doppler infrared spectra of two Fermi resonance coupled bands of carbon dioxide dimer have been obtained at 3611.5 and 3713.9 cm^{-1} using an optothermal molecular beam color-center laser spectrometer. The band origins for the complexes are red shifted by approximately 1 cm^{-1} from the corresponding $\nu_1 + \nu_3/2\nu_2^0 + \nu_3$ CO_2 bands. The higher frequency band is perturbed while the lower frequency band appears free of extraneous perturbations as determined from a precision fit to a Watson asymmetric rotor Hamiltonian. This fit and the observed nuclear spin statistical weights reveal that the complex is planar with C_{2h} symmetry (see Fig. 2.17). The C--C separation and C--C-O angle are determined to be 3.599(7)Å and 58.2(8)°, respectively. The nearest neighbor O--C distance is 3.14Å which is the same as that found in the crystal. From the centrifugal distortion analysis the weak bond stretching and symmetric bending frequencies are estimated to be 32(2) and 90(1) cm^{-1}. No interconversion tunneling is observed.

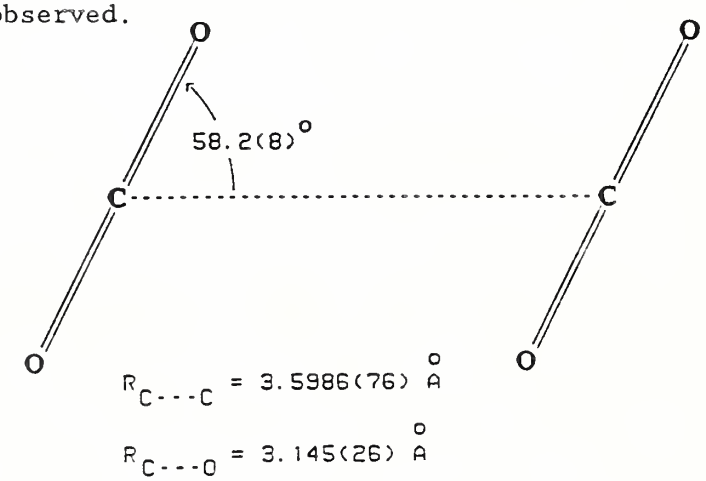

Fig. 2.17 Molecular structure of the CO_2 dimer determined from the ground state rotational constants. The complex is planar with C_{2h} symmetry.

18. Sub-Doppler Infrared Spectrum of the Carbon Dioxide Trimer (G. T. Fraser, A. S. Pine, W. J. Lafferty, and R. E. Miller)

A spectrum of the carbon dioxide trimer van der Waals species has been recorded near 3614 cm^{-1} at sub-Doppler resolution using an opthothermal (bolometer-detected) molecular-beam color-center laser spectrometer. A planar, cyclic structure with C_{3h} symmetry (see Fig. 2.18) has been determined for the complex with a carbon-carbon separation of 4.0382(3)Å. The observed perpendicular band, corresponding to an in-plane E'-symmetry vibration of the trimer, has been attributed to a localized excitation of the $2\nu_2^0 + \nu_3$ combination mode of a CO_2 subunit by virtue of its small blue shift (~0.98 cm^{-1}) from that of the isolated monomer.

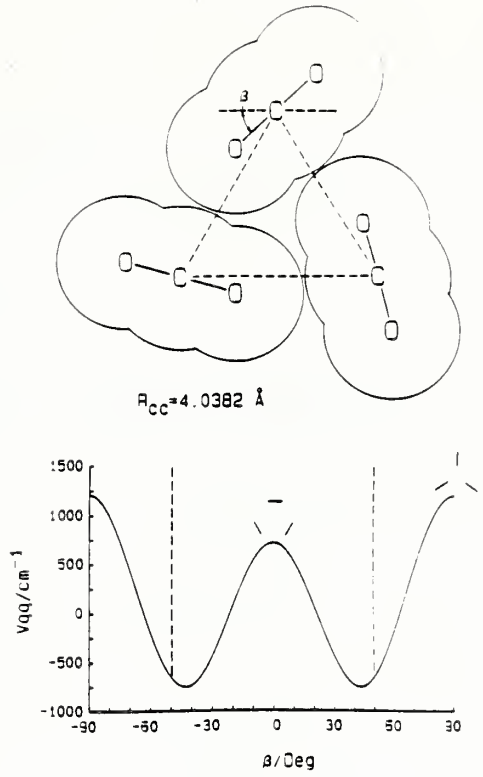

Fig. 2.18 Structure of the CO_2 trimer obtained from the spectrum assuming zero inertial defect and angle, β~43°, from minimum of the electrostatic quadrupole-quadrupole potential pictured below. The dashed lines on the potential are drawn for contact of the van der Waals radii; the D_{3h} transition state geometries are indicated at β = 0° and 90°.

19. Vibrational Predissociation in the CO_2 Dimer and Trimer and Rare Gas-CO_2 Complexes
(A. S. Pine and G. T. Fraser)

Vibrational predissociation linewidths for the CO_2 dimer and trimer and the Ne-CO_2 and Ar-CO_2 complexes have been resolved using a bolometer-detected (optothermal) molecular-beam color-center laser spectrometer. Observations were made on the pair of vibrations near 3715 and 3613 cm^{-1} corresponding to the $\nu_1 + \nu_3/2\nu_2^0 + \nu_3$ Fermi diad of CO_2. Homogeneous linewidths of from ~0.5 to ~22 MHz (FWHM) were measured for these related complexes, with Ne-CO_2 exhibiting both the broadest and the sharpest lines for the upper and lower bands, respectively. Ar-CO_2 and $(CO_2)_2$ showed mode-independent intermediate predissociation rates while only the lower band of $(CO_2)_3$ could be found. The results indicate that V → V energy transfer processes are the dominant predissociation channels with symmetry selection or propensity rules and specific resonances playing a role. The observed and calculated spectrum of the 3613 band is shown in Fig. 2.19.

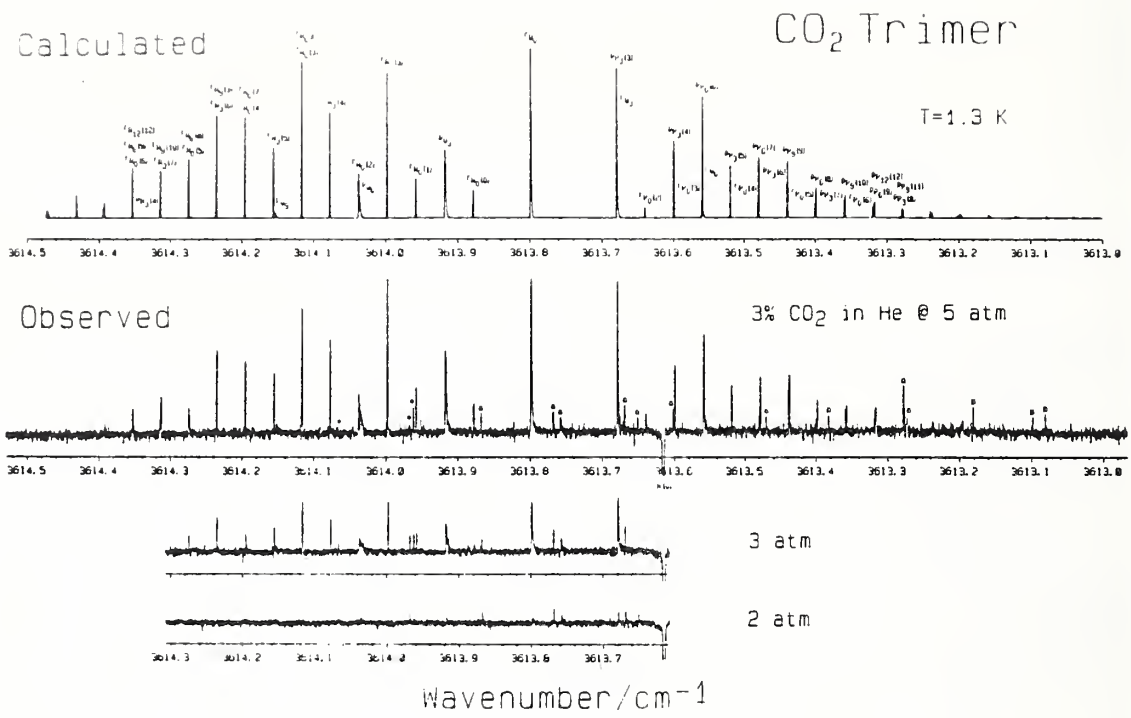

Fig. 2.19 Observed and calculated spectra of the CO_2 trimer in the region of the $2\nu_2^0 + \nu_3$ combination band of the monomer indicated by the negative-going R(0) line. Observed spectra for 3% CO_2:He mixture and 5 atm driving pressure. Asterisks indicate transitions attributed to the CO_2 dimer. Calculated transitions are simulated with Gaussian profiles of 20 MHz FWHM and an effective rotational temperature of 1.3 K.

20. Rotational Spectrum and Structure of H_2CO-HCl
(G. T. Fraser, C. W. Gillies, J. Zozom, F. J. Lovas, and R. D. Suenram)

Rotational spectra of H_2CO-$H^{35}Cl$, H_2CO-$H^{37}Cl$, D_2CO-$H^{35}Cl$, and D_2CO-$H^{37}Cl$ have been observed using a pulsed-nozzle Fourier transform microwave spectrometer. For H_2CO-$H^{35}Cl$ the following spectroscopic constants have been determined (in MHz): B = 2687.856(23), C = 2527.412(23), Δ_J = 0.0105(12), Δ_{JK} = - 0.233(10), eQq_{bb} = 14.106(19). HCl is bonded to the oxygen of H_2CO through a nonlinear hydrogen bond. For the H_2CO-$H^{35}Cl$ complex, the distance between the centers of masses of the HCl and H_2CO moieties is 3.3487Å giving an O--Cl distance of 3.21Å. From the quadrupole coupling constant, eQq_{aa}, an effective vibrationally averaged angle between the HCl axis and the a-axis of the complex is determined to be 30.5°. Centrifugal distortion analysis yields estimates of the weak bond stretching force constant and stretching frequency as 0.069(8) mdyn/Å and 85(4) cm^{-1}, respectively.

21. Electric Dipole Moments of HCl- and HCN-Hydrocarbon Complexes
(A. Weber, G. T. Fraser, and R. D. Suenram)

Electric dipole moments of several hydrocarbon-HCN and hydrocarbon-HCl complexes have been measured using a pulsed-nozzle Fourier-transform microwave spectrometer. The dipole moments (μ) and complexation-induced dipole moments ($\Delta\mu$) are (in D):

	HCl		HCN		HF[1,2]	
	μ	$\Delta\mu$	μ	$\Delta\mu$	μ	$\Delta\mu$
Acetylene	1.6032(29)	0.57	3.4130(42)	0.50	2.3681(28)	0.65
Ethylene	1.6167(15)	0.58	3.4023(27)	0.49	2.3839(45)	0.67
Benzene	1.688(10)	0.67			2.244(4)	0.59
Cyclopropane	1.7405(16)	0.71	3.5875(41)	0.67	2.5084(28)	0.78

The dipole moments for the HF complexes have been measured previously[1,2] using molecular-beam electric-resonance spectroscopy. The HCl-benzene result is in good agreement with the 1.6(1) D moment determined by Gandhi et al.[3] using electric deflection techniques. The induced dipole moments show a number of interesting features. With the same acid binding partner, the acetylene and ethylene complexes give similar induced moments while the cyclopropane complexes give the largest induced moments. Except for the benzene complexes, the induced dipole moments increase as: X-HCN < X-HCl < X-HF and do not follow the dipole moments of the acid binding partners which are ordered: HCl < HF < HCN.

1. D. D. Nelson, Jr., G. T. Fraser, and W. Klemperer, J. Chem. Phys. 82, 4483 (1985).
2. F. A. Baiocchi, J. H. Williams, and W. Klemperer, J. Am. Chem. Soc. 87, 2079 (1983).
3. S. R. Gandhi and R. B. Bernstein, Chem. Phys. Lett. 143, 332 (1988).

22. Isotope Effects in the High-Resolution Infrared Spectrum of OC-HF
(G. T. Fraser and A. S. Pine)

High-resolution infrared spectra of H-F stretching bands of natural OC-HF and enriched $O^{13}C$-HF and ^{18}OC-HF have been recorded under thermal equilibrium conditions near 195 K with a tunable difference-frequency laser. The rotational constants of the three isotopic species are consistent with the linear C-H van der Waals bond as determined by microwave spectroscopy. The isotope shifts for the band centers exhibit a curious staggering with total CO mass which we attribute to anharmonic coupling of the zero-point CO bending motion. Resolved splitting of the ℓ doublets in a hot band originating in the CO bending vibration yield tentative assignments and rotational constants for this low frequency van der Waals mode.

23. Infrared and Microwave Spectra of OCO-HF and SCO-HF
(G. T. Fraser, A. S. Pine, R. D. Suenram, D. C. Dayton, and R. E. Miller)

The H-F stretching bands of the OCO-HF and SCO-HF complexes have been studied by optothermal (bolometer-detected) molecular-beam spectroscopy. Both species exhibit spectra of a quasilinear molecule red-shifted from free HF by 52.1 and 57.5 cm^{-1}, respectively. The principal band in both molecules is accompanied by a slightly red-shifted doublet-type subsidiary band that can be interpreted as a hot band of a low

frequency bending vibration or a K=1 subband of a bent molecule. Accurate doublet splittings in the ground H-F vibrational state have been measured by pulsed-nozzle Fourier-transform microwave spectroscopy.

24. Pulsed Beam Rotational Study of the CH_2CH_2-O_3 van der Waals Complex (C. W. Gillies, J. Gillies, W. Stahl, R. D. Suenram, and F. J. Lovas)

We have recently completed a structural study of the primary ozonide of ethylene (see section on General Spectroscopic Studies). Our studies of the primary ozonide indicated that the reaction path involved a concerted 1,3-cycloaddition of ozone to the two carbon atoms of ethylene. If this were true it appeared that the van der Waals complex of ethylene-ozone would reflect this geometry and represent the transition state in the ethylene-ozone reaction which produces the cyclic primary ozonide. Using independent gas inlets to a pulsed solenoid valve, one for the Ar/CH_2CH_2 mixture and the second for the Ar/O_3 mixture, and mixing the two gases close to the nozzle exit, we have observed the rotational spectrum of O_3-CH_2CH_2 with the Fourier transform microwave spectrometer.

A geometry in which the ethylene plane is approximately parallel to the ozone plane with a C•••O distance of 3.25Å is consistent with the microwave data (see Fig. 2.20). This structure has the same symmetry (C_s) as ethylene primary ozonide. Since ethylene primary ozonide is the thermally labile 1,3-dipolar cycloaddition product of ozone plus ethylene, both species lie along the reaction coordinate predicted by orbital symmetry rules. Isotopic work is planned to further define the geometry of this complex. Future experiments will include other classical examples of 1,3-dipolar cycloadditions.

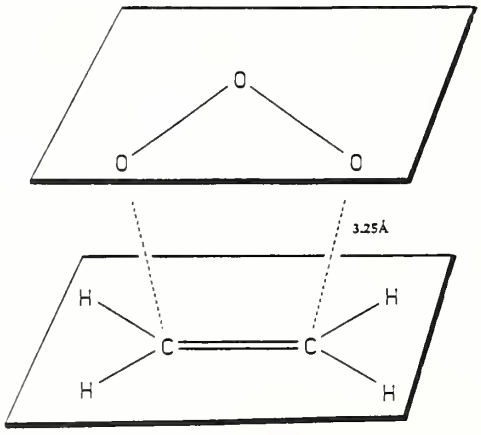

Fig. 2.20 Approximate geometry of ethylene-ozone complex showing the parallel planes of ethylene and ozone with a C•••O distance of 3.25Å.

25. Future Plans

The major emphasis of the microwave studies during the past two years has been on structural studies of molecular complexes containing water, H_2S and formaldehyde. Since water is the most important solvent, we plan to continue investigations of water complexes. A preliminary

identification of the spectrum of H_2O-H_2CO has been obtained recently and will be investigated further. Several of the experiments described above are still incomplete and these will be carried to completion next year.

A laser ablation source is now under construction and will be ready for initial tests early next fiscal year. With this source we plan to investigate complexes containing metal atoms and refractory materials.

Several modifications are planned to the optothermal molecular-beam spectrometer initially developed and successfully demonstrated for the probing of molecular complexes with a tunable color-center laser. A tunable sideband CO_2 laser system is under construction to provide access to the important 10 μm spectral region for the study of predissociation in a number of molecular complexes. The sideband generator operates by nonlinear optical mixing of microwave radiation from 8 to 18 GHz with a stabilized line-tunable CO_2 laser in a CdTe electooptic crystal. This should provide substantial coverage (>50%) throughout the 9 to 11 μm range with powers in excess of 1 mW. In conjunction with the color-center laser, this will also enable us to use infrared-infrared double resonance techniques to help identify and sort out spectra of previously uninterpreted rovibrational bands.

We are also installing quadrupole focussing fields in the drift chamber of the molecular-beam apparatus to permit us to examine the microwave spectrum of polar molecules and to provide microwave-infrared double resonance capabilities to aid in species identification and spectral assignments.

E. Rare Gas - Molecule Complexes

Since complexes involving the rare gas atoms comprise a separate category we describe our work on these in this section.

1. Optothermal-Infrared and Pulsed-Nozzle Fourier-Transform Microwave Spectroscopy of Rare Gas-CO_2 Complexes
   (G. T. Fraser, A. S. Pine, and R. D. Suenram)

Sub-Doppler infrared spectra of Ne-CO_2, Ar-CO_2, and Kr-CO_2 have been recorded near 3613 and 3715 cm^{-1}, in the region of the $2\nu_2^{\circ} + \nu_3/\nu_1 + \nu_3$ Fermi diad of CO_2, using an optothermal molecular-beam color-center laser spectrometer. In addition, pulsed-nozzle Fourier-transform microwave spectra are reported for the ground vibrational states of the complexes. The infrared and microwave spectra are consistent with T-shaped complexes as shown originally by Steed, Dixon, and Klemperer for Ar-CO_2. The infrared band origins for the Ar and Kr complexes are red shifted, from that of free CO_2, by 1.09 and 0.95 cm^{-1} for Ar-CO_2 and by 1.97 and 1.76 cm^{-1} for ^{84}Kr-CO_2. For Ne-CO_2, blue shifts of 0.15 and 0.19 cm^{-1} are observed. The lower Fermi components are free of perturbations, whereas the upper components of Ar-CO_2 and Kr-CO_2 are perturbed. For Ar-CO_2 the perturbation is strong, shifting the positions of the observed Q-branch lines of the $K_a = 1 \leftarrow 0$ subband by as much as 500 MHz.

2. Rotational-Tunneling Spectrum of Ar-H_2O and Ar-H_2S
(F. J. Lovas and R. D. Suenram)

Recently Cohen et al.[1] reported the far infrared spectrum of Ar-H_2O. They observed c-type transitions from the ground state to the upper component of a hydrogen exchange tunneling doublet (internal rotation of H_2O in the complex). Based on their rotational analysis we have confirmed their ground state assignments by observing the a-type transitions in the ground state. In order to determine the structure of the complex we have also measured the a-type spectrum of Ar-$H_2{}^{17}O$, Ar-$H_2{}^{18}O$ and Ar-D_2O. Spectral searches for the mono-deuterated species are in progress. With the information at hand, the complex appears to have the Ar bonded nearly perpendicular to the plane of H_2O at an Ar-O distance of 3.7Å. Searches for the second state produced by the tunneling motion will be carried out first on the D_2O species. We have recently detected this state for the Ar-D_2S species and will look for the spectrum of the second state in Ar-H_2S in the near future.

---

1. R. C. Cohen, K. L. Busarow, K. B. Laughlin, G. A. Blake, M. Aaverth, Y. T. Lee, and R. J. Saykally, private communication.

3. Determination of the Structure of Ar-H_2CO
(S. E. Novick, F. J. Lovas, R. D. Suenram, and G. T. Fraser)

The rotational spectrum of the weakly bound complex Ar-H_2CO has been measured using a pulsed beam Fourier transform microwave spectrometer. The rotational constants of the complex are A = 40059.961 MHz, B = 2174.589 MHz, and C = 2080.321 MHz. The argon atom sits almost directly above the carbon atom of the formaldehyde with an Ar - C distance of 3.614 Å and an Ar--C-O angle of 90°. It is likely that the hydrogen atoms of the formaldehyde execute hindered internal rotation about the C-O axis and thus their positions within the complex are not well specified.

Stark effect measurement on Ar-H_2CO yields electric dipole moment components μ_a=0.461(5) D and μ_b=2.209(10) D which are consistent with the "T-shaped" structure shown in Fig. 2.21.

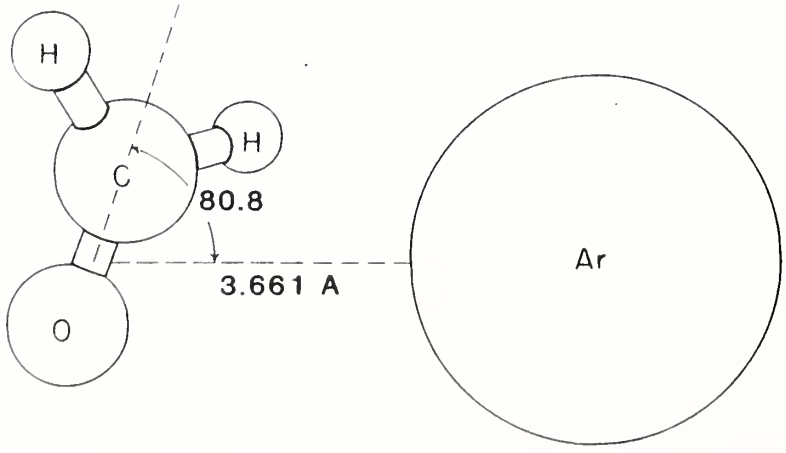

Fig. 2.21 The structure of Ar-H_2CO.

4. Rotational Spectra and Structure of Ar-CH_3OH and Kr-CH_3OH
(R. D. Suenram, G. T. Fraser, F. J. Lovas, J. Zozom, and C. W. Gillies)

Microwave spectra of Ar-CH_3OH, Ar-CD_3OH, and Kr-CH_3OH have been obtained using a pulsed nozzle Fourier transform microwave spectrometer. For each of these complexes two torsional states are observed at the ~1K rotational temperature of the expansion. These are the ground state and a metastable excited internal rotor state which correlates to the E internal rotor state of methanol. The a- and b-type ground state spectra are well characterized by the usual asymmetrical top formalism while the excited internal rotor states are complicated by the internal angular momentum. Attempts are presently underway to analyze the excited state spectra. Some preliminary spectroscopic constants for the ground internal rotor state of Ar-CH_3OH complex are (in MHz): A = 25468.82(13), B = 2084.42(2) and C = 1928.459(2).

In both complexes the rare gas atom is located approximately perpendicular to the C-O axis. For Ar-CH_3OH the distance between the centers of mass of the two subunits is 3.68 Å and the weak bond stretching force constant is 0.017 mdyn/Å (see Fig. 2.22). Similar results have been obtained for Kr-CH_3OH.

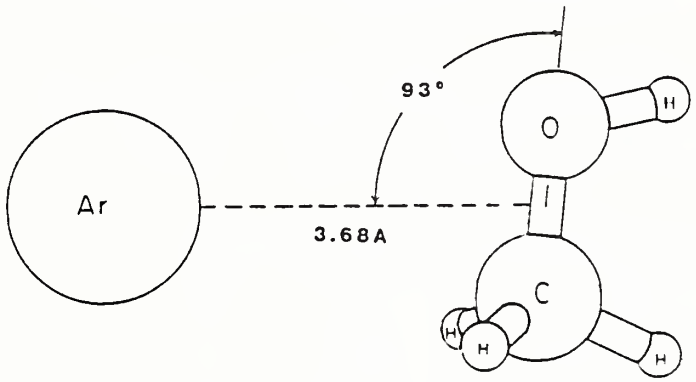

Fig. 2.22 The Structure of Ar-Methanol.

5. Microwave Spectrum, Structure, and Electric Dipole Moment of the Ar-Formamide van der Waals Complex
(R. D. Suenram, G. T. Fraser, F. J. Lovas, C. W. Gillies, and J. Zozom)

The microwave spectrum of the Ar-formamide van der Waals complex has been obtained using a pulsed-nozzle Fourier-transform microwave spectrometer. The rotational constants of the complex are: A = 10725.7524(48) MHz, B = 1771.0738(22) MHz, and C = 1548.9974(16) MHz. The complex is shown to be non-planar with an inertial defect of -6.21 $uÅ^2$. The Ar atom is located 3.62Å from the center of mass of the formamide unit at Ar-O, Ar-N, and Ar-C distances of 3.55, 3.79, and 3.93Å, respectively. The shortest Ar-H distance is 3.25Å which is similar to that observed for Ar-vinyl cyanide (3.21Å). A view of the molecular structure is shown in Fig. 2.23 which indicates the out-of-plane angle. Stark effect and hyperfine analyses yield the following values for the electric dipole

moment components and ^{14}N quadrupole coupling constants for the complex: μ_a = 0.922(1) D, μ_b = 3.407(5) D, χ_{aa} = -1.164(7) MHz, χ_{bb} = 1.906(5) MHz, and χ_{cc} = -0.742(6) MHz.

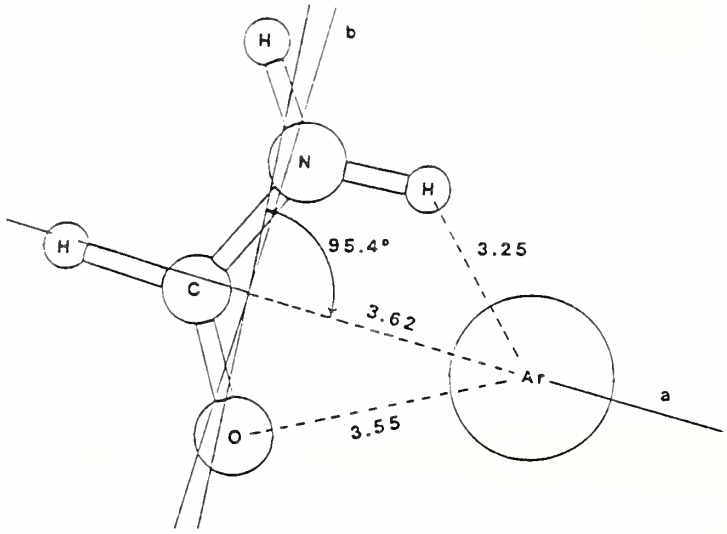

Fig. 2.23 Structure of Ar-formamide for the ground vibrational state.

6. Rotational Spectrum and Structure of Ar-CH_2CHCl
(F. J. Lovas and R. D. Suenram)

Our recent structural studies of Ar-CH_2CHCN and Ar-NH_2CHO illustrated a multicentered van der Waals interaction between Ar and these asymetric top binding partners. For the vinyl cyanide complex we also found two states which were interpreted as a double well potential produced by an inversion motion of the vinyl cyanide unit between two equivalent non-planar structural configurations. In order to determine if these structures are representative of a general configuration for rare gas complexes with asymmetric tops we have examined the rotational spectrum of Ar- vinylchloride. Indeed, we find two states for both ^{35}Cl and ^{37}Cl isotopic species. The structure shown in Fig. 2.24 is similar to those reported earlier for the vinyl cyanide and formamide complexes.

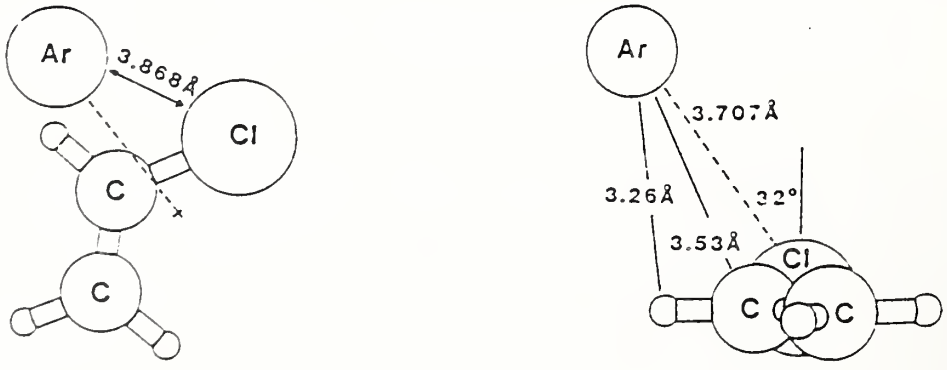

Fig. 2.24 Molecular structure of argon-vinylchloride

F. Matrix Isolation Spectra

1. Free Radical Stabilization and Spectra (M. E. Jacox)

All of the experimental studies conducted during the past two years have benefitted from the use of the BOMEM Fourier transform instrument. In each of the systems studied, the enhanced sensitivity, resolution, or spectral range has been critical to the acquisition of data suitable for positive spectral assignments and for publication.

Studies of the reaction of H atoms with HCN were completed and published. No infrared data had previously been reported for the lowest energy reaction product, H_2CN. This study led to the assignment of five of the six ground-state vibrational fundamentals of this species, which is important in nitramine decomposition and in the combustion of nitrogen-containing molecules. Earlier gas-phase studies had yielded two bands attributed to H_2CN near 285nm and extended progressions for the two deuterium-substituted species. Because of predissociation, no rotational structure was resolved. The band separation of approximately 600 cm^{-1} observed for H_2CN could be explained either by the presence of a "hot band" or by the occurrence of two partially overlapping electronic transitions. The detection of both bands in the ultraviolet absorption studies or matrix-isolated H_2CN precluded the contribution of the lower frequency absorption by a "hot band." Weak absorptions were also observed beyond the second band in the matrix observations on H_2CN, permitting a tentative vibrational assignment for all of the electronic absorption bands which have been reported for H_2CN-d_n.

Studies of the infrared spectrum of t-HOCO, obtained both by the interaction of excited argon atoms with formic acid and by the reaction of H atoms with formic acid, were also completed and published. This species is intermediate in the OH + CO reaction, the principal source of CO_2 in hydrocarbon combustion. In 1970, studies of the vacuum ultraviolet photolysis of H_2O in a CO matrix conducted in this laboratory yielded the infrared spectra of both c- and t-HOCO. Although infrared absorptions of molecules isolated in an argon or neon matrix generally appear within about 1% of the gas-phase band center, the isomeric HOCO molecules can hydrogen-bond to CO, with potentially large shifts in the infrared absorptions associated with the hydrogen stretching and bending vibrations. No subsequent reports of the spectra of the HOCO isomers have appeared. Because diatomic reactants cannot diffuse through solid argon, the yield of products in the Ar:CO:H_2O system--for which the hydrogen bonding would be avoided--would be undetectably small. The problem of hydrogen bonding was completely removed in the study in which the interaction of excited argon atoms with formic acid was the source for t-HOCO. Although only a 10 cm^{-1} shift in the C=O stretching fundamental was observed, the OH stretching fundamental of t-HOCO was found to be shifted by 150 cm^{-1} the torsion fundamental by 100 cm^{-1}, and the HOC in-plane deformation by 50 cm^{-1} as a result of hydrogen bonding with CO. In the experiments in which t-HOCO was stabilized as a product of the F + HCOOH reaction, a significant yield of t-HOCO$\cdots$HF was also observed. Thus, t-HOCO provides an interesting example of the participation of a single species in the formation of two

different types of hydrogen bond. The determination of the infrared band centers for the isolated molecule provides a basis for the search for the gas-phase spectrum of this important combustion reaction intermediate. In turn, the gas-phase observation would constitute a second stage in the development of diagnostics for the detection of t-HOCO in combustion systems.

A review chapter entitled "The Stabilization and Spectroscopy of Free Radicals and Reactive Molecules in Inert Matrices" was prepared for publication in a book entitled, Chemistry and Physics of Matrix-Isolated Species, edited by L. Andrews and M. Moskovits, which is scheduled to appear early in 1989. This review is intended to serve as an in-depth guide to scientists who are beginning studies involving free radical stabilization in matrices or who need to know the conditions under which matrix isolation studies may provide data useful as a starting point for gas-phase free radical detection.

2. Molecular Ion Stabilization and Spectra
(M. E. Jacox and W. E. Thompson)

A new series of experiments has begun in which the 16.6-16.8 eV energy of excited neon atoms is used as a photoionization source for matrix isolation studies of the spectra of molecular ions. This energy is above the photoionization threshold of virtually all molecules. Molecular cations play important roles in such diverse processes as those characteristic of the earth's ionosphere and of chemical vapor deposition and the plasma etching of microcircuits. While they are readily detected by mass spectrometers, frequently a mass probe cannot be introduced into a system and optical detection of ionic species would be desirable. Recently, high-resolution infrared spectra have been reported for a number of small molecular cations. However, for most such species the only spectral data available are those derived from low-resolution (> 50 cm^{-1}) photoelectron spectra. The development of matrix isolation studies as a survey tool for obtaining the infrared and ultraviolet spectra of molecular cations would provide an important first step in the establishment of optical diagnostics for these species.

The sampling configuration used for these experiments is shown in Fig. 2.25. A microwave discharge through a stream of neon flowing through a Vycor tube provides the neon-atom excitation. In approximately the plane of the coarse (approximately 1 mm^2) pinhole in the end of the discharge tube, a mixture of XY, the molecular ion precursor, with a several hundredfold excess of neon is introduced into the system. Approximately 2.5 cm downstream the interaction products are frozen onto a cryogenic surface maintained at 4K. Similar experiments using a beam of excited argon atoms, including those involved in the stabilization of t-HOCO, have previously been conducted at 14K. However, neon matrix experiments require the use of a cell which can be cooled to 4K, the temperature of liquid helium. Therefore, it was necessary to place in service a continuous-transfer liquid helium cell and to establish the conditions under which a stable discharge through neon could be maintained.

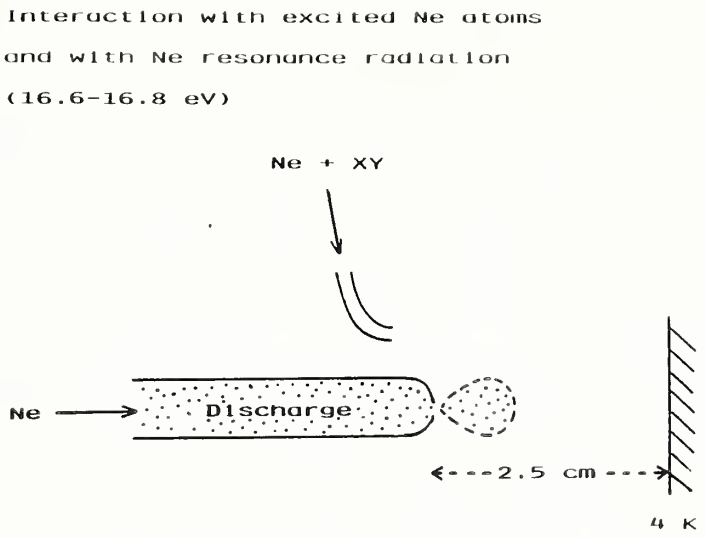

Fig. 2.25 Discharge configuration used for excited neon atom experiments.

The first molecule to be studied in this system was CO_2. High resolution infrared experiments have recently determined a gas-phase band center of 1423.1 cm^{-1} for the antisymmetric stretching fundamental, ν_3 of CO_2^+. As is shown in trace (a) of Figure 2.26 a weak to moderately intense, structured absorption appeared at 1421.7 cm^{-1} in the neon-matrix study. Isotopic substitution experiments confirmed the assignment of this absorption to CO_2^+; in trace (b) the counterpart of this peak appeared near 1380.4 cm^{-1} for a heavily carbon-12 enriched CO_2 sample, and in trace (c) the singly and doubly oxygen-18 substituted CO_2^+ species appeared at 1412.4 and 1399.8 cm^{-1}, respectively.

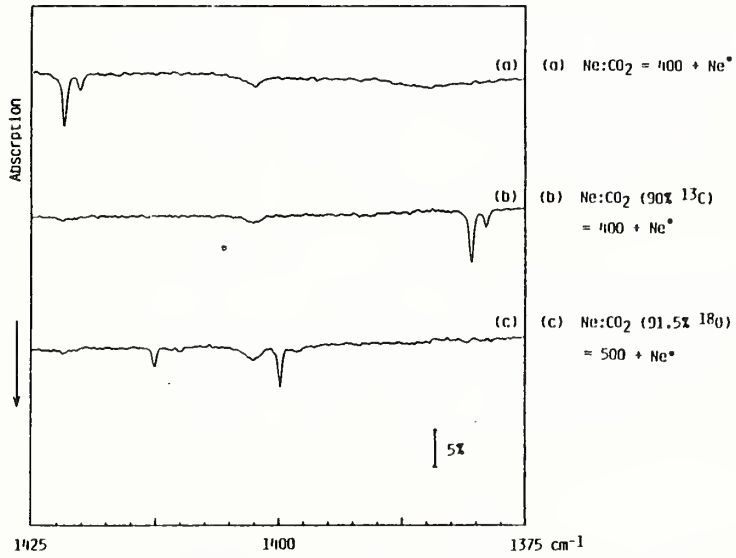

Fig. 2.26 Isotopically substituted CO_2^+ (ν_3) absorptions observed in solid neon.

In matrix isolation observations it is necessary for overall charge neutrality of the deposit to be maintained. Therefore, molecular anions must also be stabilized in these experiments. In the CO_2 experiments, an absorption appeared at 1658.2 cm^{-1} which had isotopic substitution behavior appropriate for assignment to ν_3 of CO_2^-. Earlier studies in this

laboratory of charge-transfer interaction between alkali metal atoms and CO_2 in an argon matrix had led to the identification of this fundamental of CO_2^- at 1608 cm^{-1} when sodium was used and at 1596 cm^{-1} when cesium was present in the sample. Because alkali metal atoms can diffuse through rare-gas matrices and must be quite close to the CO_2 molecule before charge transfer can occur, in the earlier experiments the CO_2^- was stabilized primarily at $M^+\cdots CO_2^-$. In the neon discharge experiments, the anion and cation concentrations are very small, and the molecular ions, which are trapped in random sites, cannot diffuse through the matrix. Therefore, it is believed that the position of the neon-matrix absorption of CO_2^-, 1658.2 cm^{-1}, most closely approximates the gas-phase band center.

A relatively broad absorption appears at 1402.4 cm^{-1} in all three of the traces of Fig. 2.26. This absorption, which is destroyed when photodetachment of electrons in the sample occurs, has tentatively been assigned to H_2O^+, formed from water desorbed from the walls of the sampling system. The ground-state bending fundamental of this important cation has been reported at 1408.4 cm^{-1} as a result of extrapolation of a long progression in this vibration in the optical emission spectrum. This value is consistent with that obtained in a study of the high resolution (ca. 2 cm^{-1}) photoelectron spectrum of H_2O. Observations on a $Ne:H_2O$ sample also yielded a product absorption near 3250 cm^{-1}, in the region in which the high resolution infrared absorptions of the two stretching absorptions of H_2O^+ were recently identified. Further experiments are planned in order to obtain a definitive assignment of the absorptions near 1402 and 3250 cm^{-1} and to establish the identity of the negatively charged species in the $Ne:H_2O$ system.

While new cation absorptions were not identified in these two experimental systems, the observation of peaks close to those of known cation absorptions demonstrates the utility of the sampling technique for producing molecular cations and supports the hypothesis that molecular vibrations of covalently bonded molecular cations, like those of free radicals, experience only small matrix shifts in solid neon.

Because O_3^+, O_4^+, O_3^-, and O_4^- are among the most important molecular ions in the D region of the ionosphere and because oxygen is frequently present as an impurity in samples used for cation formation, a series of experiments was conducted in which the excited neon was codeposited with a $Ne:O_2$ sample. As is shown in Fig. 2.27, several prominent absorptions were observed between 900 and 1400 cm^{-1} in this system. The peaks assigned to HO_2 and to NO_2^- are readily identified from previous studies of these species and are produced in the discharge because of the presence of trace impurities of water and nitrogen. The structured absorption near 1040 cm^{-1} is readily assigned to ozone, an expected product. Detailed isotopic substitution studies have provided further information on the identities of the carriers of the remaining absorptions. The prominent peak at 973 cm^{-1} can be assigned to O_4^-. Previous alkali metal codeposition experiments in this and other laboratories had determined values between 990 and 1000 cm^{-1} for this fundamental of O_4^-, stabilized as $M^+\cdots O_4^-$. Not shown in Fig. 2.27 is a moderately intense absorption at 976 cm^{-1}. This absorption lies very close to the peaks previously assigned in this laboratory to the antisymmetric stretching absorption of O_3^- in the various $M^+\cdots O_3^-$ species and has the isotopic substitution behavior appropriate for its assignment

to this fundamental of O_3^-. The isotopic substitution experiments indicate that the prominent peaks at 1164 and 1320 cm^{-1} are contributed by a single isomer of O_4^+ which has two pairs of equivalent oxygen atoms. Weak absorptions between 2600 and 2950 cm^{-1} are also contributed by O_4^+. Prior to these experiments, mass spectrometric studies had established that O_4^+ is bound by approximately 10 kcal/mol with respect to $O_2 + O_2^+$, but no infrared or ultraviolet spectrum had been detected for this important molecular cation. The two most probable structures for O_4^+ are a trans-bent chain or a rectangle. Further analysis of the isotopic data may determine which of these two structures is most appropriate.

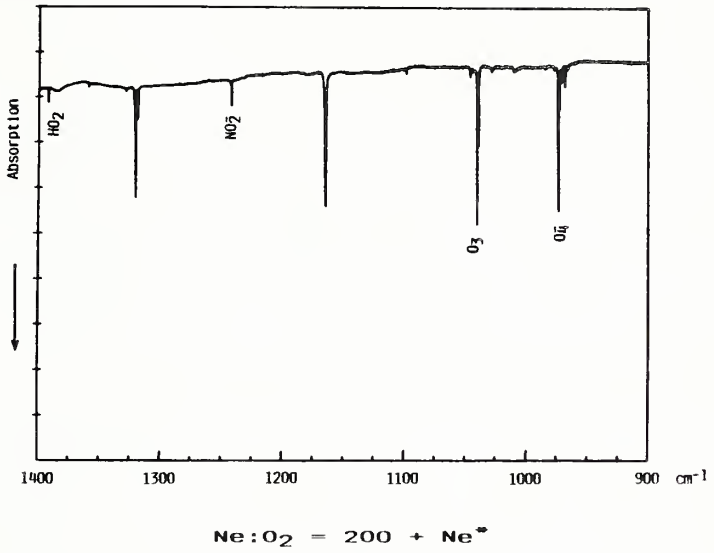

Fig. 2.27 Survey of major absorptions produced by the interaction of excited neon atoms with molecular oxygen.

3. Spectroscopy of Reaction Intermediates in Nitramine Decomposition and Combustion
(M. E. Jacox)

During the period from October 1, 1986 to June 15, 1987, this work was supported in part by the U.S. Army Research Office. The previously described studies on H_2CN and on t-HOCO were conducted as a part of this project. In addition, papers were prepared and published which present the first survey absorption spectrum for the near infrared electronic transition of HC_2 and a normal coordinate analysis for the CH_2NO_2 free radical.

4. Future Plans

a. Vibrational and Electronic Energy Levels of Transient Molecules
(M. E. Jacox)

During FY89 it is planned to complete the conversion of the vibrational frequency and electronic band center data to compiled dBase III+ files. The electronic spectral tables will continue to be updated, and a supplement to the 1984 ground-state vibrational energy level tables will be prepared for publication.

b. Free Radical and Molecular Ion Stabilization and Spectra
(M. E. Jacox and W. E. Thompson)

Before moving on to a more general study of the spectra of molecular cations, it is important to complete the characterization of molecular ions which can be derived from atmospheric molecules. In addition to being likely contributors to the spectra obtained for other samples, these ions are inherently important in the chemistry of combustion and of the terrestrial ionosphere. Like O_4^+, N_4^+ is known to be relatively stable. A search will be made for its spectrum. A search will also be made for ions derived from the various nitrogen oxides, including N_2O, NO, and NO_2.

It is of considerable interest to search for simple protonated species, such as H_2Cl^+, for which the two stretching fundamentals have recently been detected in the gas phase. If this species is identified in the matrix, attempts will be made to use a discharge through a Ne:HCl mixture and photodetachment of the proton from H_2Cl^+ as proton sources and to search for H_3O^+, the vibrational spectrum of which is quite well established. Since most molecules have proton affinities greater than that of HCl (135 kcal/mol), the successful conduct of these experiments would point the way to further studies which could yield previously inaccessible spectroscopic data for a wide variety of protonated molecules.

Because O (^1D) forms an excimer with argon, even though this species is often the primary product in photochemical O-atom generation its reaction products have been difficult to observe in an argon matrix. Published studies have indicated that O (^1D) does not react with a neon matrix, in which it has a lifetime of approximately 32 sec. It is of interest to study the 122-nm photolysis of CO_2 in a neon matrix since O (^1D), but not O (^3P), reacts with CO_2 to form CO_3. If a good yield of CO_3 is stabilized, studies of other O (^1D) reactions will be pursued. One of the early systems to be investigated would be O (^1D) + N_2O, a possible source of a chain NNOO structure which recent ab initio calculations have indicated may have a ground-state potential minimum.

c. Spectroscopy of Reaction Intermediates in Nitramine Decomposition and Combustion
(M. E. Jacox)

Most of the experimental studies described in the section entitled, "Free Radical and Molecular Ion Stabilization and Spectra" are also important in relation to the later stages of nitramine decomposition and combustion. However, an important part of the overall project on nitramine decomposition is an attempt to obtain the previously unreported spectrum of the nitramine monomer, $CH_2{=}N{=}NO_2$. The most suitable source of this species is likely to be the photodetachment of H_2 from monomethyl nitramine, CH_3NHNO_2, or of CH_4 from dimethyl nitramine, $(CH_3)_2HHO_2$. It has recently been reported that CH_4 is photodetached from a variety of amines on isolation in an argon matrix and exposure to 193 nm radiation. Thus, the use of the 185-nm mercury emission line for photolysis of these precursor molecules appears to be an especially promising route to the stabilization of $CH_2{=}N{=}NO_2$.

G. General Spectroscopy and Theory

In addition to the previously described programmatic activities a variety of research problems were pursued in response to special opportunities, and special interests of the staff and outside guest scientisits. The following are descriptions of such projects of a general nature.

1. The Ozonolysis of Ethylene. Microwave Spectrum, Molecular Structure and Dipole Moment of Ethylene Primary Ozonide (1,2,3-Trioxolane)
(R. D. Suenram, F. J. Lovas, J. Z. Gillies, and C. W. Gillies)

The gas phase structure of ethylene primary ozonide (CH_2CH_2OOO) has been determined from millimeter wave spectra of five isotopic species. Partial substitution, r_s, parameters for the lowest energy oxygen envelope conformation (C_s symmetry) are r(CC)=1.546(3)Å, r(CO)=1.417(10)Å, r(OO)=1.453(10)Å, $r(CH_{endo})$=1.088(5)Å, $r(CH_{exo})$=1.095(5)Å, Θ(CCO)=103.9(2)°, Θ(COO)=102.1(4)°, Θ(OCO)=100.1(12)°, and Θ(HCH)=111.6(3)° (see Fig. 2.28). The electric dipole moment of the normal isotopic species is 3.43(4)D. Two vibrational states, 98(6) and 171(18) cm^{-1} above the ground state, have been assigned to successive excitations of the pseudorotational mode which corresponds to a ring-twisting vibration of the five membered ring. The barrier to pseudorotation is estimated to be high (greater than 300 to 400 cm^{-1}) in agreement with ab initio MO calculations. Ethylene primary ozonide, dioxirane (CH_2OO), formaldehyde and ethylene secondary ozonide (CH_2OCH_2OO) are observed as products of the ozone ethylene reaction in the low temperature microwave cell. A mechanism of the ozonolysis of ethylene has been developed which suggests that the reaction occurs primarily in the condensed phase on the surface of the cell. Microwave techniques utilizing cis- and trans-CHD=CHD show that ozone adds stereospecifically to ethylene in the formation of ethylene primary ozonide.

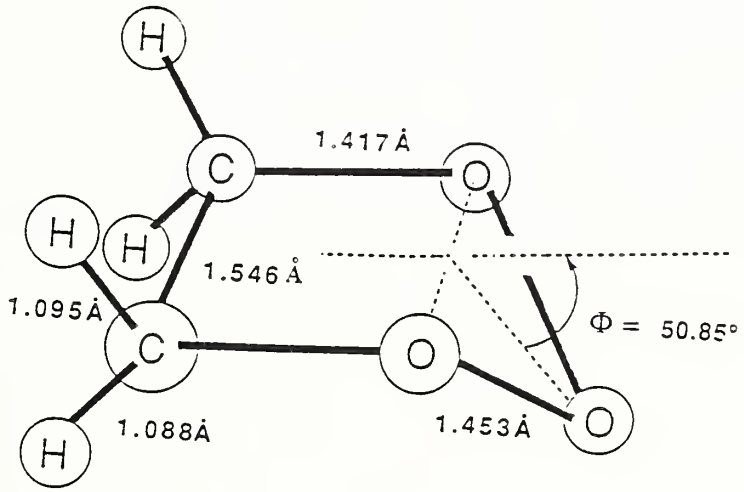

Fig. 2.28 Structure of ethylene primary ozonide.

2. Molecular Beam Studies of Larger Organic Species
(R. D. Suenram and F. J. Lovas)

In an effort to assess the feasibility of studying larger organic compounds with our pulsed molecular beam spectrometer we undertook the investigation of indole and carbazole. Both of these compounds are solids at room temperature and are fairly involatile. By placing samples of these compounds in our heated reservoir nozzle we were able to observe and assign the microwave spectra of both compounds. For indole, a nozzle temperature of 55°C with argon carrier gas proved to be adequate to produce intense rotational transitions. Carbazole was less volatile and required heating to 170°C to provide a sufficient quantity in the vapor phase to produce observable rotational transitions. For carbazole neon was used as the carrier gas instead of argon. Carbazole transitions were much weaker in argon presumably due to the formation of a significant fraction of higher polymers and complexes in the beam.

These studies, described below, have shown that the spectra of large organic molecules can be studied using a pulsed beam microwave spectrometer to simplify the spectrum. The study of carbazole by conventional technqiues would not be possible due to the large number of rotational transitions in the spectrum.

3. Microwave Spectrum and ^{14}N Quadrupole Coupling Constants of Indole
(R. D. Suenram, F. J. Lovas, and G. T. Fraser)

The microwave spectrum of indole has been observed using a conventional Stark-modulated microwave spectrometer in conjunction with a heated absorption cell. Spectral transitions were also observed in a pulsed molecular beam Fabry-Perot microwave spectrometer using a heated nozzle source. The high resolution (20 kHz) available with the Fabry-Perot instrument allows the observation of the ^{14}N nuclear electric quadrupole hyperfine splittings. An analysis of the 44 measured transitions gives the following rotational constants: A = 3877.8366(64) MHz; B = 1636.0461(48) MHz; and C = 1150.0900(19) MHz. The ^{14}N quadrupole coupling constants that were determined from the hyperfine analysis are eQq_{aa} = 1.7263(43) MHz; eQq_{bb} = 1.6525(50) MHz; and eQq_{cc} = $^{-}$3.3788(48) MHz. The observed rotational constants are compared with those obtained from a recent optical study of indole and the ^{14}N quadrupole coupling constants are compared with those of pyrrole. The accompanying figure (Fig. 2.29) illustrates the resolution of ^{14}N hyperfine structure for one of the observed rotational transitions.

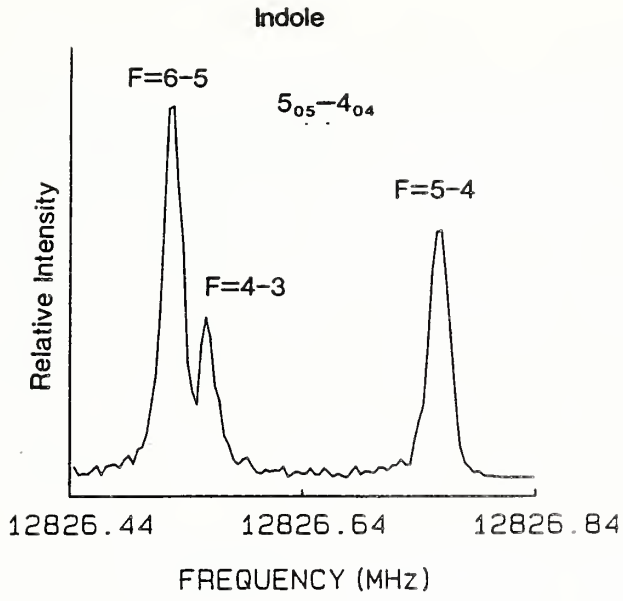

Fig. 2.29 A sample spectral window of indole in the adiabatic expansion showing the a-type 5_{05}-4_{04} rotational transition with its three most intense ^{14}N components. The F= 6-5 and F= 4-3 components are separated by ~30 kHz.

4. Microwave Spectrum and ^{14}N Quadrupole Coupling Constants of Carbazole
(R. D. Suenram, F. J. Lovas, G. T. Fraser, and P. S. Marfey)

The microwave spectrum of carbazole was observed and analyzed in the 8-14 GHz region using a pulsed molecular-beam Fabry Perot microwave spectrometer. Carbazole was vaporized in a heated nozzle source and was entrained in neon carrier gas before expansion into the Fabry Perot cavity. The rotational transitions were fitted using a rigid rotor Hamiltonian without centrifugal distortion parameters. The rotational constants are A = 2253.1985(2) MHz, B = 594.1861(2) MHz, and C = 470.3503(1) MHz. The inertial defect is small (-0.36 μÅ) and consistent with planar molecules.

The high resolution available with the instrument (~10 kHz) allowed the determination of the ^{14}N nuclear quadrupole coupling constants as χ_{aa} = 2.0697(40) MHz, χ_{bb} = 1.8719(35) MHz, and χ_{cc} = -3.9416(35) MHz. A comparison of the electronic environment of the nitrogen atom was made for the series pyrrole, indole and carbazole.

5. Quadrupole Hyperfine Splitting in the J = 1 ← 0 Rotational Transition of CCl_3F
(M. D. Marshall, H. O. Leung, and R. D. Suenram)

The hyperfine structure of the J = 1 ← 0 stransition of CCl_3F has been completely resolved for both K = 0 and K = 1 using a pulsed molecular beam Fabry-Perot cavity microwave spectrometer. Using previously available rotational constants[1] for this molecule it is shown that the hyperfine splitting is qualitatively, but not quantitatively predicted using the classic method of Wolf, et al.[2] and the effective hyperfine constants, eqQ_{zz} = 29.047 MHz and eqQ_{zz} - eqQ_{yy} = -110.95 MHz. To adequately describe

the nuclear quadrupole coupling interaction in this heavy, oblate symmetrical top molecule it is necessary to consider in addition to those matrix elements off-diagonal in the quantum number J those off-diagonal in K. Such matrix elements include not only additional ones arising from the $eqQ_{zz} - eqQ_{yy}$ term in the hyperfine Hamiltonian, but also those which find their origin in the usually ignored eqQ_{zy} term. The ability to measure this additional term will place more stringent limits on the assumption of cylindrical symmetry about the C-Cl bond.

1. J. H. Carpenter, P. J. Seo, and D. H. Whiffen, J. Mol. Spectrosc. 123, 187-196 (1987).
2. A. A. Wolf, Q. Williams, and T. L. Weatherly, J. Chem. Phys. 47, 5101-5109 (1967).

6. Millimeter- and Submillimeter-wave Surveys of Orion A Emission Lines in the Ranges 200.7-202.3 GHz, 203.7-205.3 GHz, and 330-360 GHz
(P. R. Jewell, J. M. Hollis, F. J. Lovas, and L. E. Snyder)

We have conducted a continuous spectral line survey of the Orion A position from 330.5 to 360.1 GHz. This survey covers nearly the entire 870 μm atmospheric window accessible from ground-based observations. Approximately 160 distinct spectral features composed of about 180 lines were detected, 30 of which could not be readily identified. In addition, we also surveyed Orion A from 200.7 to 202.3 GHz and from 203.7 to 205.3 GHz and detected 42 distinct, new spectral lines, including 4 that are unidentified at present. These data sets are the first thorough survey results in these spectral regions. Twenty of the known Orion A molecular species, including less abundent isotopic forms of several species, have been identified in the 870 μm survey. The largest percentage of transitions observed are attributed to SO_2 and CH_3OH. Previous surveys at 3mm and 1.2mm showed a high percentage of transitions from $HCOOCH_3$ for which only 6 transitions were identified in the present work. The data are being made available to the Astronomical Data Center at the Goddard Space Flight Center for distribution-by-request to the astronomical community.

7. Instrumental Studies for the BOMEM FTS
(W. B. Olson)

Considerable effort has been made to formulate a practical treatment of throughput or etendue in optical systems of cylindrical symmetry for the purpose of designing of optical systems of very high efficiency for the NIST BOMEM FTS. Ray transfer matrices can provide a first order solution to the problem of throughput matching of the optical subsystems required for sampling, but difficulties arise in precise interpretation when it comes to the execution of the design in practice. There are some areas of practical application where the ideal solution in terms of ray transfer matrices cannot be well translated into practice with quadric section type optical elements. These difficult areas lie in regions where the ideal solutions require a large solid angle subtended at some plane by the radiation. Non-imaging optical systems can provide a solution to this problem in principle, but in practice they are not perfect either, and it does not seem possible to derive analytical equations for actual efficiency.

Extensive three dimensional ray tracing has been done on White type multiple reflection absorption cells with two rows of images in the front mirror focal plane, and it has been found that there is a ratio of total width of the spots on the front focal plane to the separation of the two rows where optical aberrations nearly disappear.

A heat pipe of nickel has been devised and constructed for the heat pipe optical system of the BOMEM FTS. This should allow the use of high temperature fluorides in the heat pipe, which attack the current stainless steel heat pipes.

8. Analysis of the 3-μm Bands of Benzene
(J. Pliva and A. S. Pine)

A comprehensive rovibrational analysis was performed for the 3-μm absorption bands of the benzene molecule measured on a difference-frequency laser spectrometer and deconvolved to an effective linewidth of 0.0010 - 0.0015 cm^{-1}. The four strong bands observed, centered at 3047.908, 3078.614, 3100.408, and 3101.854 cm^{-1}, are due to the E_{1u} fundamental ν_{12} sharing its intensity with the E_{1u} components of the combinations $\nu_{13} + \nu_{16}$, $\nu_2 + \nu_{13} + \nu_{18}$, and $\nu_3 + \nu_{10} + \nu_{18}$ via anharmonic resonances. The bands exhibit strong perturbations due to ℓ resonances with the inactive B_{1u}/B_{2u} components of the $\nu_{13} + \nu_{16}$ and $\nu_2 + \nu_{13} + \nu_{18}$ states, and numerous localized perturbations due to overtones and combinations of the 16 low-frequency vibrations of the molecule. Symmetry arguments and values of constants such as $C\zeta$ known for the fundamentals have been used to propose tentative assignments for many of the perturbing states. The Hamiltonian matrix used for the treatment of the 8384 assigned transitions, with all the components of the main interacting states plus 18 perturbing states, was of order 34 and contained 130 parameters of which 112 were eventually adjusted. A set of spectroscopic constants was obtained which reproduces all the data with a standard deviation of 0.0012 cm^{-1}. The analysis shows that the Fermi resonance between ν_{12} and $\nu_{13} + \nu_{16}$ combined with the other anharmonic interactions shifts the fundamental down by 16.46 cm^{-1} from its unperturbed position. It was found that x,y-Coriolis and anharmonic resonances of surprisingly high order have to be invoked to account for most of the localized perturbations observed in the spectrum.

9. Influence of an AC Stark Effect on Multiphoton Transitions
(W. L. Meerts, I. Ozier, and J. T. Hougen)

A multiphoton mechanism for molecular beam transitions was developed which relies on a large first-order AC Stark effect to modulate the energy separation of the initial and final states of the multiphoton transition, but which does not require the presence of any intermediate level(s). The theoretical formalism uses ideas from the laser multiphoton literature for a two-level system interacting with a monochromatic electromagnetic radiation field, together with a close analog of the rotating wave approximation. The diagonal matrix elements of the Hamiltonian operator corresponding to the large AC Stark effect are removed by a mathematical substitution which in effect transforms these diagonal elements into transition moments involving higher harmonics of the frequency of the monochromatic radiation field. The electric field strength of the true

monochromatic radiation field is "distributed" among the higher harmonics of the effective field according to an expression involving Bessel functions. Because these Bessel functions are bounded, there exists a threshold for the magnitude of the transition dipole matrix element coupling the two levels. Below this threshold, the transition probability in a traditional one-photon molecular beam electric resonance experiment cannot be made unity simply by increasing the amplitude of the radiation field. In fact, if the coupling matrix element is small enough, the molecular beam electric resonance signal will become unobservable. The algebraic formalism described above was checked by computer solution of an initial value problem involving four real coupled linear differential equations. It was then used to explain the multiphoton transitions previously observed in molecular beam electric resonance studies on the two symmetric top molecules OPF_3 and CH_3CF_3 where the number of photons involved in a given transition varies from 2 to 40.

10. Far Infrared Spectrum of Methyl Amine. Assignment and Analysis of the First Torsional State
(N. Ohashi, K. Takagi, J. T. Hougen, W. B. Olson, and W. J. Lafferty)

The far-infrared spectrum of methyl amine has been studied in the 40 to 350 cm^{-1} region with a resolution of 0.005 cm^{-1} or better. The pure rotational spectrum in the first excited torsional state, as well as the fundamental torsional band, have been assigned. The data obtained have been combined with microwave data from the literature, and a global fit has been carried out, based on a group theoretical formalism developed previously. Over 650 transitions with $0 \leq K \leq 14$ and $K \leq J \leq 25$ were fit to 41 molecular parameters, with a standard deviation of $\pm 0.000\ 94$ cm^{-1}. This standard deviation was achieved by including J and K dependent (centrifugal distortion) corrections to the structural parameter ρ. The goodness of the fit confirms the correctness of the theoretical formalism. Problems remaining presumably arise from the neglect of five tunneling and nontunneling terms with selection rules $\Delta K = \pm 1$. Some aspects of the torsional potential function and inversion potential function in this molecule were also considered.

11. Effect of Tunneling Motions on the Hyperfine Structure of Hydrazine
(L. H. Coudert, J. T. Hougen, and R. D. Suenram)

In the present work, we attempt to describe the hyperfine structure in a molecule which exhibits significant tunneling splittings because of large amplitude inversion and internal rotation motions, but which still has a well defined equilibrium configuration. The approach involves setting up a complete quadrupole Hamiltonian for the two nitrogen atoms in hydrazine (NH_2-NH_2), which is made dependent upon the three large amplitude coordinates necessary to fully describe the various configurations of the molecule, and which contains all five elements of the electric field gradient tensor (i.e., $2q_{aa} - q_{bb} - q_{cc}$, $q_{bb} - q_{cc}$, q_{ab}, q_{ac}, and q_{bc}) at one nitrogen atom when the molecule is in one of its equilibrium configurations. The mean value of this quadrupole operator is calculated for each tunneling state. One interesting result is that for nondegenrate A or B-type levels only the sum of the two hyperfine Hamiltonians is involved, while for doubly degenrate E-type levels the sum as well as the

difference appears. The difference contains the contribution of the non-diagonal term q_{bc}, and leads to large qualitative differences in the hyperfine pattern. These results are applied to the analysis of the hyperfine structure of selected transitions that have been recorded on the NIST Fourier transform microwave instrument. After a preliminary analysis of the hyperfine structure of each transition separately, a least square fit global analysis of the data was performed. This allowed us to determine the two diagonal quadrupole coupling constants as well as the bc nondiagonal one.

12. A Two Tunneling Path IAM-Like Treatment of the Microwave Spectrum of Divinyl Ether
(L. H. Coudert)

The microwave spectrum of the cis-trans conformer of divinyl ether, previously measured by Hirose and coworkers, has been fit using a two-dimensional IAM-like treatment which accounts for the 27 MHz tunneling splitting displayed by this molecule. This two-dimensional IAM-like treatment begins by first determining the various feasible tunneling path(s) connecting the two frameworks of the molecule. For the tunneling process corresponding to an antigeared rotation of each vinyl unit about axes coinciding with the respective CO bonds, two limiting cases are considered: if the molecule goes through a planar configuration during the tunneling, only one tunneling path arises; if the intermediate configuration is not planar, two equivalent tunneling paths occur. The consequences for the J and K dependence of the splitting are examined, and using this formalism the microwave data are fitted with an RMS deviation of 0.156 MHz. The parameters related to the J and K dependence of the splitting were also determined and their values are interpreted in a favor of a two tunneling path system. A comparison with the values obtained theoretically for those parameters was also carried out.

13. WKB Potential Well Ground States without Matching?
(C. Leubner and J. T. Hougen)

Schmid[1] has recently conjectured that it might be possible in general to obtain semi-classical (WKB) ground state energies and wavefunctions for various potential surfaces without explicitly considering the problem of how wavefunctions obtained separately in the classically allowed and classically forbidden regions are to be matched across the boundary between those regions. We showed by formally expanding the energy as a power series in $\hbar$ in the usual WKB equations, that even in the one-dimensional case, Schmid's procedure yields an approximate ground state wavefunction only for potential wells which are nearly harmonic, and that the corresponding energy obtained is totally insensitive to any anharmonicity present. Furthermore, excited state wavefunctions cannot be obtained at all. Thus, despite its inherent simplicity, Schmid's method can only be of limited value in the analysis of the dynamics of real molecules on multi-dimensional potential surfaces.

---

1. A. Schmid, Ann. Phys. (NY) 170, 333 (1986).

14. Measuring Transition Moments by Means of the Herman-Wallis Effect (A. G. Maki and W. B. Olson)

In a recent study we made on using the Herman-Wallis effect to measure the transition moment of the fundamental band of ClO, it became apparent that this is a technique that has general applicability to diatomic molecules. It is not generally recognized that the theory has been well studied and the formulas for describing the Herman-Wallis effect take into account higher order terms both in the dipole moment function and also in the Dunham potential function. The Herman-Wallis effect relates the ratio of the transition moment divided by the dipole moment to the relative intensity of $\Delta J=+1$ and $\Delta J=-1$ transitions. To determine the transition moment it is necessary to know the dipole moment and a few other molecular parameters, but it is not necessary to know the number of molecules in the sample. In many cases it is extremely difficult to obtain an accurate measure of the partial pressure of the species of interest, but it is much easier to obtain the parameters needed to analyze the Herman-Wallis effect.

We are determining the Herman-Wallis effect from FTS infrared measurements on three different molecular species, LiH, NaH, and NaI. An example of this effect for NaH is shown in Fig. 2.30. Without the Herman-Wallis effect the two transitions shown would have the same intensity, to within 5%. In Table II we show the results found for NaH. A test of this technique on HF and HCl has shown that the transition moment obtained by application of this technique is within 1% of the value obtained by direct intensity and concentration measurements.

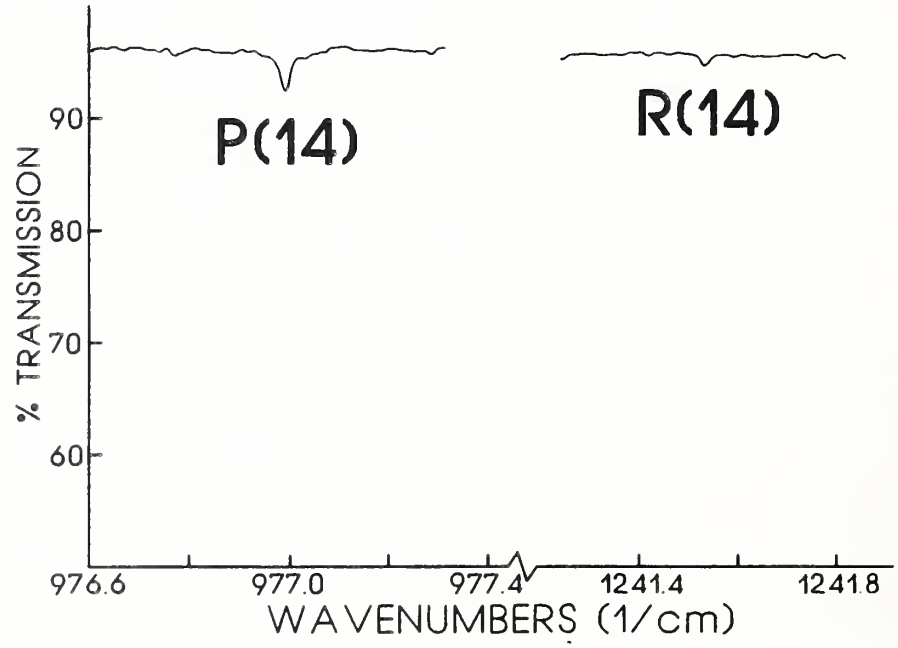

Fig. 2.30 Comparison of the relative intensities of the P(14) and R(14) lines the v=1←0 transition of NaH.

Table II. Relative Intensity Measurements and Estimated Transition Moment for the v=1-0 Transition of NaH

J	Obs. $\frac{S[R(J)]}{S[P(J)]}$	Obs.-Calc.
5	0.878	0.077
6	0.777	0.058
7	0.682	0.033
8	0.589	0.004
9	0.499	-0.028
10	0.405	-0.068
11	0.383	-0.039
12	0.323	-0.051
14	0.335	0.053

α = -0.046 ± 0.003[a]
β = 0.0[b]
μ_{10} = 0.31 ± 0.05 Debye
(assuming μ_0 = 6.6 D)

a) The uncertainty is three times the standard error.

15. The Vibrational Dependence of the Transition Moment
(A. G. Maki and W. B. Olson)

Simple harmonic oscillator theory says that the intensity of $\Delta v=1$ transitions should depend on $v''+1$ while $\Delta v=2$ transitions should have intensities that depend on $(v''+1)^2$. In a number of high temperature measurements we have qualitatively observed that this vibrational dependence is approximately correct, but conditions were never good enough to test this theory. In recent FTS measurements on the high temperature spectrum of NaI we have observed transitions from v=1←0 up to v=13←12. Since the Fourier transform spectrometer measures all wavelengths at the same time, it is particularly well suited for comparing the intensities of different transitions measured in the same interferogram. Our measurements verify the applicability of the harmonic oscillator treatment to within 5 or 10%, at least for this one case. We have good reason to believe this will be true for most other molecules.

16. An FTS Measurement of the Rotational Spectrum of LiH and LiD
(A. G. Maki and W. B. Olson)

For several years we have been measuring the high temperature infrared spectrum of diatomic molecules that are unstable in the gas phase at room temperature. Some of the species that we have studied have rather large dipole moments and small moments of inertia, making them good candidates for producing far-infrared pure rotational spectra. We have now measured the rotational spectra of LiH and LiD from 100 to 285 cm^{-1}. Transitions have been observed for both ^{6}LiD and ^{7}LiD in the v=0, v=1, and

v=2 states. Fig. 2.31 shows a segment of the pure rotational spectrum of a mixture of ^{6}LiD and ^{7}LiD.

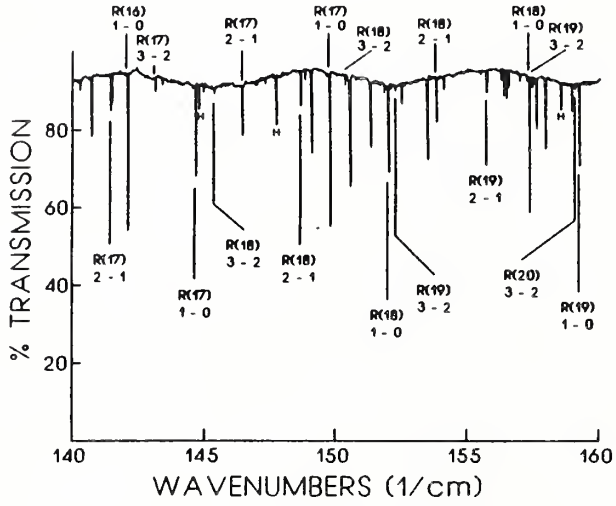

Fig. 2.31 Rotational transitions of a mixture of ^{6}LiD and ^{7}LiD from 140 to 160 cm^{-1}. Transitions labeled below the spectrum are due to ^{7}LiD and those labeled above the spectrum are due to ^{6}LiD. Lines due to LiH are indicated by an H. All other lines are due to H_2O.

17. High Temperature FTS Measurements
(A. G. Maki, W. B. Olson, G. Thompson, and A. Weber)

We have extended to longer wavelengths our high temperature measurements of the infrared spectrum of molecules unstable in the gas phase at room temperature. The BOMEM Fourier transform spectrometer (FTS) has been used to record a number of high temperature spectra in the 100 to 400 cm^{-1} region. Aside from the pure rotational spectrum of LiH and LiD mentioned above, we have measured the following spectra: KI ($\nu_0 \approx 185$ cm^{-1}), NaI ($\nu_0 \approx 255$ cm^{-1}), and TℓCℓ ($\nu_0 \approx 280$ cm^{-1}). The analysis of the TℓCℓ spectrum was more difficult because of the two thallium isotopes and the two chlorine isotopes. High resolution was essential to the measurement and analysis of these spectra.

In addition, the spectrum of NaH was measured in the 900 to 1300 cm^{-1} region. This spectrum was used to determine the transition moment of NaH from the Herman-Wallis effect, as was described above.

18. Analysis of the Infrared Spectrum of the BO_2 Radical
(A. G. Maki, J. Burkholder, C. J. Howard, and A. Sinha)

The absorption spectrum of BO_2 in the ground state, $X^2\Pi_g$, has been measured in the infrared with a high-resolution Fourier transform spectrometer. The 00^01-00^00 and 10^01-00^00 vibrational transitions have been measured for both the $^2\Pi_{1/2}$ and the $^2\Pi_{3/2}$ states. Because of the large number of vibronic levels arising from the Renner-Teller effect, there is a high likelihood of observing level crossings in this molecule and three examples of perturbations in these states are described. Improved ground state constants are reported.

19. Doppler Broadening of Raman Lines
(A. Weber)

For the purpose of determining molecular energy levels high resolution Raman spectroscopy is conducted on low pressure gases and vapors to avoid line shifts caused by velocity and phase changing collisions. Under these conditions Dicke narrowing is absent and the resolution is limited by Doppler broadening of the spectral lines, as well as instrumental effects such as the width of the exciting line and the characteristics of the spectrometer system. Conventional high resolution Raman spectroscopy of gases has reached a resolution limit of ca 0.05 cm^{-1}; this limit was, however, determined in the main by instrumental effects.

The use of currently available scanning Fourier transform spectrometers offers the possibility of achieving a nearly 10-fold improvement in the instrumental resolution capability. However, to realize such resolution in incoherent Raman scattering it is essential that line broadening effects due to the Doppler effect be minimized. A recalculation of the Doppler broadening using the laws of conservation of energy and linear momentum in their relativistic formulation gives, to a very high degree of approximation, the same result as that obtained non-relativistically. Thus, the Doppler broadened Raman linewidth (FWHM) is given by

$$\delta\nu_R = \sqrt{2\ell n2(kT/m_0c^2)}\ \sqrt{4(\nu_0^2 - \nu_0\nu_R)\sin^2(\theta/2) + \nu_R^2} \qquad (1)$$

where $\nu_R = \nu_0 - \nu_{scatt}$ is the Raman displacement ($\nu_R>0$ for Stokes scattering, $\nu_R<0$ for anti-Stokes scattering, ν_{scatt} = frequency of scattered photon) and θ is the scattering angle. The calculation also yields a term that describes a velocity dependent Raman line shift due to the recoil experienced by the molecule in the scattering process.

When combining Raman spectral data with those obtained by infrared absorption spectroscopy in a unified analysis of the molecular energy levels it is desirable to have a quantitative estimate of the quality of the Raman data relative to the data obtained by infrared spectroscopy. Figure 2.32 shows the ratio $\delta\nu_R/\delta\nu_{IR}$ as a function of scattering angle,

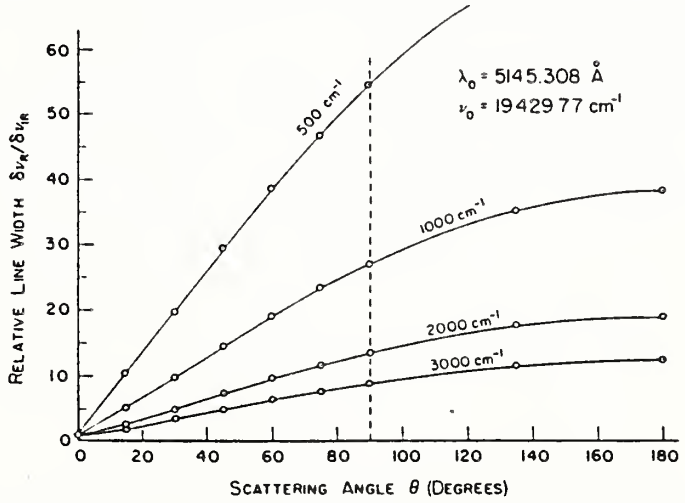

Fig. 2.32 Ratio of Raman to infrared Doppler line widths for Stokes Raman displacements of 500, 1000, 2000, and 3000 cm^{-1}.

where $\delta\nu_R$ is the Raman Doppler line width given by Eqn. (1) and $\delta\nu_{IR}$ is the Doppler line width for an infrared absorption line of the same frequency (wave number), for Stokes Raman displacements of 500, 1000, 2000, and 3000 cm^{-1} generated by the Ar 5145Å laser line. The Doppler widths of the Raman and infrared lines are seen to be equal only for the "forward" scattering configuration ($\theta=0°$). When Raman frequencies obtained with scattering arrangements with $\theta>0$ are to be combined with infrared data they should be weighted, for equal signal to noise ratios, at least by the inverse square of their relative Doppler widths. This weight would have to be augmented by additional factors which account for other causes of line broadening (e.g., pressure effects). Eqn. (1) gives the Doppler width of a Raman line for a static gas in thermodynamic equilibrium. It is equally applicable to incoherent as well as to coherent Raman scattering (but not CARS). In coherent Raman gain spectroscopy, however, the "forward" scattering geometry is automatically assured as part of the usual experimental configuration.

20. High Resolution Spectroscopic Studies of CH_2F_2: The ν_8 Band at 1435 cm^{-1}
(R. D'Cunha, P. K. Wahi, V. B. Kartha, and A. Weber)

Fourier transform infrared spectra of methylene fluoride were recorded with the NIST BOMEM DA3.002 spectrometer with an apodized resolution of 0.004 cm^{-1}. Detailed assignments up to $J_{max} = 25$ have been made for the ν_8 parallel A type band centered at 1435 cm^{-1}. Watson's A type reduced Hamiltonian in the I^r representation was used to obtain upper state molecular parameters. These reproduce the observed data to within the limits of the experimental accuracy.

3. MOLECULAR DYNAMICS GROUP

M. P. Casassa, L. B. Elwell, B. R. Foy, E. J. Heilweil, D. S. King, J. C. Stephenson, Molecular Spectroscopy Division

and

J. D. Beckerle, S. A. Buntin, R. R. Cavanagh, and L. J. Richter
Surface Science Division

A. Condensed Phase Energy Transfer

B. Decomposition of Molecules from Metastable Vibrational States

1. Overtone Photodissociation of Molecules: HN_3

2. Dynamics of van der Waals Molecules: $(NO)_2$

C. Molecular Desorption from Surfaces

This group primarily performs quantum-state specific studies of molecular dynamics. A common factor in the research described below is the role of energy transfer in the spectroscopy and kinetics of molecules. Research on molecular dynamics of molecules on surfaces is done in collaboration with the Surface Science Division.

A. Condensed Phase Energy Transfer

(J. D. Beckerle, M. P. Casassa, R. R. Cavanagh, E. J. Heilweil, and J. C. Stephenson)

We have used picosecond lasers to measure the vibrational population relaxation times (T_1) for the CO (v=1) stretching modes ($\nu \approx 2000$ cm^{-1}) of carbon monoxide bound to metal atoms. Data were obtained for (1) metal carbonyl molecules, general formula $M_x(CO)_y$, in room temperature CCl_3H and CCl_4 solutions; (2) $M_x(CO)_y$ molecules supported on a SiO_2 surface; (3) CO chemisorbed on large (ca. 30 Å diameter) Pt and Rh metal clusters on a SiO_2 support. We expected, based on theory and on our earlier experimental results, that $M_x(CO)_y$ species with a small number of metal atoms in the metal core would exhibit long T_1 times characteristic of multiphonon relaxation to lower frequency molecular modes. However, for larger metal cores, a different and more efficient relaxation mechanism, coupling of the vibrational energy to metal conduction electrons (electron-hole pair damping), was theoretically predicted to dominate and give rise to much shorter T_1 lifetimes. Our experiments support these expectations.

As in our earlier experiments, we used a one color picosecond (ps) infrared (ir) transient bleaching method to determine T_1. A tunable ir pulse is generated as the difference frequency between two ps visible laser pulses. Resonant with the CO v=0 → v=1 transition, each pulse is split into a pump (> 99%) and weak probe (< 1%), which is delayed in time with respect to the pump. The pump partially saturates the v=0 → v=1 absorption of the sample, causing a transient increase in sample transmission. The change in absorbance, which is proportional to the population in CO(v=1), is monitored by the weak probe pulse. The measured absorbance change vs. pump-probe time delay (t_D) gives the characteristic population decay time for the excited mode: $CO(v=1) \propto \exp(-t_D/T_1)$.

The transition-metal carbonyl molecules $Rh_2(CO)_4Cl_2$, $Rh_4(CO)_{12}$, $Co_4(CO)_{12}$, and $Rh_6(CO)_{16}$ in chloroform solution all showed very long relaxation times for the high frequency CO stretching modes. Specifically, T_1 was the same for the B_1(2092 cm^{-1}, 710 ± 130 ps) and B_2(2036 cm^{-1}, 750 ± 90 ps) modes of $Rh_2(CO)_4Cl_2$, and T_1 was also long for $Rh_4(CO)_{12}$ (2075 cm^{-1}, 610 ± 65 ps) and $Rh_6(CO)_{16}$ (2077 cm^{-1}, 700 ± 100 ps). $Co_4(CO)_{12}$ (2068 cm^{-1}) exhibited a fast decay (47 ± 5 ps) followed by a slow decay (400 ± 70 ps). In all these molecules the vibrational frequencies (except the CO stretches) are very low: MCO bends ≈ 550 cm^{-1}; M-C stretches ≈ 450 cm^{-1}; M-M modes ≈ 110-120 cm^{-1}. Therefore, when a CO(v=1) mode relaxes at least 4 quanta must simultaneously be created in these lower frequency modes to conserve energy. These high order multiquantum processes are theoretically expected to be improbable, which is why T_1 is so long (40,000 CO vibrational periods) for these molecules. The fast (47 ps) relaxation in $Co_4(CO)_{12}$ probably arises from fast coupling of the pumped mode with

other CO stretching modes in the molecule, followed by the slower (400 ps) decay of the coupled CO stretches to the lower frequency molecular modes.

In a related study of the molecule $Rh(CO)_2(C_5H_7O_2)$, the same T_1 was measured for the symmetric (2084 cm^{-1}, 90 ± 10 ps) and antisymmetric (2014 cm^{-1}, 87 ± 10 ps) metal carbonyl modes. That these T_1 times are shorter than those for more complicated molecules like $Rh_6(CO)_{16}$ suggests that vibrational energy flows (across the Rh atom) in a nearly resonant process to the CO modes of the 2,4-pentanedionate ligand (ν=1553, 1513 cm^{-1}).

When the molecules $Rh_2(CO)_4Cl_2$ (2096 cm^{-1}, 180 ± 39 ps; 2040 cm^{-1}, 187 ± 19ps), $Co_4(CO)_{12}$ (2070 cm^{-1}, 98 ± 11ps), and $Rh_6(CO)_{16}$ (2084 cm^{-1}, 173 ± 34 ps) are chemisorbed on a silica (SiO_2) surface (in vacuum), the relaxation times for the CO stretching modes are decreased by a factor of 4 compared to the results in CCl_3H solution. This increase in rate demonstrates the importance of vibrational energy transfer from CO(v=1) to create two quanta in the 1000 cm^{-1} Si-O stretching modes of the substrate.

As in our earlier studies, we find no correlation between measured T_1 lifetimes and the total density of molecular vibrational states in these molecules. T_1 is the same for $Rh_2(CO)_4Cl_2$ and $Rh_6(CO)_{16}$ while $\rho(E_{vib})$ of the states pumped by the laser increases from 10^{11} to 10^{36} states/cm^{-1}. There is also no correlation between ir spectral bandwidths and T_1. The uncertainty principle broadening associated with a 100 ps lifetime is only 0.05 cm^{-1}, which is negligible compared to the observed 10 cm^{-1} absorption bandwidths.

It was also discovered that the decay data are sensitive to IR frequency and pump pulse fluence. Anomalous T_1 decays and transient absorptions can be observed if the pulse bandwidth overlaps higher overtone transitions (the metal-carbonyl anharmonicity ranges from 10-20 cm^{-1}). This is avoided by using carefully chosen high frequency and low power pump pulses.

To probe the relaxation of CO(v=1) bound to larger metal particles, metal clusters were prepared by reducing Rh and Pt salts supported on SiO_2. Transmission electron microscopy (TEM) measurements of these particles of poorly defined shape indicated mean particle diameters of 35 ± 6Å (Rh ≈ 1600 atoms) and 20 ± 10Å (Pt ≈ 400 atoms). $CO/Rh/SiO_2$ samples exhibit characteristic CO absorption features which originate from the same species as $Rh_2(CO)_4Cl_2$ directly deposited on SiO_2 plus a broad band associated with CO adsorbed on large metal particles. Transient IR experiments were performed on these bands first using 20 ps FWHM infrared pulses. Two features arising from $Rh_2(CO)_4$ type surface species yielded a T_1 = 140 ± 20 ps (compared to ~180 ps for directly deposited $Rh_2(CO)_4Cl_2$) while metal-CO particle absorption produced nearly pulse-width limited decays with $T_1 \leq$ 20 ps as an upper limit. These results indicate that CO relaxes at drastically different rates when adsorbed on various sites in these types of inhomogeneously distributed "catalyst" samples. Pt/SiO_2 samples, however, exhibit only a single broad CO-particle absorption and give a similar limiting value for T_1.

The short time behavior of the CO-particle relaxation was further explored using IR pulses of 2 ps duration (FWHM). Fig. 3.1 shows a decay for one Pt sample; Rh gave a similar response. This initial decay indicates a lifetime of approximately 7.5 ps. The fast rise and immediate fall of the signal indicate T_1 contributions of less than 7 ps may still be present. Related measurements using much shorter IR pulses are needed to resolve the short time behavior.

This dramatic increase in relaxation rate, by about a factor of 15 compared to the Rh carbonyl compounds supported on SiO_2, can not be due to multiphonon relaxation to lower frequency vibrational states. The enhanced rate presumably arises from coupling to electronic degrees of freedom of the large metal particles, i. e., electron-hole pair damping. Short T_1 values (≈1 ps) have been estimated theoretically for adsorbates on metal single crystal surfaces due to this damping mechanism.

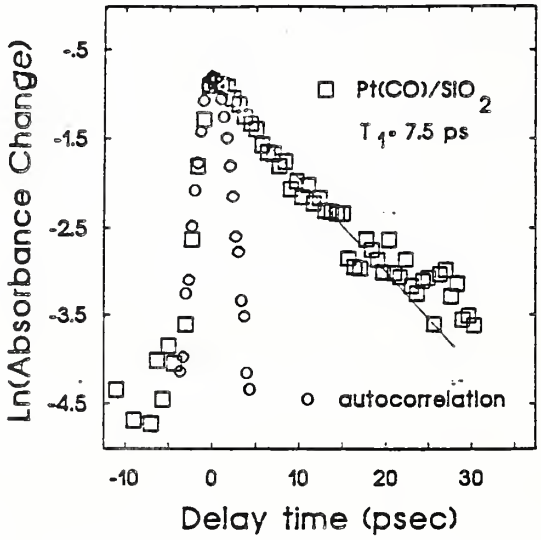

Fig. 3.1 Time dependence of the ir transient bleaching signal (ν_{laser}=2090 cm^{-1}) for CO chemisorbed on Pt particles (d ~ 30Å) supported on SiO_2 at T=20°C. Also shown is laser pulse autocorrelation, indicating experimental time resolution.

During the next year we plan to focus on two goals. We will try to directly measure where the vibrational energy goes when the initially excited CO(v=1) mode is deactivated. For metal carbonyl molecules in the gas phase, in solution, and on dielectric surfaces we intend to probe transient populations in other ir active modes by time-resolved two color ir absorption spectroscopy. There are several picosecond and femtosecond laser techniques that we are investigating in order to accomplish this goal, including direct ir absorption, and broadband ir absorption followed by up-conversion to the visible spectral region with multichannel detection. For strong Raman active modes such as M-C stretches, spontaneous anti-Stokes Raman scattering may also be useful for detecting transient low frequency vibrational populations.

The second goal is to measure T_1 for an ordered monolayer of CO on a metal single crystal prepared and characterized under UHV conditions. Interpretation of T_1 results on a single crystal are expected to be more

straightforward and unambiguous than the interpretation of the transient bleaching signals for the polydisperse inhomogeneous supported metal particles discussed above.

This research is supported in part by the Air Force Office of Scientific Research.

B. Decomposition of Molecules from Metastable Vibrational States
(M.P. Casassa, B.R.Foy, D.S.King, and J.C. Stephenson)

1. Overtone Photodissociation of Molecules: HN_3

State-to-state photodissociation experiments provide an exceptionally detailed view of the dynamics of rovibrationally excited molecules, and have particular significance when complemented by high resolution photodissociation spectra and linewidth data. We have measured nascent distributions of kinetic, vibrational, and rotational energy, along with unimolecular decomposition rates and photodissociation spectra for the collision-free laser-induced reactions:

$$HN_3\ (X\ ^1A') \longrightarrow HN\ (X\ ^3\Sigma^-) + N_2\ (X) \qquad \Delta H = 15\ \text{kcal/mol},$$
$$\longrightarrow HN\ (a\ ^1\Delta) + N_2\ (X) \qquad \Delta H = 51\ \text{kcal/mol}.$$

An important feature of this system is that the minimum enthalpy channel is spin-forbidden, with a 36 kcal activation barrier to singlet-triplet crossing. The reactions were initiated in two different ways. Direct single-photon excitation of the 4th and 5th NH-stretching overtone transitions of HN_3 populated individual rovibrational states with sufficient energy to decompose via the triplet (spin-forbidden) channel. The second type of experiment used multiphoton pumping (IRMPD) of DN_3 by a CO_2 laser, which produced both singlet and triplet products.

The measurements were performed using low pressure HN_3 or DN_3 samples in a flow cell, and using HN_3 cooled in a supersonic expansion. The 10ns duration overtone pump laser operated at 575 (v_1=6←0) or 662 nm (v_1=5←0) with a spectral bandwidth ≈0.4 cm^{-1}. In experiments with higher resolution, this laser produced a ≈0.03 cm^{-1} bandwidth. The IRMPD experiments employed a CO_2 laser with temporal "square wave" pulses of 50 ns duration focussed to I=10GW/cm^2. Most product state data were obtained with the CO_2 P(18) laser line at 946 cm^{-1}. The HN/DN fragments were probed by laser-induced fluorescence of the $A^3\Pi$ - $X^3\Sigma^-$ or $c^1\Pi$ - $a^1\Delta$ transitions using a frequency-doubled dye laser with a bandwidth of 0.7 cm^{-1} (etalon-narrowed to 0.05 cm^{-1} for the measurement of Doppler profiles). For lifetime measurements of the v_1=5 level, the time delay between pump and probe was stepped electronically in 1 ns increments. To measure the lifetime of the v_1=6 state, picosecond lasers were used, as in our earlier work on the vibrational predissociation lifetime of the NO dimer.

The experimental observations yield information about the distribution of energy in the reactant, the microscopic reaction rates, the location of barriers to dissociation, and the geometry of the transition states. Excitation of the NH-stretching overtone transitions of HN_3 to v_1 = 5 and 6 resulted in predissociation to $HN(X^3\Sigma^-)$ and $N_2(X)$ with lifetimes of 210 ± 110 and 1.0 ± .2 ns, respectively (see Fig. 3.2). Following

excitation of either overtone under collisionless conditions, the HN ($X^3\Sigma^-$) molecules were formed predominantly in the symmetric F_1 and F_3 spin-rotation states with no significant population (≤4%) in the anti-symmetric F_2 levels. Fragment Doppler profiles showed that most of the available energy (>96%) went into translational motion. The distribution of rotational population in the F_1, F_3 states was Boltzmann-like, characterized by a rotational "temperature" 280 ± 50 K for $v_1 = 5$ photodissociation, and 570 ± 60 K for $v_1 = 6$. There was no significant population (<5%) in excited HN ($^3\Sigma^-$) vibrational levels.

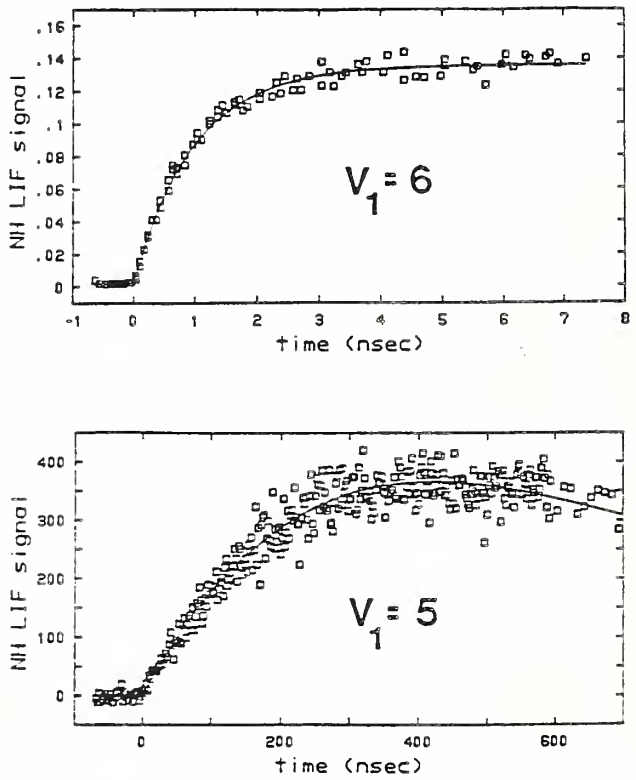

Fig. 3.2 Time-resolved appearance of X NH(v=0) product following excitation of V_{NH}=5 (lower) or V_{NH}=6 (upper) vibrational states of HN_3 in a molecular beam, giving lifetimes of 210 and 1.0ns, respectively.

Interestingly, the high resolution overtone photodissociation spectra revealed that the N-H stretching states are strongly mixed with background vibrational levels. Lines expected for a simple asymmetric top vibrational band are split into groups of 3 to 6 lines appearing with comparable intensity. We are working to analyze these spectra and exploring whether the dissociation dynamics depend upon the eigenstate excited within an overtone band.

Multiphoton vibrational excitation of DN_3 by a CO_2 laser led to dissociation forming DN in both $X^3\Sigma^-$ (spin forbidden) and $a^1\Delta$ (spin allowed) electronic states. The DN ($^1\Delta$) products were formed preferentially in the symmetric (A'), e-labeled lambda doublet levels: $\Delta(A')/\Delta(A") = 1.44$. The DN ($^1\Delta$) was formed with no vibrational excitation (<2%); the rotational state population distributions were Boltzmann-like

with a rotational "temperature" of 425K. Doppler profiles gave a total kinetic energy of about 1500 cm^{-1} in the singlet channel. That the most probable value of fragment kinetic energy was not zero implies the presence of a small barrier in the singlet reaction. As in the overtone experiments, the DN ($X^3\Sigma^-$) molecules were formed predominantly in the F_1 and F_3 spin-rotation states with little population in the F_2 levels, and there was no significant population in excited DN ($X^3\Sigma^-$) vibrational levels. The distribution of rotational states was characterized by $T_R \approx 920K$ for the F_1 and F_3 states. Doppler profiles showed a large kinetic energy release of about 10,100 cm^{-1} total in the triplet channel.

Dramatic HN/DN spin selectivity, no fragment vibrational excitation, little rotational excitation and essentially total (>96%) kinetic energy release occurred in both the overtone pumping and IRMPD experiments. The large increase in unimolecular reaction rate with vibrational energy in the overtone experiments is inconsistent with the scaling of rate with state density ρ, $k_{uni}(E) \approx A\rho(E-E_a)/\rho(E)$, expected for statistical reactions, which predicts $k_{uni}(6\nu_1)/k_{uni}(5\nu_1) \approx 3$; the experimental ratio is 200. According to the calculations of Alexander and coworkers [J.Chem.Phys.89, 1388(1988)] F_1 and F_3 spin selectivity arises from the symmetry of the spin-orbit operator matrix elements for a planar transition state. A similar argument pertains to the population of Λ-doublets in the spin-allowed channel. Little product vibrational and rotational excitation occurs because the HN and NN bonds in the singlet-triplet crossing region have free-molecule lengths, the impact parameter is very small (linear NNN, $\Theta_{HNN} \approx 90^o$), and there is little anisotropy in the exit channel of the potential surface.

During the next year we expect to complete many additional overtone chemistry experiments. Photodissociation spectra of the HN_3 overtone rotation-vibration levels will be obtained at high resolution using a cw ring dye laser pulse amplified at 20 Hz to produce very intense 10ns pulses with a bandwidth ≤ .002 cm^{-1} FWHM. For the $v_1=6$ state and combination bands like $5\nu_1 + \nu_3$ (ν_3 is the "reaction coordinate," i.e., the 1264 cm^{-1} N-N stretch) we will compare spectral linewidths, which give the dephasing decay times of the excited states, to the time-resolved dissociation rates of these states. This will show if rates of intramolecular vibrational relaxation (IVR) are faster than the reaction rates. Time- and state-resolved experiments will be done for the $v_1=7$ level, which is near the threshold for formation of $NH(a^1\Delta)$. Competition between the spin-allowed and spin-forbidden channels may be studied as a function of the HN_3 (V, J, K) state initially excited. We will try to do similar experiments on other molecules such as $CH_3N_3 \rightarrow CH_3N_3(v_{CH}=5) \rightarrow CH_3N(X\ ^3A_2) + N_2$ or $CH_2N_2 \rightarrow CH_2N_2(v_{CH}=5) \rightarrow CH_2(a\ ^1A_1) + N_2$. The CH_3N may be probed via LIF of the $A\ ^3E \leftarrow X\ ^3A_2$ system and CH_2 via LIF of the $b\ ^1B_1 \leftarrow a\ ^1A_1$ system.

This research is supported in part by the Air Force Office of Scientific Research.

2. Dynamics of van der Waals Molecules: $(NO)_2$

Progress in our studies of vibrational predissociation of weakly bound molecular clusters has included a full characterization of the single

quantum infrared photodissociation of the nitric oxide dimer. Excitation of either the symmetric (1869 cm^{-1}) or the antisymmetric (1790 cm^{-1}) NO stretching modes leads to fragmentation of the complex since the energy of either mode exceeds the 800 cm^{-1} dimer bond energy. The 1986 report described preliminary experiments which showed a dramatic mode specific effect, with the higher energy mode leading to a longer lifetime than the lower energy mode (880 ps vs 39 ps). Since 1986, picosecond experiments determined that the mode specific decay rates are independent of the NO fragment state which is probed, and product state distribution measurements showed no dependence on the initially excited mode. The latter effect was surprising, but may be understood if both modes dissociate via a channel involving a nonadiabatic transition. Infrared photodissociation spectra obtained using a pulsed difference frequency laser system gave the expected dimer band contours, and showed that such a technique is feasible for obtaining high resolution IR photodissociation spectra of clusters.

We hope to obtain higher resolution photodissociation spectra of the NO dimer and other vdW molecules by using a new infrared excitation source. Tunable ir pulses of about 10ns duration and $\leq .003$ cm^{-1} spectral width will be generated as the difference frequency between a frequency doubled pulsed single mode Nd-YAG laser and the pulse amplified cw ring dye laser. Uncertainty principle broadening of the NO dimer lines due to the 880 ps and 39ps dissociation lifetimes is .006 and .13 cm^{-1}, respectively. Lifetime studies (by linewidth or timeresolved measurements) of different isotopes of the NO dimer may establish the mechanism responsible for the fast, mode specific dissociation i.e., anharmonic potential coupling vs. non-adiabatic curve crossing. For instance, if crossing to a repulsive triplet state occurred at an energy resonant with v_4 (but not v_1) for the normal isotope, this could account for the much faster v_4 dissociation rate. If so, a heavy isotope like $(^{15}N^{18}O)_2$ with different v_1, v_4 vibrational frequencies should give significantly different lifetimes. If instead anharmonic coupling caused the dissociation, then large lifetime changes upon isotopic substitution are not expected. Other vdW molecules which may be studied include the acetylene dimer and HF•NO. In both, mode specific dissociation rates, product energy states, and perhaps vibrational energy transfer across the vdW bond may be observed.

C. Molecular Desorption from Surfaces

(S. A. Buntin, R. R. Cavanagh, D. S. King, and L. J. Richter)

Recent experiments on the laser-induced desorption of nitric oxide (NO) from Pt(111) have shown that low energy photons can drive non-equilibrium electron-molecule chemistry on metal substrates. This was a surprising result since, unlike semiconductors, the lifetime of non-thermal conduction electrons in metals is very short ($\leq$ 1 psec). The implication of hot electrons in driving molecular desorption was based on conflicting results from a series of state resolved experiments where laser induced desorption was compared to conventional thermal desorption.

The experiments were performed in an ultrahigh vacuum chamber equipped with surface diagnostics to assess the cleanliness and order of the Pt(111) sample. This substrate was saturated with NO at a temperature of 120 K. Experiments were performed on this sample, for which the NO coverage was

about 0.4 monolayer, and for samples which had been annealed to 200 K, producing a coverage of 0.25 monolayer (predominantly in top sites). The heating laser was based on a 15 ns duration (FWHM) Q-switched YAG. The YAG output wavelength was varied either by harmonic generation or Raman shifting. The energy of the heating laser pulses was adjusted, at each wavelength to provide sample temperature jumps of about 100 K. The desorbed NO species were probed using laser induced fluorescence at a typical distance of 4 mm from the surface. The probe laser was a narrow-band frequency doubled dye laser. Two types of experiments were performed to obtain internal and kinetic energy distributions for the desorbing species from: 1) Velocity-selected rotational excitation spectra and 2) Internal-state selected time of flights (TOFs).

Results for time of flights (λ pump = 532nm) taken probing those NO species desorbing in a single quantum state - the J=8.5 rotational level of the vibrationless level of the F_1 spin-orbit state - are shown in Fig. 3.3 for three different sample preparations. The middle trace is for a sample with 0.25 monolayer coverage in top sites (200 K anneal). For this sample, there is a single component in the TOF. Although the peak surface temperature induced by the YAG laser did not exceed 300 K, this kinetic energy distribution was characterized by a temperature of 1200 K. The bottom trace was obtained for an unannealed sample, for which the TOFs showed contributions from two desorption channels - one similar to the energetic channel observed for the annealed sample and one of a thermal nature not observed for the annealed sample. The top trace was obtained for a sample annealed to 320 K. This annealing leaves a surface coverage of 0.1 monolayer (in a bridge-bonded site), with no top-site bound species. For this sample, there was no observable laser induced desorption despite the fact that the NO coverage is approximately half that which led to the signal in Fig. 3.3b. The observed desorption behavior following 100 K temperature jumps using visible and near-visible laser-induced desorption can be summarized as follows: no desorption takes place from the bridge sites, energetic species are desorbed from the top sites, and thermal desorption occurs from the low energy binding state. Most of our efforts to date have been spent in characterizing the energetic desorption channel which can be cleanly studied for samples annealed at 200 K.

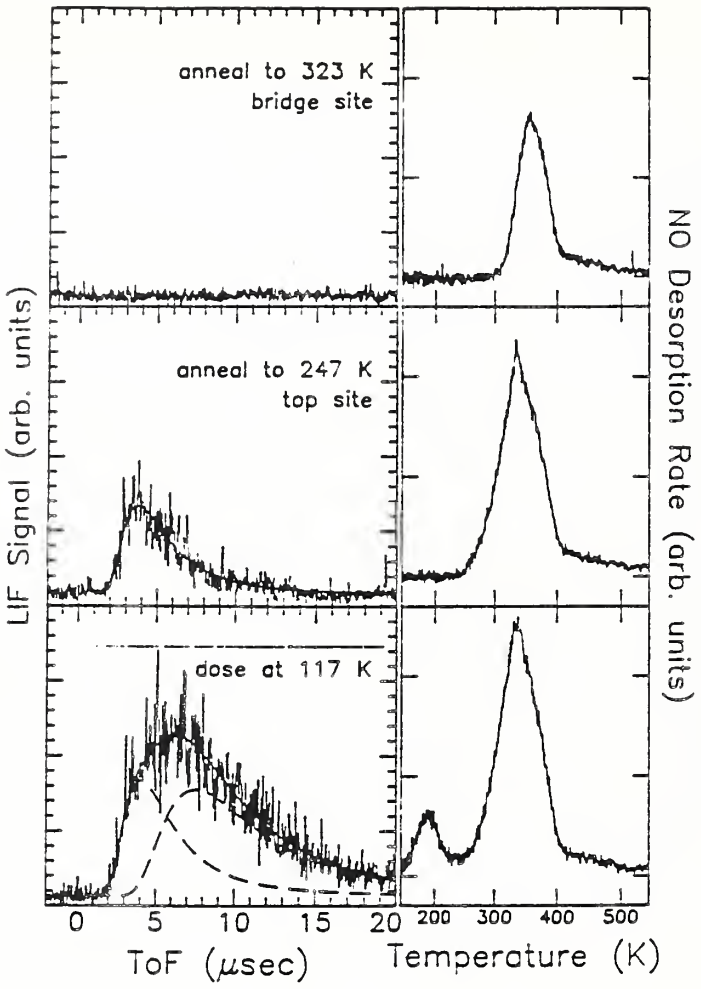

Fig. 3.3 Internal-state selected time of flights for the 532nm laser-induced desorption of NO(J=8.5; F_1) from Pt(111) for different initial surface coverages. The right-hand panels show thermal desorption results for the respective initial conditions.

The desorption mechanism responsible for these signals has to be consistent with a binding energy for the top sites of about 25 kcal/mole, 1.08 eV. When the heating laser wavelength was 532 or 355 nm, the desorbed NO had kinetic energies of 1200 to 2000 K, some 4 to 7 times the peak surface temperature with the measured value increasing with internal energy. Under these desorption conditions some 4% of the desorbed NO was in the v=1 vibrational level. For a heating laser wavelength of 1064 nm (1.17 eV) the kinetic energies were roughly 35% lower and there was no observable population in the v=1 level. The internal state population distributions were essentially the same for all heating wavelengths studied. Notably, there was an inversion in the spin-orbit state populations. The rotational population distribution at low J was independent of rotational energy, falling off rapidly with rotational energy above 300 cm^{-1}.

In the model we propose, the initial absorption of the incident photon is in the near-surface region of the metal. Some fraction of the nascent photogenerated electrons migrates to the surface layer and interacts with the adsorbed NO through its unoccupied $2\pi^*$ levels (shown by inverse

photoemission to lie in the range from 1 to 2 eV above the Fermi level). Electron capture and neutralization drives the desorption process. In the case of the 1064 nm experiments, only electrons with the full 1.17 eV photon energy can participate in this desorption mechanism due to the energy requirements. For these electrons, desorption into the vibrationally excited v=1 level is not possible. In this model, the propensity for populating the higher energy F_2 spin-orbit state is due to symmetry constraints in the charge neutralization/desorption step.

There are a number of tests still to be performed to prove (or disprove) this mechanism. These include using heating laser photons of energy lower than the 1.08 eV binding energy, using heating pulses of varied time duration and examination of co-adsorbate systems such as NO/CO where the lowest unoccupied levels of the CO are near 3 eV. Experiments are currently underway using Raman shifting techniques to generate laser pulses at energies of 0.6 and 0.85 eV.

Hot carrier assisted desorption mechanisms have previously been proposed for semiconductor systems. One such system is NO/Si(111) where NO desorption has been observed following optical excitation above the Si band gap. We plan to study the desorption dynamics manifest by thermal and hot carrier assisted desorptions from such semiconductor systems.

The interactions of hydrogen at surfaces are believed to be prototypical for a broad range of gas-surface processes. Recombinative desorption of H_2 from hydrogen covered surfaces of metals and semiconductors are typical of such interactions, in that a surface reaction leads to the formation of a new chemical bond, the H-H bond. We are presently exploring four-wave mixing techniques in order to generate vacuum ultraviolet wavelengths suitable for state-resolved studies of molecular hydrogen. In these desorption studies we plan to investigate both thermally driven H atom recombination, and recombinative desorption driven by optically excited carriers.

This work was supported in part by the U.S. Department of Energy, Office of Basic Energy Sciences.

4. QUANTUM CHEMISTRY GROUP

H. Basch, D. Garmer, P. S. Julienne, M. Krauss, F. H. Mies
S.-H. Pan, W. J. Stevens, and L. Vahala

A. Introduction

B. Electronic Structure

1. Ab Initio Reaction Field Program

2. Theoretical Studies of Hydrogen Bonding

a. $CH_3OH + NH_3$ and $H_2O + NH_3$

b. $CO_2 + H_2O + H_2O$

c. $H_2NCOOH + H_2O$

d. $HCOOH + HCOO^-$

3. Selectivity of Metal Cation Binding to Proteins

4. Binding of Pt Ammines to DNA

5. Electronic Structure of the P-O and P-S Bonds

6. Anion Binding to Polar Molecules

C. Scattering Program

1. Molecular Photodissociation

a. Overlapping Resonance Effects on Predissociation Line Shapes in O_2

b. Predissociation of the B and C States of CO

c. Intense Laser Photodissociation of H_2^+

2. Generalized MCQDT Applications

a. Whole and Half Collision Matrix Methods for Multichannel Curve Crossing Problems

b. Factored Frame Transition Half Collision Analysis of Collisions

c. Unified Half Collision Analysis of Photodissociation, Collisional Redistribution of Light, and Atomic Collisions

d. Generalized MCQDT Analysis of Molecular Bound States and Collision Cross Sections Involving Molecular Charge Transfer States

3. Theory of Ultracold Atomic Collision Phenomena

a. Molecular Photoassociation Spectroscopy

b. Associative Ionization Cross Sections of Na(3p) + Na(3p) at 0.001 K

c. Intense Laser Effects on Cross Section in Optical Traps

d. Collision-Induced Optical Trap Loss Processes

e. Quantum Threshold Effects in Ultracold Collisions

f. Ultracold Collisions in Magnetic Fields

A. Introduction

The Quantum Chemistry Group is at a time of transition. The biotechnology competence has evolved into a new entity, the Center for Advanced Research in Biotechnology (CARB), while the scattering program is to be expanded to support a new NIST competence on the physics of very slow atoms. Dr. Walter Stevens will leave the group in October 1988 to become the Associate Director of CARB. He is already representing NIST interests in the administrative structure of CARB. Scientific projects initiated in the competence will continue as collaborative efforts between the Quantum Chemistry Group and Stevens. The slow atom competence extends support to an already successful collaboration between Dr. Fred Mies and Dr. Paul Julienne with experimental groups at both NIST and the University of Maryland. An additional scattering theorist will be hired in the next fiscal year. With a new postdoctoral fellow and an occasional foreign guest scientist, the effort can attain a necessary critical mass. The electronic structure group, on the other hand, is reduced to one permanent scientist but the collaborations with CARB and guest scientists will maintain a research program in this area. The scientific direction of the group will not change from the general directions indicated by the work of the last two years described below.

B. Electronic Structure

1. Ab Initio Reaction Field Program
(W. J. Stevens, D. Garmer, M. Krauss, and H. Basch)

Final tests have been made of the first version of an ab initio reaction field computer program which will be used for quantum mechanical studies of complex systems. The reaction field approach divides a large molecular complex into an "active" region, which is to be characterized quantum mechanically, and a "spectator" region that may be modeled as an assembly of polarizable molecular fragments that are not directly involved in the chemistry. How the boundary between the active and spectator regions is chosen depends on the properties or chemistry one wishes to study. We are currently choosing the boundary so that the interactions between fragments in the two regions is of the nonbonded type. The Hamiltonian of the active region consists of the normal Hamiltonian for the active electrons and nuclei, plus an effective Hamiltonian that describes the electrostatic and exchange repulsion interactions between the active and spectator regions, and a perturbation Hamiltonian that accounts for the polarization of the spectator fragments. It is the polarization term that provides the "reaction" of the spectator region to molecular structure changes that occur in the active region.

Tremendous saving of computer time is possible through the reaction field approach, since only the electrons in the active region need to be considered explicitly, and the effective Hamiltonian between the active and spectator regions involves only one-electron integrals. We have developed methods for obtaining the parameters for the effective Hamiltonians from ab initio calculations on prototypical molecular fragments. These parameters

appear to be transferable at the functional group level, so very complex spectator regions can be modeled by a collection of predetermined "fragment potentials."

The electrostatic potential due to a molecular fragment with a frozen electronic charge distribution can be represented by a collection of distributed multipolar expansions located at the atomic centers and bond midpoints [A. J. Stone, Chem. Phys. Lett. 83, 233 (1981)]. However, such expansions are convergent only at infinite distance from the expansion centers. At finite distances, one must account for penetration of the electronic charge distribution. We have used a functional form which gives the total electrostatic potential of a fragement as a sum of an exact nuclear part and an electronic part that includes a cutoff function to account for penetration.

$$\phi_{Tot} = \sum_{n} \frac{Zn}{r} + \sum_{k} \phi_{k}^{elec} \quad [1 - Ae^{-\alpha r2}]$$

where ϕ_k^{elec} is the distributed multipolar expansion derived from the frozen electron density of the fragment, and A and α are parameters determined by a least squares fit to the quantum mechanical electrostatic potential in a volume surrounding the fragment. The electrostatic contribution to the active region energy is given by

$$E_{estat} = \langle \psi_{act} \mid V_k^{spec} \mid \psi_{act} \rangle$$

which is an easily evaluated one-electron integral.

Modeling the exchange repulsion (and orthogonality) interaction between the active and spectator regions requires some ad hoc assumptions about the localization of exchange operators. We initially tried a simple one-electron representation of the repulsive energy of the form

$$E_{rep} = \sum_{k} \langle \psi_{act} \mid V_k^{spec} \mid \psi_{act} \rangle$$

where V_k are exponential or gaussian functions centered at the atoms of the spectator fragment. The parameters defining V_k are determined by fitting ab initio calculations on prototypical fragments. While this functional form correctly mimics the repulsive interaction energy for a given pair of active and spectator fragments in a particular orientation, the V_k were found not to be transferable to different environments. We then tried a similar two-center energy term of the form

$$E_{rep} = \sum_{k} \langle \psi_{act} \mid V_k^{spec} \mid \psi_{act} \rangle + \sum_{\ell} \langle \psi_{spec} \mid V_k^{act} \mid \psi_{spec} \rangle$$

This is more complicated, since it requires the electron density of the spectator fragments, but it still involves only one-electron integrals. In this case, the potentials, V_k, are found to be transferrable between interacting systems. The transferability is good enough that one can generate the V_k by fitting the interaction between prototype fragments and a spherical "probe" atom (we use argon). Due to the short-range nature of

the repulsive exchange interactions, in practical calculations the terms need to be evaluated only at the boundary between the active and spectator regions.

The polarization contribution to the active/spectator interaction energy is calculated perturbatively. The dipole polarizability of each spectator fragment is expanded in terms of electron-pair polarizabilities located at the centers of charge of the bond pairs and lone pairs that comprise the fragment. The electron-pair polarizabilities are obtained from ab initio calculations on prototypical fragments using a localized orbital formalism. These polarizabilities are found to be transferable at the functional group level. The energy contribution due to the polarization of the spectator fragments is given by

$$E_{pol} = \sum_{k} F_k \, \bar{\bar{\alpha}}_k \, F_k$$

where F_k represents the active region electric field evaluated at a polarizable point in the spectator region

$$F_k = \langle \psi_{act} \left| \frac{r}{r^3} \right| \psi_{act} \rangle .$$

The induced moments in the spectator region can be added into the active region electrostatic interaction energy term, and the electronic wavefunction of the active region can be redetermined, iteratively, until a self-consistent polarization energy is achieved.

We have successfully tested this reaction field approach on a variety of hydrogen-bonded complexes consisting of water, formamide, and glycine. We find that the interaction energy surface for any pair of molecules can be reproduced to within 10-20% when either of the molecules is replaced by the reaction field Hamiltonian. The largest absolute errors are due to the representation of the electrostatic interaction, which is truncated at octupoles for each expansion center. We have also treated complexes of formamide hydrogen-bonded to two water molecules, and find the cooperativity in the hydrogen-bonding is predicted very accurately when both waters are replaced by reaction field Hamiltonians.

The next steps in the reaction field development include testing the transferability of the parameters in larger molecules such as proteins, testing the validity of the distributed dipole polarizability approximation in interactions of charged species (particularly anions), the addition of dispersion terms to the perturbation Hamiltonian, and the development of integral gradients that are needed for geometry optimization. Long range goals include the development of molecular mechanical methods for modifying the geometric structure in the spectator region in response to changes in the active region. Applications of the reaction field program in the coming year will include models of the active site of carbonic anhydrase with different metal substitutions, and a model of the active site in aspartyl proteases to determine the electrostatic potential and the relative energetics of proton transfers.

2. Theoretical Studies of Hydrogen Bonding
(W. J. Stevens and H. Basch)

It is well established that ab initio SCF calculations using reasonable atomic basis sets can provide accurate data for the structure and stability of hydrogen-bonded complexes. It also is possible to analyze the theoretical calculations to determine the dominant contributions to hydrogen-bond energies and properties. We have studied a variety of hydrogen-bonded dimers during the past year, some of which have also been studied spectroscopically by the microwave group (see above, section 2).

2a. $CH_3OH + NH_3$ and $H_2O + NH_3$

The structure of the methanol-ammonia dimer was determined by the microwave group (see section 2). Stark measurements indicated a rather large dipole moment enhancement (0.96 D) upon complex formation. The analogous water-ammonia dimer has a smaller dipole enhancement (0.59 D) even though the dipole moment of water is 0.18 D larger than that of methanol. We carried out ab initio SCF calculations on both methanol-ammonia and water-ammonia at the experimental equilibrium conformations. The frozen fragment reduced variation space analysis developed in this laboratory by Dr. Stevens and Dr. Fink [Chem. Phys. Lett. 139, 15 (1987)], was used to isolate the factors which determine the dipole moment enhancement for each complex. The results indicated that methanol-ammonia should have a larger enhancement than water-ammonia by virture of the larger polarizability of methanol. The enhancement due to ammonia polarization was virtually identical for the two complexes, since the local electric field near the -OH group is the same in methanol and water.

2b. $CO_2 + H_2O + H_2O$

Another study carried out in collaboration with the microwave group (see section 2) involved a cluster of CO_2 plus two waters. The positions of the heavy atoms in this complex were obtained from the analysis of the microwave spectrum. However, the proton positions could not be determined with any certainty because of the insensitivity of the moments of inertia to in-plane rotations of the waters about their centers of mass. The dipole moment of the complex was determined from Stark measurements. Ab initio calculations were carried out with the heavy atoms fixed in the positions predicted by the microwave analysis. The orientations of the two waters in the complex were varied until the calculations predicted a dipole moment that was compatible with the Stark measurements. A full quantum mechanical optimization of the structure was impossible due to the flatness of the potential energy surface and the large basis set required to correctly describe the electrostatic interactions and the polarization effects. The final predicted structure has one water bonded to the CO_2 in a nearly optimum orientation with the water oxygen pointing at the CO_2 carbon. A second water forms a bridge between the CO_2 and the first water by acting as a proton donor to the CO_2 oxygen and a proton acceptor from the first water. The water-water hydrogen bond is quite distorted, but the energy gained from the two water interactions with CO_2 more than compensates for the energy loss in the distorted hydrogen bond. The ab initio calculations find the complex to be planar, in agreement with the microwave analysis.

2c. $H_2NCOOH + H_2O$

We have carried out complete ab initio calculations, including geometry optimizations and electron correlation studies, on cyclic complexes of glycine with water. This work was stimulated by the discovery in this group of a highly stable, cyclic complex of formamide and water that was subsequently verified by microwave spectroscopy. The stability of such cyclic complexes is due to the formation of two hydrogen bonds. Each bond is distorted somewhat from an ideal linear configuration, but the binding energy obtained from the two distorted hydrogen bonds exceeds that of any single hydrogen bond that can be formed. Glycine-water complexes have not been observed experimentally, but our calculations predict two cyclic structures that are quite stable with binding energies of approximately 9 kcal/mol. The two structures are shown in Fig. 4.1. Both involve a cyclic, double hydrogen-bonded configuration between water and the carboxyl moiety. The difference in the two structures is a 180 degree rotation about the C-C bond in glycine, which also distinguishes two of the

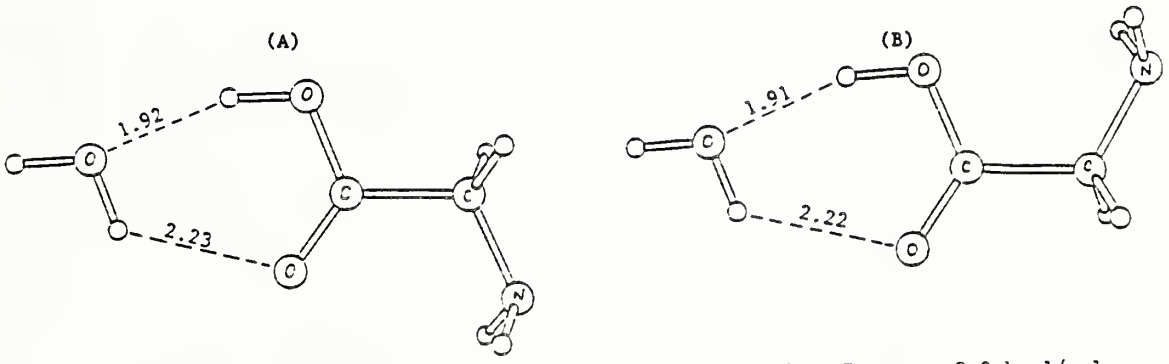

Fig. 4.1 Structure of water-glycine complexes.

conformers of the glycine monomer. As expected, the monomer geometries are not distorted by the hydrogen bond formation. The energy separation between these two complexes is a little less than the separation in the glycine monomer conformers, presumably due to some cooperative polarization of the hydroxyl group by the water and the amine group. Other cyclic structures were examined that involve water binding between the carboxyl and amine groups, but these were found to be weakly bound and much less stable.

2d. $HCOOH + HCOO^-$

In the three dimensional structure of proteins, it is very common to find two carboxyl groups in close proximity to each other, particularly in metal binding sites or sites involved in hydrolysis reactions. We have begun a series of ab initio calculations aimed at characterizing these protein fragments in terms of structure, stability, proton mobility, and

the influence of the protein environment. The first study involves the formate-formic acid complex, for which there is gas phase data on the stability but not the structure. We have carried out a full energy gradient optimization of the structure of the complex within the SCF approximation. The interaction energy surface is quite flat. We are currently investigating the proton-transfer reaction coordinate at both the SCF level and the MP2 correlated level. The next phase of the investigation involves the introduction of a water molecule, which will yield many new interesting structures as well as several proton transfer possibilities. Eventually, we will introduce a protein environment via the reaction field method and attempt to make predictions about stable structures and proton positions as a function of protein mutation.

3. Selectivity of Metal Cation Binding to Proteins
(M. Krauss and W. J. Stevens)

Ab initio molecular orbital calculations of the binding energy of metal cations to octahedral clusters of water, formamide, and formate ligands are used to model the enthalpies of metal substitution reactions at Ca binding sites in proteins. Since the binding of the cation to the first shell ligands substantially exceeds ligand-ligand binding energies, the conformation of the first shell in the bulk is essentially determined by the equilibrium geometry of the first shell cluster. A satisfactory model for calculating binding enthalpies is based on the first shell energetics and the Born model for determining the polarization interaction of the first shell with the environment. Cluster reaction enthalpies are calculated for transferring Mg^{+2}, Ca^{+2}, and Na^{+1} cations from a water cluster to the protein model cluster. The metal is bound to the lone pair electrons of the oxygen atoms in these ligands. Cluster size is determined by the metal to oxygen distance and is found to strongly affect cation binding selectivity between cations of the same and different charges. The selectivity is a function of both steric and electrostatic interactions. The selectivity between Mg and Ca is primarily dependent on steric factors which restrict the formation of optimal electrostatic bonds. However, there is also an electrostatic component independent of steric influences which is selective between cations of different charge.

The model is tested by a calculation of Na, Mg, and Ca cation enthalpies in water. Including dispersion and zero-point energies in the first shell cluster energetics, these enthalpies agree within 5% with the experimentally deduced values. Enthalpies are compared for clusters with different numbers of waters. It is evident that the W6 cluster is most stable for Mg and Na. However, for Ca, W6 and W9 yield comparable enthalpies reflecting the tendency for Ca to be found in variable first shell environments.

The model metal reaction enthalpies have been applied to an analysis of the binding sites in the protein, Subtilisin BPN'. For the A site, the energy of reaction is 20 kcal/mol favoring Ca binding over Mg. Desolvation energies determine the ion selectivity between Mg and Ca. Steric interaction between the protein ligands are larger than in water and prevent as optimal Mg-O bonds from forming in the protein cluster. For an optimal B site type cluster, Ca is bound by 13 kcal/mol over Mg. As the

metal to oxygen bond distance is increased, Ca is even more strongly bound than Mg. Competition between Na and Ca is only possible if the protein site is substantially rigid. If the clusters around both the Ca and Na cations can achieve optimal bond distances, then the Ca cation will always be very energetically favored. When the cluster conformation is determined primarily by forces in the protein and not by the cation-ligand interaction, then several different conformations between the cations and ligands are possible and, for an appropriate cluster size, the enthalpy of reaction will approach zero. If the cluster containing one formate, one water, and four formamide ligands is fixed with the M-O bond distance 2.8Å or larger, the reaction enthalpy favors Na binding to the protein model cluster. Crystallographic analysis indicates the site is of comparable size for either Ca or Na binding, but each metal binds in a unique manner. The Ca ion binds to the carboxylate anion of an ASP residue, the carbonyl oxygen of a backbone residue, and four waters. It does not penetrate into the binding site but remains near the surface and bound to the ASP anion. The Na is found bound to three carbonyl oxygens of residues near the bottom of the site but still interacting at a longer distance with the residues at the surface containing the anionic moiety. The Na binding energy in the cluster varies slowly with the position in the cluster, but, because of the charge of Ca, the binding energy varies rapidly with position for Ca with the Ca more strongly bound in an optimal conformation with the formate anion. Binding energies of these different cluster conformations permit a rationalization of the experimental geometries. The relative rigidity of the B site in the protein is ascribed to ionic bonds in the second shell of residues around the site. Metal substitution and hydration enthalpies will be studied for other metal cations and the models extended to clusters with more than one formate or formic acid ligand.

4. Binding of Pt Ammines to DNA
(H. Basch, M. Krauss, and K. Miller)

Metal cation bonds to nucleic acid bases have large intrinsic bond energies. The binding of cis-diammineplatinum (DP) to single- or double-strand oligomers of DNA substantially alters the local helix geometry at the point of bonding. Experimental evidence suggests that DP binds preferentially to the N7 sites of the guanine (G) base in a GpG chelate, which can interfere with the physiological properties of DNA. Earlier we proposed a theoretical model for DP binding which showed a 'kinked' distortion of the DNA is feasible without seriously disturbing the duplex base-paired hydrogen binding. The details of the kinked structure have been examined with both quantum and classical mechanics modeling. Valence self-consistent-field (SCF) calculations of the energetics of clusters of DP, a phosphate anion, and water molecules indicate that the structure of the adduct depends on the hydrogen bonding of the polarized ammine ligand to nucleophillic sites in DNA. The possibility of water bridges significantly increases the number of types of structures. The cation can bind directly to the phosphate or it can bind to water which is in turn hydrogen bound to the phosphate. Direct or through-water binding of DP to phosphate is calculated to be competitive and the kinked conformations are dependent on the interaction with the environment and the extent to which the interacting species can be solvated. Detailed geometries obtained by molecular mechanics minimization are reported for the interaction of DP

with the pentamer duplex, (AT, GC, CG, AT) and a number of water molecules. Binding of the DP to the carbonyl oxygen of the thymine (T) base is observed in the molecular mechanics conformations and the energetics of such a bond was also examined with SCF calculations. Binding of substituted DP was also investigated to determine the relative importance of steric and hydrogen binding on the adduct formation. Computer modeling of a series of cis- $Pt(NH_2R)_2^{+2}$, where R=H, CH_3, cyclopropane, cyclobutane, and cyclopentane, to the pentamer duplex of DNA shows that the receptor site geometry and the conformation of the DNA is changed little for binding all mono-substituted ammines. The binding energy decreases with the substituent size faster than the slight increase in van der Waals energy resulting from the increasing number of atoms. The reduction of binding is correlated with the decrease in physiological activity.

5. Electronic Structure of the P-O and P-S Bonds
(H. Basch, M. Krauss, and W. J. Stevens)

The electronic structure of the P-O and P-S bonds is studied because of the importance of phosphates and phosphorothioates in biological systems. Although the study concentrated on these systems, the following molecules were examined to study the bonds in a variety of molecular environments: H_3PO, PO_3^-, $H_2PO_4^-$, and H_3PO_4, and their mono-substituted sulfur analogues. The analysis of the bonding was based on the gross atomic populations, plots of the charge density and appropriate difference-densities, and the electrostatic potential. For the phosphate anion and the thio analogue, the water binding energy was calculated to provide a more direct example of binding to the oxygen and sulfur sites to compare with the electrostatic potentials. The P-O and P-S bonds are found to be very polar in all the molecules. Population analysis shows an appreciable d population on P related to π back transfer. However, the strength of the bond and the short bond distance is related to the polar character of the bond and not the hypervalent or multiple bond character. The P-O and P-S bonds in the phosphorothioate anion show significant charge transfer from P to both O and S. The large negative potential near both atoms leads to ionic hydrogen bonding of water to both O and S. The bond energy to O is about 4 kcal/mol larger because of the closer approach of water to O. The electronic structure of the P-O bond is now being compared to the V-O bond. Vanadate substrates have been suggested as a replacement for phosphates to create a stable transition state analogue. We will compare the electronic structure of the V-O and P-O bonds to determine the validity of the concept.

6. Anion Binding to Polar Molecules
(H. Basch, M. Krauss, and W. J. Stevens)

The electrostatic interaction between an anion and a highly polar molecule is large and bound adducts are expected. However, adducts are possible for more than one set of reactants or channel that are accessible to one another by a substitution reaction. Whether the adducts are stable intermediates in channels other than the lowest energy one will depend on the magnitude of the binding energy and the barrier associated with reaction to a lower energy channel. A number of stable adducts or

intermediates have been explored for phosphates with the general formula composition, $H_4PO_5^-$, or chlorine substituted phosphate anions, $H_3PO_4Cl^-$ and $H_2PO_3Cl_2^-$. Cl substitution for OH allows an exploration of the effect of the size and electronegativity of the interacting species. The polar nature of the P-O and O-H bonds suggests that the nucleophillic addition of an anion to both P and O sites would lead to stable adducts. Considering proton transfer between reactants, the following hydrogen-bonded adducts are possible:

1. $H_2PO_4^-$ ••• H_2O,
2. H_3PO_4 ••• OH^-,
3. HPO_3Cl ••• H_2O,
4. $H_2PO_4^-$ ••• Cl^-,
5. $PO_2Cl_2^-$ ••• H_2O,
6. H_2PO_3Cl ••• Cl^-.

The stabilities of the OH^- and Cl^- adducts are interesting since we calculate binding energies of nearly 70 and 40 kcal/mol, respectively, which far exceed the binding energies observed for normal polar-anionic interactions. For example, the binding energy of water to the phosphate anion is of the order of 15 kcal/mol. Both electrostatic or hydrogen-bonded and five-coordinate adducts were studied. The electronic structure of the five-coordinate trigonal bipyramid adduct was examined as a function of Cl substitution in equatorial and apical positions. Both adducts 1 and 2 are stable, but the five-coordinate analogue structure is an intermediate local minimum. Adduct 1 is the lowest energy structure and the barrier to proton affinity exists to allow a stable adduct 2. The approach of OH^- to phosphoric acid induces a rotation of the all OH bonds around each P-O bond so that the acid adopts an umbrella conformation with three OH bonds pointed at the OH^-. The binding energy is comparable to three times the bond energy between OH^- and water. The Cl structures are not as strongly bound because of the larger size of Cl and the differences in the proton affinities of the anions. However, a reaction field analysis of the ionic hydrogen bonds reveals the electrostatic interaction is dominant as expected. The Cl substitution manifests itself by reducing the polarity of the neighboring P-O bonds and producing a concomitant reduction of the proton affinities of the substituted phosphate anions. This leads to the proton abstraction without a barrier by OH^- from the substituted molecules.

The apical OH ligands in the five-coordinate complexes are very polar and the central P atom of the equatorial moiety is quite positive with over one electron transferred to the surrounding ligands. For the Cl substituted five-coordinate structures, the stability and binding energy trends are related to the local polarity of the P-X bond and not the overall electronegativity of OH and Cl. Cl is more electronegative but still stable five-coordinate intermediates only have equatorial chlorines. When the chlorines are in apical positions, the structures are always found to be transition states and are dissociative for a chlorine ion. The local polarity influence on adduct formation for anions containing second row atoms will be examined more systematically for halide substitution and replacement of OH by SH. Reaction field methods will be used to analyze the interactions.

C. Scattering Program

We are actively involved in a variety of problems which can be classified as the spectroscopy of colliding molecular fragments. For example, a photon may be absorbed during a collision, or a photon may cause the dissociation of a molecule or the association of fragments to form a molecule. Such problems occur in a wide variety of areas in chemical physics, e.g., laser spectroscopy, development of new lasers, spectral line shapes, radiative redistribution and transport, excimer lasers, chemistry of planetary atmospheres, ultracold collision phenomena. We use two complementary approaches: (1) numerical state-of-the-art close coupled quantum scattering methods combined with ab initio calculations of interaction potentials and (2) powerful analytic tools based on the generalized form of the multichannel quantum defect theory (MCQDT). This combined numerical and analytic approach gives a comprehensive and unified ab initio quantum methodology for describing a variety of experimental observables. Our applications of this theory in FY87-88 are described below for the following topics:

C.1. Molecular photodissociation.
  a. Overlapping resonance effects on predissociation line shapes in O_2.
  b. Predissociation of the B and C states of CO.
  c. Intense laser photodissociation of H_2^+
C.2. Generalized MCQDT applications.
  a. Whole and half collision matrix methods for multichannel curve crossing problems.
  b. Factored frame transformation half collision analysis of collisions.
  c. Unified half collision analysis of photodissociation, collisional redistribution of light, and atomic collisions.
  d. Generalized MCQDT analysis of molecular bound states and collision cross sections involving molecular charge transfer states.
C.3. Theory of ultracold atomic collision phenomena.
  a. Molecular photoassociation spectroscopy.
  b. Associative ionization cross sections of Na(3p) + Na(3p) at 0.001K.
  c. Intense laser effects on cross section in optical traps.
  d. Collision-induced optical trap loss processes.
  e. Quantum threshold effects in ultracold collisions.
  f. Ultracold collisions in magnetic fields.

C.1

a. Overlapping Resonance Effects on Predissociation Line Shapes in O_2 (P. S. Julienne, F. H. Mies, and L. Vahala)

The Schumann-Runge bands of O_2 have long been known to be predissociated. These bands play an important role in upper stratospheric photochemistry, since they control the penetration of the solar flux in the 200-175 nm range. Numerous experimental studies of these bands have been carried out over several decades, and are still current today. Several years ago we (Drs. Julienne and Krauss) carried out an ab initio study of the predissociation line widths, and explained the basic mechanism of the predissociation in terms of 4 different molecular states which cross the bound $B^3\Sigma_u^+$ state. All experimental modelling of the widths, as well as our theory, assumed the standard Lorentzian model of the predissociation line

shape. The blending of triplet fine structure components in the bands has made the extraction of lineshapes from experimental data difficult. Theory predicts different widths and level shifts for each fine structure component. Theory also predicts that two of the fine structure components of the same J but different N can interfere and give rise to non-Lorentzian line shapes. Such interfering resonances are called overlapping resonances (predissociating bound states are scattering resonances).

We have applied our two-fold approach to the question of the photodissociation line shapes of the Schumann-Runge bands. We have calculated line shapes using both a multichannel close coupled scattering calculation and an analytic theory based on the generalized MCQDT which uses parameters obtained by perturbation theory. We find the two methods to be in excellent agreement. The calculation gives an excellent illustration of the power of the MCQDT formalism to introduce the effect of multistate couplings into molecular spectroscopy problems involving both bound states and continua.

We have used our numerical close coupling code to calculate the spectral line shape for transitions from specific O_2 $X^3\Sigma_g^-$ ground state fine structure levels to the upper multichannel continuum which represents the two closed fine structure bound state channels interacting with multiple continua. The bound closed channels represent the F_1 and F_3 triplet fine structure components of the same J and respective N = J-1 and J+1. We have carried out model studies including both single and multiple continuum interactions. Fig. 4.2 illustrates a typical profile for the two interfering $^NP_{13}(3)$ and $P_3(3)$ lines predissociated by interaction with the $^3\Sigma_u^+$ state. The non-Lorentzian character of the lines in this model calculation is evident in comparison with the correct line shape obtained by close coupling.

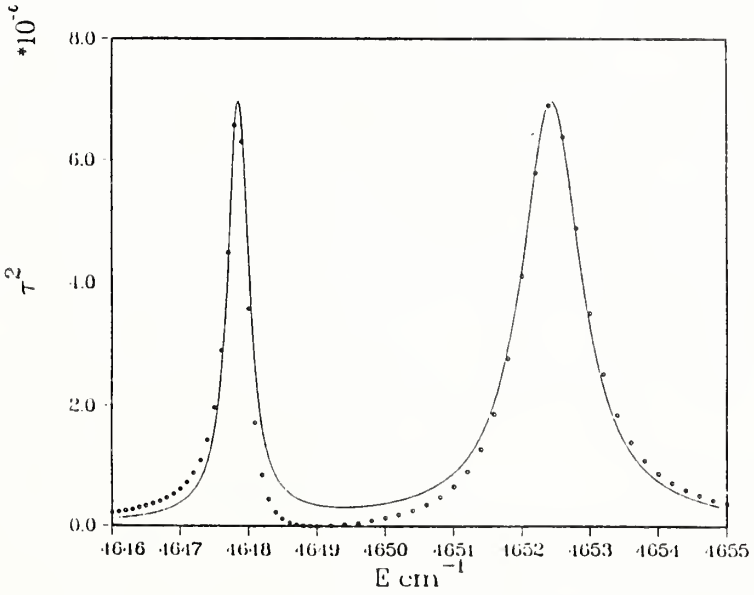

Fig. 4.2 Lorentzian fit to two interfering fine-structure lines in predissociating O_2. Solid points indicate exact numerical results of close-coupling codes.

The MCQDT analysis of the line shape uses the analytic structure of the excited state multichannel wavefunction to give an analytic representation of the line shape. The expression is:

$$|\tau(E)|^2 = \tilde{\underline{D}}\ \underline{L}(E)\ \underline{D},$$

where $\underline{D}$ is a 2 component vector containing the product of Franck-Condon and Hönl-London amplitudes for the two interfering lines and L(E) is a 2 x 2 matrix line shape function which can be expressed in terms of ordinary molecular spectroscopic perturbation matrix elements. It contains both the effects of the spin-spin and spin-rotation interactions and the predissociation by one or more continua including the effects of width and level shift. The MCQDT theory allows for interference between the two bound levels. In Fig. 4.3 the MCQDT profile is in excellent agreement with the numerical close coupled profile. The MCQDT formalism is expected to have much utility in molecular spectroscopy, since it can treat bound and continuum interactions equally well in a consistent way.

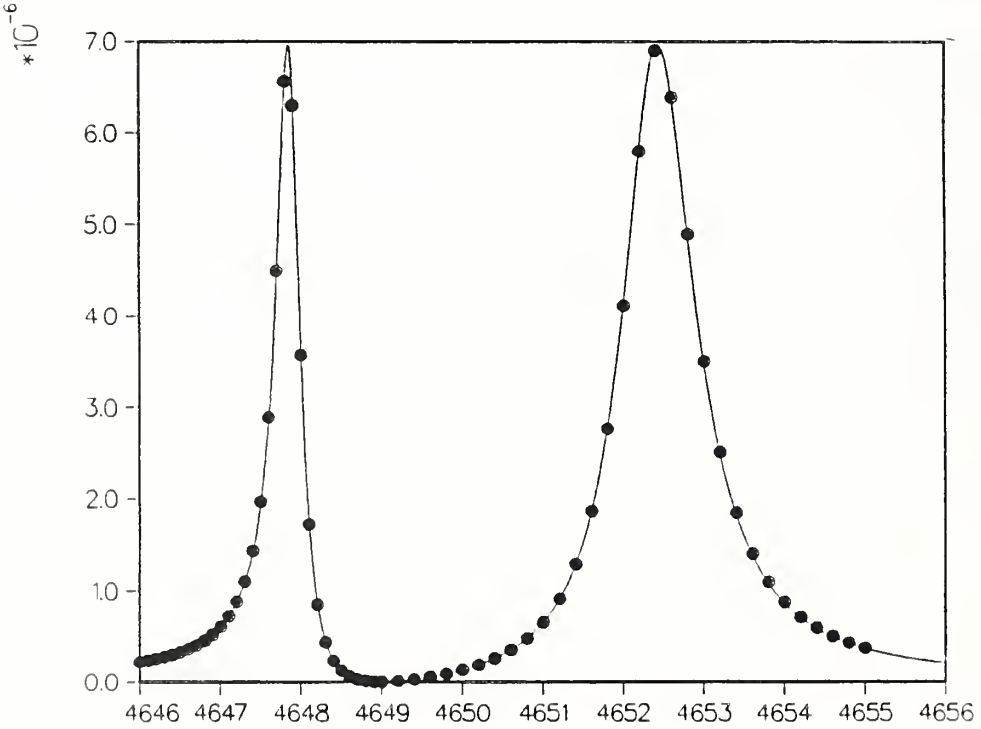

Fig. 4.3 Resultant exact fit to interfering predissociating lineshapes in O_2 using analytic expressions predicted by MCDQT.

b. Predissociation of the B and C states of CO
(P. S. Julienne and F. Rostas)

CO is an astrophysically important molecule which can be photodissociated by light with wavelength shorter than 112 nm. The photodissociation between 112 and 90 nm only occurs in discrete bands which are predissociated. New high resolution absorption and emission spectra for a number of bands in this region have recently been obtained by F. Rostas and coworkers at the Observatory of Paris, Meudon, France. We have

been analyzing these data in collaboration of the group at Meudon in order to interpret the predissociations and obtain a predictive model of the predissociations in the ns and np $^1\Sigma$ Rydberg series perturbed by the D$'^1\Sigma$ valence perturber.

The positions and intensities of the vibrational and rotational levels of the B $3s\sigma$ $^1\Sigma$ and C $3p\sigma$ $^1\Sigma$ Rydberg states are perturbed due to strong interactions with the nearby D $^1\Sigma$ valence state. These are especially evident in the B state, where the vibrational spacings depart significantly from the spacings in the CO^+ molecular ion. An anomalous rotational constant is found for B v=2, and the rotational levels become diffuse and break off with increasing J. Although the C state is higher in energy than the B state and also crossed by the D' state, vibrational levels to v=4 are observed, and v=0, 1, and 2 are seen in emission. Level shift perturbations are also seen for the C levels, but these are much smaller than for the B state.

We have constructed a model to explain these data. The model uses deperturbed spectroscopic constants to construct model diabatic potentials for the B, C, and D' states. The D' state is known in its R_e region from 4 observed vibrational levels. It is necessary to extrapolate the left limb to small R in the region of crossing with the B and C states, for which the R_e is the same as for the molecular ion. Diabatic coupling matrix elements are assumed by the model, and curves and couplings are adjusted to account for the level positions, predissociation widths, and absorption intensities, assuming diabatic transition dipoles.

The coupling matrix element between diabatic B and D' states is so large, 3000 cm^{-1}, that a strong coupling model is necessary to treat the problem. Our numerical close coupling code is set up as a three channel scattering problem to calculate the predissociation line shapes for the B and C bound levels which are strongly coupled to the D' continuum. Perturbation theory based on either a diabatic or adiabatic weak coupling model predicts the wrong results. It is necessary to calculate the predissociation widths and shifts in a strong coupling model which solves the coupled equations which treat the strong coupling between the B and D' states. One important consequence of this calculation is that the C state predissociation, which is much weaker than that of the B state, can be calculated using Fermi Golden Rule perturbation theory, but only if the golden rule matrix element is calculated between the unperturbed C state and the strongly coupled two channel B-D' mixed state. The correct C state widths can not be calculated by either a diabatic or adiabatic model of the D' state alone.

This work is still in progress to fine tune the parameters of the model. The model is capable of accounting for the magnitudes of the width and level shift perturbations, as well as the band oscillator strengths of the various B-X and C-X bands. The model is expected to predict the predissociation behavior of the higher members of the Rydberg series.

c. Intense Laser Photodissociation of H_2^+
(F. H. Mies and A. Giusti)

We are performing a joint theoretical study of the influence of intense laser fields on the photodissociation of diatomic molecules. This is motivated by experimental studies in Saclay, France [see C. Cornaggia, et al., Phys. Rev. A34, 207 (1986)] where non-linear contributions to the photodissociation of H_2^+ in a strong laser field has been observed in a multiphoton experiment involving the H_2 molecule. A four photon process leads to the production of the $H_2^+(1s\sigma_g)$ in a variety of vibrational rotational states depending on the laser frequency. (The ion is produced by photoionization of the $H_2(E^1\Sigma_g^+)$ excited state which is accessed by a three photon process). At field intensities in excess of $I = 10^{11} W/cm^2$ the observed photodissociation rate

$$H_2^+(1s\sigma_g, v^+) + h\nu \rightarrow H_2^+(2p\sigma_u, \epsilon) \rightarrow H(1s) + H^+ + \epsilon$$

exceeds the predictions of conventional weak-field theory, which ignores any field-induced distortions of the molecular states, and yields a linear dependence on I.

A photodissociation process may be viewed as a laser-induced predissociation of field-dressed molecular bound state imbedded in a field-dressed dissociation continuum with a radiative coupling strength $V_{rad}=eE\cdot d$ which is proportional to $|E| = (2I/c)^{1/2}$. In the weak-field limit the resultant predissociation rate is equivalent to the photodissociation rate and is proportional to I. In the strong-field limit the width and position of the field-dressed resonance state exhibits non-linear effects, and eventually adjacent vibrational states begin to overlap and lead to profound saturation effects.

Preliminary calculations using rigorous closed-coupled scattering codes and algorithms which solve driven equations needed to describe a bound-continuum transition yield results which are consistent with experimental observations. Our collaboration involves a number of interesting theoretical studies concerned with the proper gauge that is needed to describe the H_2^+ transition dipole; the comparison of complex variable methods versus multichannel close-coupled scattering codes applied to the laser-induced predissociation; and the proper description of a three-particle continuum that is needed to rigorously describe the simultaneous ionization-dissociation of the H_2 molecule.

Future experiments will be conducted at Saclay using two lasers of different frequency and intensity. This will provide a much more thorough analysis of the intense laser field modifications associated with the final photodissociation process and our theoretical calculations will be directed toward a rigorous description of such two-color experiments.

C.2 Generalized MCQDT applications.

a. Whole and Half Collision Matrix Methods for Multichannel Curve Crossing Problems
(F. H. Mies and Y. Band)

We have developed two new numerical methods of solving coupled quantum scattering equations which are most convenient for treating the dynamics of conventional atom collisions, which can be called a "full collision" process, as well as processes that proceed from an initial bound state, such as photodissociation, which can be viewed as a "half collision" process. In both cases we can also describe the scattering under the influence of intense laser fields. To describe any scattering process we begin by choosing a set of channel states sufficient to describe all the dynamic observables. For a given set of channels we must then construct an associated interaction matrix U(r) which contains all the physics of the collision process of interest. The dynamics is then completely defined by the resultant scattering matrix S which is obtained by solving the usual multichannel second-order Schrödinger equation.

Our new methods consist of replacing the multichannel second-order Schrödinger equation by an equally exact set of first order equations which allow us to numerically propagate a specially designed Half Collision Matrix X(r) which asymptotically defines the usual scattering matrix

$$S = e^{i\xi}X(X^*)^{-1}e^{i\xi}.$$

The method requires us to <u>choose</u> a set of diagonal reference potentials V(r) which then define a diagonal set of reference phase shifts ξ. Given our choice of V(r), which is completely at our disposal and can be chosen for our convenience in propagating the coupled equations, the resultant half collision amplitude X(r), which now incorporates all the non-adiabatic couplings between our reference channel states, is rigorously defined.

The matrix X(r) can only be propagated in classically open regions of configuration space. However, we can always derive a stable first-order algorithm for propagating the associated Full Collision Matrix $\Sigma(r) = X(X^*)^{-1}$ which is valid throughout all configuration space, and also asymptotically yields the required scattering matrix $S = e^{i\xi}\Sigma e^{i\xi}$. The numerical methods were applied to a multichannel curve crossing in atom diatom vibrational energy transfer collisions. Exact results (i.e., agreement with conventional close-coupled results for S were obtained using the Full Collision Matrix Method throughout all space, or applying the Half Collision Matrix Method in classically allowed regions. Many improvements, elaborations and applications of these numerical techniques will be developed in future collaborations.

In addition to these rigorously defined Matrices, a Classical Half Collision Matrix $Z(r) = e^{+\beta}X(r)e^{-i\beta}$ can be defined by introducing a WKB-like phase function $\beta(r)$ for each channel and then neglecting rapidly oscillating terms in the propagation of the first-order equations for Z(r) that are associated with the sum of such phases $\exp(\beta_i+\beta_f)$ and only retaining terms multiplied by phase differences $\exp(\beta_i-\beta_f)$. Although this random phase approximation is only valid if the non-adiabatic coupling is

restricted to classically accessible regions of coordinate space, it is quite a useful and generally valid approximation for most molecular dynamics. It has the important consequence that $Z(r)$ and hence the half collision amplitude is unitary, such that $X(r)X^{\dagger}(r)=1$ for all r. In this case, since we are no longer solving the coupled equations exactly, the choice of reference potentials $V(r)$ is much more critical. Fortunately, the best choice is generally made quite obvious simply by examining the exact interaction matrix $U(r)$ which defines the dynamics. This multichannel semiclassical approximation has many powerful applications in scattering theory and molecular spectroscopy. It is presently being applied to multichannel curve crossings, lineshape theory, and final state distributions of fine-structure states in photodissociation.

b. Factored Frame Transformation Half Collision Analysis of Collisions
(F. H. Mies)

Often is would appear that the complete dynamics of a multichannel scattering process can be physically separated into two or more distinct regions of space with uniquely different interactions and distinctly different combinations of channels which are strongly coupled. Such a situation is especially evident in atom-atom scattering and diatomic dissociation where strong chemical and electronic interactions, often represented in Hund's case (a) or (b), are prevalent at short distances, while weaker spin-orbit interactions dictate a predominately case (c) coupling only at intermediate distances, and ultimately, as $r\rightarrow\infty$, and nuclear angular momentum becomes dominant, we approach a pure case (e) representation. Further refinements are required if atomic hyperfine splittings are present, and of course external Stark and Zeeman fields will introduce further separate regions of dynamic couplings on the way to the asymptotic set of fragment internal states which define the scattering cross-sections. Let us choose to designate say i=1,N distinct regions of internuclear separation r

$$\text{Region(1)} \qquad 0 \leq r < r_1$$

$$\text{Region(i)} \qquad r_{i-1} < r < r_i$$

$$\text{Region(N)} \qquad r_{N-1} < r \leq \infty$$

based on the assumption that each region has some dynamically distinct feature which we choose to isolate for special consideration. In general, we can imagine that region N is where the hyperfine dynamics is dominant and all other couplings, such are couplings between any fine-structure states of the atoms have become negligible. The simple criterion for such a separation is that the fine-structure splittings of the atomic fragments are large compared to any residual molecular state interactions, but which, in turn, may be large or comparable to any hyperfine splittings. We can always include a complete set of channels that carry us from region 1 to region N and solve the complete dynamics exactly. However we choose these separate regions for our numerical convenience in blocking the complete interaction matrix $U(r)$ into dynamically uncoupled sub-sets of channels at various ranges of the internuclear coordinate r. Our intention is to solve the close-coupled dynamics separately in each region using these

substantially smaller subsets, and obtain an appropriately blocked half collision amplitude $X_i(r)$ at $r=r_i$ derived with the initial boundary condition $X_i=1$ at $r=r_{1-1}$. These can always be combined to obtain the exact asymptotic amplitude.

$$X(\infty) = X_1(r_1)\cdot X_2(r_2)\cdots X_i(r_i)\cdots X_N(\infty)$$

which then yields the complete scattering matrix $S = e^{i\xi}X(X^*)^{-1}e^{i\xi}$.

In general this separation is not especially useful since the form of the coupled equations for the amplitude $X_i(r)$ beginning at $r=r_{i-1}$, even with the initial boundary condition $X_i=1$, depends on the resultant amplitude $X_{i-1}(r_{i-1})$ obtained from the preceeding region. Fortunately, one very simplifying feature of most atomic collision processes, is that, except for the smallest region i=1 where curve crossings and predissociations are assumed to occur, all couplings between the atomic fragments generally occur in classically accessible regions. This implies that

$$X_i(r)X_i^{\dagger}(r) = 1 \text{ for all r and } i>1$$

In this case the propagation of $X_i(r)$ for $i>1$ is independent of the preceeding amplitude, and we can perform the scattering calculations separately in each region. The final structure of the scattering matrix takes the very useful form

$$S = [e^{i\xi}X_N\cdots X_2e^{-i\xi}]\ S_1\ [e^{-i\xi}X_2\cdots X_Ne^{i\xi}]$$

where S_1 is the scattering matrix defined by the short range interactions in the absence of the final state interactions contained in the product of amplitudes $X_N\cdots X_2$.

The structure of this factorized scattering matrix offers a multitude of powerful applications in spectroscopy and atom dynamics. The most immediate applications are being made in atomic lineshapes theory and in developing criteria for the use of frame transformation theory especially for product state distributions in photodissociation and predissociation.

c. Unified Half Collision Analysis of Photodissociation, Collisional Redistribution of Light, and Atomic Collisions
(P. S. Julienne)

The half collision methods which we have developed can be used to give a unified picture of a variety of collisional processes. In particular we have shown how the half collision factorization of the T matrix elements can be used to analyze and give a unified description of several kinds of processes which superficially seem to be different. Specifically the analysis is applied to collisional redistribution of light, molecular photodissociation, and atomic energy transfer collisions. In particular, we analyze recent experiments which involve the collision of two atoms, one of which is aligned or oriented. In one type of experiment, an atom is aligned in one frame prior to a collision in a beam frame, and the production of products measured as a function of angle between the two frames. In other experiments, a polarized photon is absorbed during a

collision or used to photodissociate a molecule, and the alignment of a product atom is detected. The underlying theme in the unified picture is a common half collision description of the collision dynamics.

We first obtain a separation of the cross sections into geometric factors which define the various experiments and reduced dynamical factors which are independent of experimental geometric parameters such as laser polarization direction or angle between laser and beam frames. The reduced dynamical factors depend on the angular momentum quantum numbers, but not space projection quantum numbers, and on T matrix elements calculated for a given total angular momentum J. These T matrix elements are the ones that would be found by a standard close coupling calculation for the coupled equations for the given J.

At this point approximations are introduced into the theory. We make the usual MCQDT separation into different zones of internuclear separation R characterized by distinct physics. There will always be a long range or asymptotic zone which describes the noninteracting separated atoms. There will also be one or more short range zones characterized by one or more molecular Born-Oppenheimer potentials and some Hund's coupling case. The collision dynamics describes the transitions between these different molecular zones and the asymptotic zones. We introduce the assumption that the transition in question between some initial and final molecular Born-Oppenheimer states occurs in a short range clasically allowed molecular zone where the reference states can be chosen so the interaction is described by weak coupling. The connection between the short range and asymptotic zones can be characterized by strong coupling in either the initial or final states. With these assumptions the half collision factored form of the T matrix can be used:

$$T(f \leftarrow i) = N_f t\, N_i ,$$

where N_i and N_f describe the respective initial and final state half collision dynamics which connect the asymptotic and short range transition zones and t describes the weak coupling Franck-Condon type transition at short range.

When the above factorization is used in the reduced dynamical cross section expressions, much physical insight about the collision dynamics can be obtained from constructing models of the N matrices. One such model is a sudden or recoil limit model which has been used widely in photodissociation experiments. We have also worked out the limiting expressions of this model for several different types of redistribution and aligned atom collision cases. The usual recoil limit model does not explain alignment experiments well because it neglects axis rotation dynamics. We have introduced a more accurate model of the N matrix, obtained by solving coupled semiclassical equations, to account for axis rotation dynamics. The model gives a satisfactory account of collisional redistribution experiments, and corresponds to a picture where the orbital alignment follows the rotating molecular axis over the short range part of its trajectory. The same N matrix model predicts that an aligned atom collision is described by an asymmetry parameter whose magnitude depends on the long range part of the trajectory where the alignment is <u>not</u> coupled to the rotating axis.

d. Generalized MCQDT Analysis of Molecular Bound States and Collision Cross Sections Involving Molecular Charge Transfer States
(F. H. Mies and S.-H. Pan)

Fully quantal calculations for the vibrational bound levels and adjoining continuum of alkali-halide charge transfer states have been made using new algorithms derived from the Milne quantum number function for the radial motion of the diatom. Because of the asymptotic coulombic interaction, the molecular potential actually supports an infinite number of bound vibrational states which conform to a Rydberg-like spectrum and can be characterized by a vibrational quantum defect. As predicted by conventional quantum defect theory for perturbed Rydberg series, we also observe that the vibrational quantum defect extrapolates across the dissociation limit to yield the threshold elastic scattering phase shift for the dissociative continuum state. The implicit dependence of the defect on the rotational state of the molecule yields a complete description of the rotational-vibrational spectrum. Because the system is heavy, the mass and rotational dependence of the computed quantum defects generally conform to appropriate WKB-like predictions. These numerical results are critical ingredients that are needed to describe the photodissociation spectra and predissociation of the alkali-halides.

Since the so called ionic or charge-transfer state of the alkali-halide molecule XM dissociates into a positively charged alkali metal $M^+(^1S)$ and a negatively charged halide ion $X^-(^1S)$, it must correspond to a non-degenerate $^1\Sigma^+$ state of the molecule. Asymptotically, this state lies just above the lowest $^1\Sigma^+$ state which correlates with the neutral ground state fragments $M(^2S) + X(^2P)$. Together these two $^1\Sigma^+$ states can be expected to dominate the two body collisional charge transfer processes. For example, the asymptotic splitting of the LiI system that we will be studying

$$Li(^2S) + I(^2P) \rightleftarrows Li^+(^1S) + I^-(^1S)$$

is just 2.329 eV. We use the prevalent diabatic representation of these states and designate $1^1\Sigma^+$ as the predominantly ionic state which describes the ground electronic state at r_{eq}, "diabatically" crosses the neutral $2^1\Sigma^+$ state at larger r_c, and asymptotically dissociates into ionic fragments.

Between the ionic and neutral thresholds the bound rotational-vibrational levels of the ionic $1^1\Sigma^+$ state will be predissociated by diabatic coupling to the dissociating covalent $2^1\Sigma^+$ state. Our calculations of the unperturbed bound and continuum states of the isolated ionic state are needed as preliminary data to our subsequent multichannel quantum defect analysis (MCQDA) of the predissociation and photodissociation of these molecules. The bound state phase $\nu_J(E)$ required in the MCQDA, $\nu_J(E) = \pi N_J(E)$ is simply the modular-π equivalent of the vibrational number function $N_J(E)$ for an isolated charge-transfer state. This analytic function defines the bound states by the condition $\tan \nu_J(E) = 0$ as $E \rightarrow E_{J,v}$ and is precursor to a more thorough and systematic analysis of the complete spectroscopy and dynamics of charge transfer systems. In particular the energy dependence of $\nu_J(E)$ is required to give exact analytic representations of the predissociation lineshapes and level shifts.

In previous studies of the charge-transfer dynamics only the diabatic coupling between the neutral and charge-transfer $^1\Sigma^+$ electronic states were included. Although the $1^1\Sigma^+ \rightarrow 2^1\Sigma^+$ coupling certainly dominates the dynamics, there are a total of 12 covalent electronic states ($^1\Sigma^+$, $^1\Pi$, $^3\Sigma$, $^3\Pi$) which correlate with the neutral ground state fragments and cross the ionic state. When combined with the angular momentum states of the rotating collision complex, six of the electronic states form channel states of the same parity and total angular momentum state J as the ionic collision complex, and a completely rigorous description of the scattering requires solving a seven channel close-coupling problem. However, our preliminary analysis of the predissociation suggests it is adequate to merely include additional coupling to the neutral $^3\Pi_0^+$ state and simply develop a three channel model. Using these three channels from pure case(c) molecular states, with appropriate radial, rotational and spin-orbit couplings, we have evaluated the partial widths for predissociation into the specific j=½ and j=3/2 fine-structure states of the $X(^2P)$. We have utilized a rigorous analytic multichannel quantum defect representation of this resonance scattering in order to isolate the effect of varying fine-structure splitting on the charge-transfer spectra for different alkali-halogen systems.

C.3. Theory of Ultracold Atom Collision Phenomena

Experimental methods for cooling and trapping atoms at ultracold temperatures have matured to the point that collisions of such atoms can now be observed. The collision cross section for associative ionization of two excited Na atoms has now been measured at NIST in an optical trap with T < 1 mK. Collisional processes are believed to limit the densities which are possible in neutral atom traps. Experimental studies of cooling and trapping of several other atomic ground and excited metastable species is currently in progress in various laboratories. We therefore expect that collisional and spectroscopic studies of ultracold collisions will become increasingly important in the future. The very low collision energy, long deBroglie wavelength, and long time scale associated with ultracold collisions result in many novel features of such collisions. We are beginning a program to develop the theory of ultracold collisions. The theoretical tools we have been developing for collisions in a radiation field and for MCQDT analysis of collisions can be naturally and readily applied to ultracold collisions. Some of our applications are described below.

a. Molecular Photoassociation Spectroscopy
(P. S. Julienne, H. Thorsheim, and J. Weiner)

The availability of ultracold atom sources offers the possibility of doing a new kind of high resolution molecular spectroscopy which can be used both as a probe of the collision and as way to access new Franck-Condon regions of the molecular spectrum. This is photoassociation spectroscopy, which can be represented by the equations,

$$A + A + \hbar\omega \rightarrow A_2^*$$
$$A_2^* \rightarrow \text{fluorescence} + A_2.$$

The process is very similar to the familiar laser induced fluorescence (LIF). The main difference is that the initial state in photoassociation is a continuum or scattering state instead of a bound state. During a collision of A with another A atom, the absorption of a photon excites a bound vibrational rotational level of an excited molecular state, which is then detected by its fluorescence. Having an ultracold source offers a great advantage over a normal or room temperature source. First, the excitation spectrum (fluorescence signal versus ω) will be very sharp, since thermal broadening due to the kT spread of collision energies is very small, e.g., kT/h = 21 MHz for T = 1 mK. Second, the cross section for the process near threshold will be much larger than at higher temperatures. A simple semiclassical reason for this is that the very slow moving atoms have much longer time to interact with the photon. Our theoretical calculations suggest that it should be possible to generate high enough photoassociation fluorescence signals to be measured.

We have carried out specific calculations for the magnitude of the photodissociation rate coefficient and spectrum for the case of collision of two ground state Na atoms. We treated the case of both the $^1\Sigma_u \leftarrow {}^1\Sigma_g$ and $^3\Sigma_g \leftarrow {}^3\Sigma_u$ absorptions. Note that in a collision the latter is just as likely as the former, so that the triplet spectrum is readily accessible. We used the well known molecular Born-Oppenheimer potentials and transition dipoles to calculate the spectra. A typical example is shown in Fig. 4.4, for absorption to v' = 130 of $^1\Sigma_u$ at a collision temperature of 10 mK. The spectrum shows well resolved rotational structure, with a rapid drop off to high N due to inability to penetrate the ground state centrifugal barrier. The transitions to N' = 3 and 5, and to a lesser extent, N' = 4 and 6, show enhancements due to shape resonances in the respective lower N" = 4 and 5 levels. Note that photoassociation Franck-Condon factors will favor high v' in the excited state, where the transition takes place at long range. Also note that the spectrum not only contains information about the excited state energy levels, but also about the lower state scattering resonances. A study of spectral intensities will give information about collision dynamics, and possibly can be used to improve the ground state potentials.

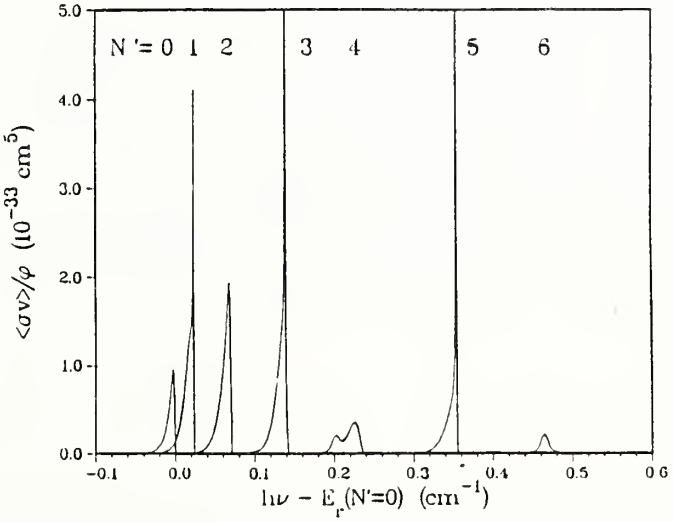

Fig. 4.4 Model photoassociation spectra at T = 0.01K for Na_2. The broadening of the lines is due to the thermal spread of collision energy in the ground state.

Our calculation suggests the feasibility of photoassociation experiments. The theory used was very simple and needs to be improved for realistic conditions. It is necessary to take into account the small relativistic electron and nuclear spin terms which affect the collision and especially the spectroscopy of the $^3\Sigma \rightarrow {}^3\Sigma$ transition. It is also necessary to take into account the true quantum threshold behavior of the cross section and the linewidth of the excited state due to spontaneous emission. We will continue to study the ultracold photoassociation process.

b. Associative Ionization Cross Sections of Na(3) + Na(3p) at 0.001 K.
(P. S. Julienne, W. D. Phillips, H. Thorsheim, and J. Weiner)

The NIST experimental laser cooling and trapping group of Dr. W. D. Phillips has succeeding in constructing an optical trap in which Na atoms are trapped at a density of 10^{10} cm^3 and temperature of 0.75 mK. Due to the strong laser tuned near the Na $^2P_{3/2} \leftarrow {}^2S_{1/2}$ resonant transition, there is a large fraction of excited atoms present in the trap. By measuring the current of Na_2^+ ions formed in the trap, the group measured the cross section for the associative ionization of two excited Na atoms to make molecular ions:

$$Na^* + Na^* \rightarrow Na_2^+ + e^-.$$

The cross section, 9×10^{-14} cm^2, is quite large and is about three orders of magnitude larger than the measured cross section at room temperature.

We have begun theoretical studies of such threshold cross sections. These are described more fully below. However, the plausibility of a large cross section can be readily established. The cross section can be written in the form,

$$\sigma = \pi(\lambda/2\pi)^2 \, (\ell_{max}+1)^2 \, P,$$

where ℓ_{max} partial waves are assumed to contribute and P is the probability of association ionization averaged over partial waves. P is a complicated dynamical quantity which depends on the molecular potentials, nonadiabatic mixings, spin-orbit and hyperfine interactions, and all other quantities which control the dynamics. Even if only a single s-wave is assumed to contribute to the cross section, an upper limit to the cross section can be found by assuming that P = 1. The upper limit is 6×10^{-13} cm^2, which is nearly an order of magnitude larger than the measured value. This shows that P is actually much less than unity, as we would expect. At room temperature P is known to be around 0.1.

c. Intense Laser Effects on Cross Sections in Optical Traps
(P. S. Julienne)

The laser intensity in the optical trap described in the previous section in which the associative ionization cross section was measured is very large, corresponding to a Rabi frequency of about 1400 MHz and an AC Stark shift in molecular potential energy which is about 50 times kT when

the two excited Na atoms are far apart. Since the Na_2 molecule detunes from and becomes decoupled from the laser field during the course of a collision because of the R-dependent molecular potentials, the nature of the molecule-field interaction changes dramatically during the course of the collision. We have therefore set up a simple model to describe the interaction of two like atoms which interact with each other and also with the laser field. We only consider interactions through the first order dipole-dipole multipole interaction term. It is necessary to introduce a 4-state model with treats the case of two ground state atoms, the degenerate case of one ground, one excited atom, and the case of two excited atoms. The model describes the separated atoms as two field-dressed atoms which interact with each other at long range with $1/R^3$ potentials in all 4 states. The atoms when close together form a molecule which is decoupled from the laser field. The adiabatic potentials which are found by diagonalizing the 4 x 4 interaction matrix give effective potentials on which the atoms move.

There are two important features of the model. First, the R-dependent decoupling of the molecule from the field at small R causes the asymptotic AC Stark shift to vanish at small R, thereby providing an R-dependent drop in the effective potential which accelerates the atoms towards one another and increases their collision velocity while the atoms are still far apart, $R > 100\ a_0$. Second, the long collision time makes it possible for spontaneous emission to be a significant loss process for collision processes involving excited states. In a strong field, strong coupling to the excitation laser occurs to short enough distance that the long range acceleration ensures a short enough collision time that spontaneous emission is not significant. However, in a weak field, there is little field induced acceleration and the decoupling from the exciting field occurs at such long distance that spontaneous emission prevents the excited state collision from continuing. The simple model therefore predicts that the associative ionization cross section at low collision energy will behave dramatically differently in strong and weak laser fields.

When the above simple model is applied to the conditions in the NIST optical trap, the model predicts about a 4 order of magnitude decrease in associative ionization cross section in optical molasses as compared to the optical trap. Since the NIST experiment is a time-alternating experiment between molasses and trap conditions, this prediction can be tested by time-resolving the ion and excited state fluorescence signals between the two conditions. In a recent experiment at NIST by Phillip's group, the qualitative theoretical prediction was dramatically confirmed! The ratio of ion signal in the trap to that in molasses was found to be about 50 with the present signal to noise, in spite of the fact that the fluorescence (excited state density) varied by less than a factor of 2. Thus, we have theoretical prediction and experimental confirmation that the nature of the collision dynamics is strongly influenced by the strength of the laser field. A reaction can be turned off or on by field-induced modification of collision dynamics.

d. Collision-induced Optical Trap Loss Processes
(P. S. Julienne, S.-H. Pan, H. Thorsheim, and J. Weiner)

Collisions between the species in an atom trap can lead to loss of atoms from the trap, and thereby limit the density of atoms which can be trapped. One example is the associative ionization process discussed above, which destroys two atoms in the trap. Other collisional trap destruction processes of an unknown nature have been observed by other groups. We have examined the following collisional loss process:

$$Na(3p) + Na(3s) \rightarrow Na(3s) + Na(3s) + \hbar\omega.$$

If the emitted photon is red shifted by $\Delta = \hbar\omega - \hbar\omega_0$ from the resonance transition frequency ω_0, an atom will escape from the trap if its kinetic energy $\Delta/2$ is greater than the trap depth D. This process is just the far red wing emission from the pressure broadened Na resonance line. Therefore, we need to calculate the spectrum and calculate the rate of emitting a photon with red shift greater than 2D. Since we have shown that a strong radiation field can have a large effect on collision dynamics, we will first consider only the case of a weak optical field in the trap.

We have calculated the emission spectrum by using the known long range form of the Na_2 potentials and transition dipoles. There are several possible transitions which contribute to the emission when a $Na\,^2P_{3/2}$ atom collides with a rare gas atom, namely, $0_u^+ \rightarrow 0_g^+$, $1_g \rightarrow 0_u^-$ or 1_u, $0_g^- \rightarrow 0_u^-$ or 1_u, and $1_u \rightarrow 0_g^+$. We have carried out fully quantum mechanical calculation of the spectrum for the $0_u^+ \rightarrow 0_g^+$ transition. We have also carried out a semiclassical calculation using the usual stationary phase and random phase approximations which give the quasistatic expression for the spectrum. Other than quantum oscillations about the envelope of the smooth semiclassical spectrum, the two are in quite good agreement even for a collision energy of 0.001 mK. It might at first glance seem surprising that semiclassical theory should work so well at large R where the interaction potential is only a few mK, but we find that the criterion for applicability of the WKB approximation, $d\lambda(R)/dR \ll 1$, is well satisfied here for the long range C_3/R^3 potential of the excited state. Therefore, the semiclassical theory can be used for all transitions. The semiclassical theory is analytically very simple, and for each transition only depends on the long range C_3 coefficient and transition dipole. The final expression for the rate coefficient for trap loss due to collisions with temperature T for a trap of depth T_D (both in Kelvin) takes on the simple form,

$$K(T,T_D) = F_s \times 1.3 \times 10^{-11}/(T^{1/6}T_D^{5/6})\ \text{cm}^3\ \text{sec}^{-1},$$

where F_s is a factor which takes into account the probability of survival versus spontaneous emission in the long range approach of the two atoms. The survival factor F_s is difficult to calculate accurately, but can be estimated from classical trajectory calculations. It is a sensitive function of T, but is between 0.1 and 0.01 for T on the order of 1 mK. The loss rate is comparable in magnitude to that due to associative ionization.

e. Quantum Threshold Effects in Ultracold Collisions
(P. S. Julienne)

The very low collision energy, and large deBroglie wavelength, in ultracold collisions raises the question of the nature of quantum threshold effects which might affect the cross section. The threshold laws for inelastic scattering processes are well known as a function of partial wave quantum number for different kinds of long range potentials. What is needed in this case is a study of actual cases using realistic potentials and masses of colliding atoms. The basic ideas can be readily stated in terms of the MCQDT formulation of the threshold behavior, although the ideas can be traced back at least as far as H. Bethe's 1935 study of threshold neutron scattering from atomic nuclei. The range of internuclear separation is divided into two zones. In the inner zone the wavefunction is approximated by the WKB wavefunction $\sin\beta(R)/k(R)^{1/2}$. In the long range zone the wavefunction is a linear combination of the regular and irregular Bessel functions, but the irregular function can not contribute as E→0 and the phase shift vanishes. The long range function is determined by energy normalization, and the short range WKB component must be matched to the long range form. The matching requires that the short range part be multiplied by a R-independent factor C(E) which depends on collision energy. When E is sufficiently large the WKB and long range Bessel function can always be matched by a WKB connection between large and small R, and C(E) = 1. As E→0 the small R decaying tail of the long range Bessel function can not be matched to the short range WKB function except by a function $C(E) \propto k_\infty^{1/2}$ in the case of an s-wave.

The T matrix element for a process which only occurs in the short range molecular zone will be proportional to the short range wavefunction, and therefore has the form,

$$T(E) = C(E)\, T_{short},$$

where T_{short} represents the amplitude for the short range process and is relatively insensitive to total energy. It is nearly constant as E→0. Therefore, the threshold behavior can be estimated by examining the C(E) function. This assumes the approximation that only a single potential is important. In reality, the asymptotic states are usually not nondegenerate, especially if hyperfine interactions are included, and several potentials can contribute. A full theory will require that we treat the long range multichannel interactions. However, a single channel theory is useful for estimating qualitative effects.

Therefore, we have calculated the C(E) function for a variety of cases. We have treated model cases involving collisions of Na atoms and collisions of two He ^3S metastable atoms. The latter are the subject of laser cooling efforts at the Ecole Normal Superieure in Paris, are likely to be cooled to $T \approx 30\ \mu K$ in a atom trap, and are known to Penning ionize in collisions at 20 K. Two s state atoms interact at long range with a potential which varies as $1/R^6$. The C(E) function shows the expected power law behavior at low enough collision energy. The critical energy where C(E) changes from its high energy value of unity depends on the potential and mass of colliding atoms. In particular the threshold shape is quite sensitive to the proximity of the last bound state of the potential to threshold. C(E)

can manifest structure due to shape resonances for angular momentum quantum number $\ell \geq 1$. Even an s-wave, $\ell = 0$, can exhibit "resonance" like structure if a bound state exists sufficiently close to threshold. For two ground state Na atoms, C(E) shows departure from unity for collision energies on the order of 1 mK and less, with power law threshold behavior evident below 100 μK. It is possible for s, p, and perhaps also d waves to contribute to Na scattering at 1 mK. However, He ^{3}S meta-stable collisions show departure from unity for collision energies on the order of 10 mK. Only s waves are likely to contribute at 30 μK. The detailed shape of C(E) is very sensitive to the whole potential, since it depends on the position of the last bound state. Ultracold collisions are likely to sample the range of collision energies where quantum threshold effects are important, but the extreme sensitivity of the threshold behavior to the details of the potential will make predicitive calculations difficult. Perhaps experimental studies can be used to refine experimental or theoretical potential models.

Collisions of ground and excited states of like atoms with $1/R^3$ potentials will be much less sensitive to the potentials. The C(E) function remains unity even to temperatures below 1 μK, and semiclassical theory can be used just as at higher temperatures. This was discussed above in the discussion on collision-induced trap loss processes.

The near threshold magnitude of the cross section for an inelastic exothermic process is likely to be very large. In fact, the cross section diverges as 1/v as the collision velocity $v \rightarrow 0$ at threshold. This was pointed out long ago by Bethe (1935) in connection with threshold neutron scattering. The collision rate coefficient, $T\sigma$, remains finite, however. The observed large value of near threshold cross section for Na^* associative ionization is consistent with this general expectation of large threshold cross section for such processes.

f. Ultracold Collisions in Magnetic Fields
(F. H. Mies, P. S. Julienne, and C. J. Williams)

Since some varieties of neutral atom traps use a magnetic field in the trapping process, it is necessary to develop the theory needed to describe collisions in a magnetic field. Collisions in a magnetic field may result in trap loss processes, just as for collisions in an optical field. Since Zeeman shifts, just like AC Stark shifts, can be many times kT, the magnetic field can cause large perturbations on the collision just as a laser field can. In many ways it is simpler to formulate the problem of collisions in a static magnetic field than in an oscillating electromagnetic field, since the problem of spontaneous emission during the collision need not be considered for the former if only ground state collisions are treated.

We have begun to develop the Hamiltonian matrix necessary to set up a close coupled calculation of the cross sections which describe scattering of two like atoms in ^{2}S ground states with nuclear spin I. We consider the ordinary molecular electronic-rotational Hamiltonian, the various spin-dependent interactions (electron-electron, electron-nuclear, and nuclear-nuclear), and the magnetic field interaction. We have formulated the frame transformation between the Hund's case (a) basis in the molecular frame and

the asymptoptic basis in the laboratory frame in which the Zeeman sublevels are quantized along the magnetic field axis. The molecular $^1\Sigma_g^+$ and $^3\Sigma_u^+$ potentials are defined in the former frame, and the asymptotic scattering states are defined in the latter. We intend to treat the cases of H (I=1/2) and Na (I=3/2). We have written a computer code to calculate the S-matrix for these cases. Detailed calculations will be carried out in the future.

5. PUBLICATIONS

(a) Publications in Print, October 1986 - September 1987

Basch, H., Krauss, M., and Stevens, W. J., "Electronic Structure of Diammine (ascorbate) Platinum II and the Trans Influence on the Ligand Dissociation Energy," Inorg. Chem. 25, 4777 (1986).

Basch, H., Krauss, M., and Stevens, W. J., "Cation Binding Effect on Imidazole Tautomerism," Int. J. Quant. Chem. 31, 405 (1987).

Burgess, D. R., Jr., King, D. S., and Cavanagh, R. R., "Kinetics and Dynamics of the Nitric Oxide/Ammonia Interaction on Pt(111)," J. Vac. Sci. Tech. A5, (1987).

Burkholder, J. B., Hammer, P. D., Howard, C. J., Maki, A. G., Thompson, G., and Chackerian, C., "Infrared Measurements of the C10 Radical," J. Mol. Spectrosc. 124, 139-161 (1987).

Casassa, M. P., Stephenson, J. C., and King, D. S., "Vibrational Predissociation of the Nitrix Oxide Dimer," Faraday Discuss. Chem. Soc. 82, 251, (1986).

Casassa, M. P., Woodward, A. M., Stephenson, J. C., and King, D. S., "Picosecond Measurements of the Dissociation Rates of the Nitric Oxide Dimer ν_1 (v=1) and ν_4 (v=1) Levels," J. Chem. Phys. 85, 6235 (1986).

Coudert, L., Maki, A. G., and Olson, Wm. B., "High Resolution Measurements of the ν_2 and $2\nu_2$-ν_2 Bands of SO_2," J. Mol. Spectrosc. 124, 437-442 (1987).

Fraser, G. T. and Pine, A. S., "Van der Waals Potentials from the Infrared Spectra of Rare Gas-HF Complexes," J. Chem. Phys. 85, 2502 (1986).

Fraser, G. T., Suenram, R. D., and Lovas, F. J., "Nearly Free Internal Rotation in Ar-CH_3Cl," J. Chem. Phys. 86, 3107-3114 (1987).

Fraser, G. T., Pine, A. S., Lafferty, W. J., and Miller, R. E., "Sub-Doppler Infrared Spectrum of the CO_2 Trimer," J. Chem. Phys. 87, 1502 (1987).

Heilweil, E. J., Casassa, M. P., Cavanagh, R. R., and Stephenson, J. C., "Population Lifetimes of OH(v=1) and OD(v=1) Stretching Vibrations of Alcohols and Silanols in Dilute Solution," J. Chem. Phys. 85, 5004 (1986).

Heilweil, E. J., Casassa, M. P., Cavanagh, R. R., and Stephenson, J. C., "Picosecond Studies of Vibrational Energy Transfer in Molecules on Surfaces," J.O.S.A. B3, No. 8, Part 2, P140 (1986).

Heilweil, E. J., Casassa, M. P., Cavanagh, R. R., and Stephenson, J. C., "Population Lifetimes of OH(v=1) and OD(v=1) Vibrations in Alcohols, Silanols, and Crystalline Micas," in Ultrafast Phenomena IV, Springer-Verlag Series in Chemical Physics Vol. 46, 465-468 (1986).

Heilweil, E. J., Cavanagh, R. R., and Stephenson, J. C., "Population Relaxation of CO(v=1) Vibrations in Solution Phase Metal-Carbonyl Complexes," Chem. Phys. Lett. 134, 181 (1987).

Hinz, A., Wells, J. S., and Maki, A. G., "Heterodyne Measurements of Hot Bands and Isotopic Transitions of N_2O Near 7.8μm," Z. Phys. D5, 351-358 (1987).

Hougen, J. T., "Hydrogen Migration Tunneling Effects in the Rotational and Vibrational Spectrum of Protonated Acetylene $C_2H_3^+$," J. Mol. Spectrosc. 123, 197-227 (1987).

Jacox, M. E. and Olson, Wm. B., "The A $^2\Pi$ - X $^2\Sigma_g^+$ Transition of HC_2 Isolated in Solid Argon," J. Chem. Phys. 86, 3134-3142 (1987).

Jacox, M. E., "Comparison of the Electronic Energy Levels of Diatomic Molecules in the Gas Phase and in Inert Solid Matrices," J. Mol. Struct. 157, 43-59 (1987).

Jacox, M. E., "Analysis of the Vibrational Spectrum of the Nitromethyl Free Radical," J. Phys. Chem. 91, 5038-5041 (1987).

Jasien, P. G., Stevens, W. J., and Krauss, M., "Ab Initio Calculations of the Rotational Barriers in Formamide and Acetamide: The Effects of Polarization Functions and Correlation," J. Mol. Struct. Theochem., 139, 197-206 (1986).

Jucks, K. W., Huang, Z. S., Dayton, D., Miller, R. E., and Lafferty, W. J., "The Structure of the Carbon Dioxide Dimer from Near Infrared Spectroscopy," J. Chem. Phys. 86, 4341 (1987).

Julienne, P. S. and Mies, F. H., "Nonadiabatic Theory of Atomic Line Broadening: Redistribution Calculations for Sr(^{1}P $\leftarrow$ ^{1}S) + Ar," Phys. Rev. A34, 3729 (1986).

Julienne, P. S. and Vahala, L. L., "Close Coupled Theory of Fine Structure Transitions in Collisional Redistribution," in Spectral Line Shapes, Vol. 4, ed. by R. Exton (Deepak Publishing, Hampton, VA) 1987, pp. 397-411.

Lafferty, W. J., Suenram, R. D., and Lovas, F. J., "The Microwave Spectra of the $(HF)_2$, $(DF)_2$, HFDF, and DFHF Hydrogen-Bonded Complexes," J. Mol. Spectrosc. 123, 434 (1987).

Lovas, F. J., "Erratum: Recommended Rest Frequencies for Observed Interstellar Molecular Microwave Transitions - 1985 Revision, J. Phys. Chem. Ref. Data 16, 251-252 (1987).

Lovas, F. J., Suenram, R. D., Ross, S., and Klobukowski, M., "Rotational, Structural, Ab Initio and Semirigid Bender Analysis of the Millimeter Wave Spectrum of H_2CO-HF," J. Mol. Spectrosc. 123, 167-186 (1987).

Lovas, F. J. and Suenram, R. D., "Pulsed Beam Fourier Transform Microwave Measurements on OCS and Rare Gas Complexes of OCS with Ne, Ar, and Kr," J. Chem. Phys. 87, 2010-2020 (1987).

Mialocq, J.-C. and Stephenson, J. C., "Picosecond Laser Induced Flurorescence Study of the Collisionless Photodissociation of Nitrocompounds at 266 nm," Chem. Phys. 106, 281 (1986).

Mies, F. H., Julienne, P. S., Band, Y. B., and Singer, S. J., "A Converged Analysis of Radiative Matrix Elements in Atomic Lineshape Theory," J. Phys. B19, 3249 (1986).

Nelson, D. D., Jr., Fraser, G. T., Peterson, K. I., Zhao, K., Klemperer, W., Lovas, F. J., and Suenram, R. D., "The Microwave Spectrum of the K=0 States of Ar-NH_3," J. Chem. Phys., 85, 5512 (1986).

Ohashi, N. and Hougen, J. T., "The Torsional-Wagging Tunneling Problem and the Torsional-Wagging-Rotational Problem in Methylamine," J. Mol. Spectrosc. 121, 474-501 (1987).

Olson, Wm. B., "Method for First-order Design of a Transfer Optics System to Throughput Match a Fourier Transform Spectrometer to a Sample Cell Without Use of a Field Lens at the Cell Input," Appl. Optics 26, 2441-2445 (1987).

Peterson, K. I., Fraser, G. T., Nelson, D. D., Jr., and Klemperer, W., "Intermolecular Interactions Involving First Row Hydrides: Spectroscopic Studies of Complexes of HF, H_2O, NH_3, and HCN," in Comparison of Ab Initio Quantum Chemistry with Experiment: State-of-the-Art, ed. by R. J. Bartlett (Reidel, NY) (1986).

Pine, A. S., and Looney, J. P., "N_2 and Air Broadening in the Fundamental Bands of HF and HCl," J. Mol. Spectrosc. 122, 41-55 (1987).

Pine, A. S., "Vibrational Anomalies and Dynamic Coupling in Hydrogen-Bonded van der Waals Molecules," in NATO Workshop on Structure and Dynamics of Weakly Bound Molecular Complexes, ed. by A. Weber (Reidel, Holland) (1987).

Stevens, W. J. and Fink, W. H., "Frozen Fragment Reduced Variational Space Analysis of Hydrogen Bonding Interactions. Application to the Water Dimer," Chem. Phys. Lett. 139, 15 (1987).

Thompson, G. A., Maki, A. G., Olson, Wm. B., and Weber, A., "High Resolution Infrared Spectrum of the Fundamental Band of LiCl at a Temperature of 830°C," J. Mol. Spectrosc. 124, 130-138 (1987).

Thorsheim, H., Weiner, J., and Julienne, P. S., "Laser Induced Photoassociation of Ultracold Sodium Atoms," Phys. Rev. Lett. 58, 2420 (1987).

Weber, A., Ed. Molecular Spectroscopy Division, Technical Activities, 1986, NBSIR-86-3483, (1986).

Weber, A., "The Molecular Spectroscopy Division of the National Bureau of Standards," Applied Spectroscopy, 41, 1085 No. 7, (1987).

Zink, L. R., Wells, J. S., and Maki, A. G., "Heterodyne Frequency Measurements on N_2O near 1060 cm^{-1}," J. Mol. Spectrosc. 123, 426-433 (1987).

(b) Publications in Print, October 1987 - September 1988

Alexander, M. H., Andersen, P., Bacis, R., et al., "A Nomenclature for Lambda Doublet Levels in Rotating Linear Molecules," J. Chem. Phys. 89, 1749 (1988).

Band, Y. and Mies, F. H., "Half and Full Collision Methods," J. Chem., Phys. 88, 2309 (1988).

Basch, H., Krauss, M., and Stevens, W. J., "Cation Binding Effect on Imidazole Tautomerism," Int. J. Quantum Chem., 31, 405, (1987).

Buck, U., Meyer, H., Nelson, D., Jr., Fraser, G. T., and Klemperer, W., "Fragmentation of NH_3 Dimers by Electron Impact Ionization," J. Chem. Phys. 88, 3028 (1988).

Buntin, S. A., Richter, L. J., Cavanagh, R. R., and King, D. S., "Optically Driven Surface Reactions: Evidence for the Role of Hot Electrons," Phys. Rev. Letts. 61, 1321 (1988).

Burgess, D., Jr., King, D. S., and Cavanagh, R. R., "Kinetics and Dynamics of the Nitric Oxide/Ammonia Interaction on Pt(111)," J. Vac. Sci. Tech. A5, 2959 (1987).

Burgess, D., Jr., Cavanagh, R. R., and King, D. S., "Laser-induced Desorption: Thermal and Non-thermal Pathways," J. Chem. Phys. 88, 6556 (1988).

Callomon, J. H., Hirota, E., Kuchitsu, K., and Lafferty, W. J., "Structure Data of Free Polyatomic Molecules," Vol. 7A Landolt-Börnstein, Springer Verlag, Berlin (1988).

Casassa, M. P. "Direct Time Resolved Observations of Vibrational Energy Flow in Weakly Bound Complexes," Chem. Rev. 88, (1988).

Casassa, M. P., Stephenson, J. C., and King, D. S., "Vibrational Predissociation Dynamics of the Nitric Oxide Dimer," in Atomic and Molecular Processes with Short Intense Laser Pulses, edited by A. D. Bandrauk, NATO ASI Series B171, 367, (1987).

Casassa, M. P., Stephenson, J. C., and King, D. S., "Time- and State-Resolved Measurements of Nitric Oxide Dimer Infrared Predissociation," J. Chem. Phys. 89, 1966 (1988).

Cavanagh, R. R., Casassa, M. P., Heilweil, E. J., and Stephenson, J. C., "Vibrational Relaxation of Adsorbed Molecules: Comparison with Relaxation Rates of Model Compounds," J. Vac. Sci. Technol. A, 5, 469 (1987).

Cavanagh, R. R., Heilweil, E. J., and Stephenson, J. C., "Time-Domain Measurements of Vibrational Relaxation at Surfaces: CO(v=1) in Metal Carbonyl Systems," J. Electron Spectroscopy and Rel. Phenom., 45, 31-40 (1987).

Coudert, L. H., Lovas, F. J., Suenram, R. D., and Hougen, J. T., "New Measurements of Microwave Transitions in the Water Dimer," J. Chem., Phys. 87, 6290-6299 (1987).

Coudert, L. H. and Hougen, J. T., "Tunneling Splitting in the Water Dimer: Further Development of the Theory," J. Mol. Spectrosc. 130, 86-119 (1988).

Foy, B. R., Casassa, M. P., Stephenson, J. C., and King, D. S., "Unimolecular Dynamics Following Vibrational Overtone Excitation of HN_3, ν_1=5, and ν_1=6: $HN_3(X; \nu,J,K) \rightarrow HN (X^3\Sigma^-; \nu,J,\Omega) + N_2(X\ ^1\Sigma_g^+)$," J. Chem. Phys. 89, 608 (1988).

Fraser, G. T., Suenram, R. D., and Lovas, F. J., "Nearly Free Internal Rotation in Ar-CH_3Cl," J. Chem. Phys. 86, 3107 (1987).

Fraser, G. T., Pine, A. S., Lafferty, W. J., and Miller, R. E., "Sub-Doppler Infrared Spectrum of the CO_2 Trimer," J. Chem. Phys. 87, 1502 (1987).

Fraser, G. T., Gillies, C. W., Zozom, J., Lovas, F. J., and Suenram, R. D., "Rotational Spectrum and Structure of H_2CO-HCl," J. Mol. Spectrosc. 126, 200-209 (1988).

Fraser, G. T. and Pine, A. S, "Isotope Effects in the High Resolution Infrared Spectrum of OC-HF," J. Chem. Phys. 88, 4147 (1988).

Fraser, G. T., Pine, A. S., and Suenram, R. D., "Optothermal-Infrared and Pulsed-Nozzle Fourier-Transform Microwave Spectroscopy of Rare Gas-CO_2 Complexes," J. Chem. Phys. 88, 6157-6167 (1988).

Fraser, G. T., Suenram, R. D., Lovas, F. J., and Stevens, W. J., "Microwave Spectrum of the CH_3OH-NH_3 Complex," Chem. Phys. 125, 31 (1988).

Gould, P. L., Lett, P. D., Julienne, P. S., Phillips, W. D., Thorsheium, H. R., and Weiner, J., "Observation of Associative Ionization of Ultracold Laser Trapped Sodium Atoms," Phys. Rev. Letts. 60, 788 (1988).

Heilweil, E. J., Cavanagh, R. R., and Stephenson, J. C., "CO(v=1) Population Lifetimes of Metal-Carbonyl Cluster Compounds in Dilute $CHCl_3$ Solution," J. Chem. Phys. 89, 230 (1988).

Heilweil, E. J., Cavanagh, R. R., and Stephenson, J. C., "Population Relaxation of CO(v=1) Vibrations in Solution Phase Metal-Carbonyl Complexes," Chem. Phys. Letts. 134, 181 (1987).

Heilweil, E. J., Cavanagh, R. R., and Stephenson, J. C., "Vibrational Relaxation of Carbon Monoxide on Metal Clusters," Ultrafast Phenomena V, Springer-Verlag (1988).

Hougen, J. T., "Hydrogen Migration Tunneling Effects in the Rotational and Vibrational Spectrum of Protonated Acetylene C_2H_3+," J. Mol. Spectrosc. 123, 197-227 (1987).

Jacox, M. E. and Olson, W. B., "The A $^2\Pi$ - X $^2\Sigma_g^+$ Transition of HC_2 Isolated in Solid Argon," J. Chem. Phys. 86, 3134-3142 (1987).

Jacox, M. E., "Comparison of the Electronic Energy Levels of Diatomic Molecules in the Gas Phase and in Inert Solid Matrices," J. Mol. Struct. 157, 43-59 (1987).

Jacox, M. E., "Analysis of the Vibrational Spectrum of the Nitromethyl Free Radical," J. Phys. Chem. 91, 5038-5041 (1987).

Jacox, M. E., "Vibrational and Electronic Spectra of the H + HCN Reaction Products Trapped in Solid Argon," J. Phys. Chem. 91, 6595-6600 (1987).

Jacox, M. E., "The Vibrational Spectrum of the t-HOCO Free Radical Trapped in Solid Argon," J. Chem. Phys. 88, 4598-4607 (1988).

Jacox, M. E., "Electronic Energy Levels of Small Polyatomic Transient Molecules," J. Phys. Chem. Ref. Data 17, 269-511 (1988).

Jasien, P. G. and Stevens, W. J., "Theoretical Calculations of Diatomic Metal Oxides, CrO and CrO^+," Chem. Phys. Letts. 147, 72 (1988).

Jucks, Z., Huang, S., Miller, R. E., Fraser, G. T., Pine, A. S., and Lafferty, W. J., "Structure and Vibrational Dynamics of the CO_2 Dimer from the Sub-Doppler Infrared Spectrum of the 2.7μm Fermi Diad," J. Chem. Phys. 88, 2185 (1988).

Julienne, P. S. and Vahala, L. L., "Close Coupled Theory of Fine Structure Transitions in Collisional Redistribution," in Spectral Line Shapes, Vol. 4, ed. by R. Exton (Deepak, Hampton, VA) (1987).

Julienne, P. S., "Laser Modification of Ultracold Atomic Collisions in Optical Traps," Phy. Rev. Letts. 61, (1988).

Krauss, M., Basch, H., and Miller, K. J., "Comparison of Direct and Through Water Binding of Pt Ammines to the Phosphate Amion," J. Am. Chem. Soc. 110, 4517 (1988).

Krauss, M., Regan, R. M., Konowalow, D. D., "Rare-gas Interaction Energy Curves," J. Phys. Chem. 92, 4329 (1988).

Krauss, M., Basch, H., and Miller, K. J., "Hydrogen Bonding in Pt Ammine Complexes," J. Chem. Phys. Lett. 148, 577 (1988).

Lafferty, W. J., Suenram, R. D., and Lovas, F. J., "The Microwave Spectra of the $(HF)_2$, $(DF)_2$, HFDF and DFHF," J. Mol. Spectrosc. 123, 434-452 (1987).

Leubner, C. and Hougen, J. T., "WKB Potential Well Ground States without Matching?" Ann. Phys. (NY) 181, 284-289 (1988).

Lovas, F. J., Suenram, R. D., Ross, R., and Klobukowski, M., "Rotational, Structural, Ab Initio and Semirigid Bender Analysis of the Millimeter Wave Spectrum of H_2CO-HF," J. Mol. Spectrosc. 123, 167-186 (1987).

Lovas, F. J. and Suenram, R. D., "Pulsed Beam Fourier Transform Microwave Measurements on OCS and Rare Gas Complexes of OCS with Ne, Ar, and Kr," J. Chem. Phys. 87, 2010-2020 (1987).

Lovas, F. J., Suenram, R. D., Fraser, G. T., Gillies, C. W., and Zozom, J., "The Microwave Spectrum of Formamide-Water and Formamide-Methanol Complexes," J. Chem. Phys. 88, 722-729 (1988).

Maki, A. G. and Lovas, F. J., "The Infrared Spectrum of the $\Delta v=2$ Transitions of Lead Sulfide (PbS)," J. Mol. Spectrosc. 125, 188-195 (1987).

Maki, A. G., "High Resolution Measurements of the ν_2 Band of HNO_3 and the ν_3 Band of trans-HONO," J. Mol. Spectrosc. 127, 104-111 (1988).

Maki, A. G., Olson, W. B., Wells, J. S., and Vanek, M. D., "Heterodyne and FTS Measurements on the OCS Hot Bands near 1890 cm^{-1}," J. Mol. Spectrosc. 130, 69 (1988).

Maki, A. G., Burkholder, J. B., Sinha, A., and Howard, C. J., "Fourier Transform Infrared Spectrum of the BO_2 Radical," J. Mol. Spectrosc. 130, 238 (1988).

Nelson, D. D., Jr., Klemperer, W., Fraser, G. T., Lovas, F. J., and Suenram, R. D., "Ammonia Dimer: Further Structural Studies," J. Chem. Phys. 87, 6364-6372 (1987).

Nelson, D. D., Jr., Fraser, G. T., and Klemperer, W., "Does Ammonia Hydrogen Bond?" Science, 238, 1670 (1987).

Novick, S. E., Suenram, R. D., and Lovas, F. J., "Determination of the Structure of OCS CO_2," J. Chem. Phys. 88, 687-690 (1988).

Ohashi, N. and Hougen, J. T., "The Torsional-Wagging Tunneling Problem and the Torsional-Wagging-Rotational Problem in Methylamine," J. Mol. Spectrosc. 121, 474-501 (1987).

Ohashi, N., Takagi, K., Hougen, J. T., Olson, W. B., and Lafferty, W. J., "Far Infrared Spectrum and Ground State Constants of Methyl Amine," J. Mol. Spectrosc. 126, 443-459 (1988).

Olson, W. B., Hunt, R. H., Young, B. W., Maki, A. G., and Brault, J. W., "Rotational Constants of the Lowest Torsional Component (OG) of the Ground State and Lowest Torisional Component (1G) of the First Excited Torsional State of Hydrogen Peroxide," J. Mol. Spectrosc. 127, 12-34 (1988).

Pan, S.-H. and Mies, F. H., "Rydberg-like Properties of Rotational Vibrational Levels in Alkali-Halide Charge Transfer States," J. Chem. Phys. 89, 3096 (1988).

Pine, A. S. and Looney, J. P., "N_2 and Air Broadening in the Fundamental Bands of HF and HCl," J. Mol. Spectrosc. 122, 41-55 (1987).

Pine, A. S., "Vibrational Anomalies and Dynamic Coupling in Hydrogen-Bonded van der Waals Molecules," Structure and Dynamics of Weakly Bound Molecular Complexes, NATO ASI Series C 212, 93-105 (1987); ed. by A. Weber (D. Reidel, Holland).

Pine, A. S. and Fraser, G. T., "Vibrational Predissociation in the CO_2 Dimer and Trimer and Rare Gas-CO_2 Complexes," J. Chem. Phys. 89, 100 (1988).

Pliva, J. and Pine, A. S., "Analysis of the 3 μm Bands of Benzene," J. Mol. Spectrosc. 126, 82-98 (1987).

Schaeffer, R. D., Lovejoy, R. W., W. B. Olson, and Tarrago, G., "High-resolution Infrared Spectrum of $^{28}SiH_3D$ from 1450 to 1710 cm^{-1}," J. Mol. Spectrosc. 128, 135-150 (1988).

Stephenson, J. C., Casassa, M. P., and King, D. S., "Energetics and Spin and Λ-doublet Selectivity in the Infrared Multiphoton Dissociation $DN_3 \rightarrow DN(X^3\Sigma, a^1\Delta) + N_2(X)$: Experiment," J. Chem. Phys. 89, 1378-1387 (1988).

Stevens, W. J. and Fink, W. H., "Frozen Fragment Reduced Variational Space Analysis of Hydrogen Bonding Interactions. Application to the Water Dimer," Chem. Phys. Lett. 139, 15 (1987).

Suenram, R. D. and Lovas, F. J., "Microwave Spectrum of the Ar-Vinyl Cyanide van der Waals Complex," J. Chem. Phys. 87, 8 4447-4455 (1987).

Suenram, R. D., Lovas, F. J., and Fraser, G. T., "Microwave Spectrum of ^{14}N Quadrupole Coupling Constants of Indole," J. Mol. Spectrosc. 127, 472-480 (1988).

Thorsheim, H. R., Weiner, J., and Julienne, P. S., "Laser-induced Photo-dissociation of Ultracold Sodium Atoms," Phys. Rev. Letts. 58, 2420 (1987).

(c) Publications in Progress

Burgess, D., Jr., Cavanagh, R. R., and King, D. S., "NO/NH_3 Coadsorption on Pt(111): Kinetic and Dynamical Effects in Rotational Accommodation," submitted to Surface Science.

Fraser, G. T., Suenram, R. D., and Lovas, F. J., "Electric-Dipole Moments of H_2O-Formamide and CH_3OH-Formamide," J. Mol. Struct. (in press).

Fraser, G. T., Suenram, R. D., Lovas, F. J., Pine, A. S., Hougen, J. T., Lafferty, W. J., and Muenter, J. S., "Infrared and Microwave Investigations of Interconversion Tunneling in the Acetylene Dimer," J. Chem. Phys. (in press).

Fraser, G. T., Pine, A. S., Suenram, R. D., Dayton, D. C., and Miller, R. E., "Infrared and Microwave Spectra of OCO-HF and SCO-HF," J. Chem. Phys. (submitted).

Fraser, G. T., "The Vibrational Exchange Upon Interconversion Tunneling in $(HF)_2$ and $(HCCH)_2$," J. Chem. Phys. (submitted).

Garmer, D. R. and Anderson, J. B., "Potential Energies for the Reaction F + $H_2 \rightarrow$ HF + H by the Random Walk Method," J. Chem. Phys. (in press).

Garmer, D. R., "Effective Diffusion Quantum Monte Carlo without Time-Step Errors," J. Comp. Chem. (in press).

Gillies, J. Z., Gillies, C. W., Suenram, R. D., and Lovas, F. J., "The Ozonolysis of Ethylene. Microwave Spectrum, Molecular Structure and Dipole Moment of the Primary Ozonide," J. Am. Chem. Soc. (in press).

Goldman, A., Burkholder, J. B., Howard, C. J., Escribano, R., and Maki, A. G., "Spectroscopic Constants for the ν_9 Infrared Band of HNO_3," J. Mol. Spectrosc. (in press).

Gould, P. L., Lett, P. D., Watts, R. N., Westbrook, C. I., Julienne, P. S., Phillips, W. D., Thorsheim, H. R., and Weiner, J., "Associative Ionization of Ultracold Laser-trapped Sodium Atoms," in Proceedings of the Eleventh International Conference on Atomic Physics (in press).

Heilweil, E. J., Stephenson, J. C., and Cavanagh, R. R., "Measurements of CO(v=1) Population Lifetimes: Metal-carbonyl Cluster Compounds Supported on SiO_2," J. Phys. Chem. (in press).

Heilweil, E. J., Cavanagh, R. R., and Stephenson, J. C., "Picosecond Study of the Population Lifetime of CO(v=1) Chemisorbed on SiO_2-supported Rhodium Particles," J. Chem. Phys. (in press).

Heilweil, E. J., Cavanagh, R. R., and Stephenson, J. C., "Vibrational Relaxation Measurements of Carbon Monoxide on Metal Clusters," Proceedings of the Sixth International Conference on Ultrafast Phenomena, Springer Verlag Pub. (in press).

Jacox, M. E., "The Stabilization and Spectroscopy of Free Radicals and Reactive Molecules in Inert Matrices," in Chemistry and Physics of Matrix Isolated Species, L. Andrews and M. Moskovits, Eds. (North-Holland Physics Publishing, Amsterdam, The Netherlands), (in press).

Jewell, P. R., Hollis, J. M., Lovas, F. J., and Snyder, L. E., "Microwave Surveys of Orion A Emission Lines in the Ranges: 200.8-202.3 GHz, 203.8-205.3 GHz, and 330-360 GHz," Astrophys. J. Suppl. (submitted).

Julienne, P. S. and Frommhold, L., "Roundtable Discussion on Laser-induced Collisions and Collision-induced Spectra," in Spectral Line Shapes, Vol. 5, ed. by J. Szudy (submitted).

King, D. S. and Cavanagh, R. R., "Molecular Desorption from Solid Surfaces: Laser Diagnostics and Chemical Dynamics," in Molecular Surface Interactions, K. Lawley, ed., Advances in Chemical Physics (J. Wiley and Sons, London).

Krauss, M. and Stevens, W. J., "A Theoretical Model of Metal Binding Sites in Proteins," Proceeding of the 1988 Oholo Conference (in press).

Leung, H. O., Marshall, M. D., Suenram, R. D., and Lovas, F. J., "Microwave Spectrum and Molecular Structure of the N_2-H_2O Complex," J. Chem. Phys. (in press).

Lovas, F. J. and Suenram, R. D., "Microwave Spectral Tables III. Hydrocarbons, CH to $C_{10}H_{10}$," J. Phys. Chem. Ref. Data (in press).

Maki, A. G. and Olson, W. B., "Infrared Spectrum of the ν_6, ν_7, and ν_8 Bands of HNO_3," J. Mol. Spectrosc. (in press).

Meerts, W. L., Ozier, I., and Hougen, J. T., "Influence of an AC Stark Effect on Multiphoton Transitions," J. Chem. Phys. (in press).

Meijer, G., Heinze, J., Meerts, W. L., ter Meulen, J. J., and Hougen, J. T., "High-Resolution Spectroscopy on the A^1B_1 (0,6,0) $\leftarrow$ X^1A_1 (0,0,0) Transition in $SiCl_2$," Chem. Phys. Lett. (in press).

Ohashi, N., Takagi, K. Hougen, J. T., Olson, W. B., and Lafferty, W. J., "Far Infrared Spectrum of Methyl Amine. Assignment and Analysis of the First Torsional State," J. Mol. Spectrosc. (in press).

Pine, A. S. and Pliva, J. M., "Doppler-limited Spectra of the C-H Bending Overtone of Fluoroform," J. Mol. Spectrosc. (in press).

Pine, A. S., Fraser, G. T., and Pliva, J. M., "Molecular Beam Spectrum of the Highly Perturbed C-H Stretching Region of Fluoroform," J. Chem. Phys. (in press).

Pine, A. S. and Fraser, G. T., "Vibrational, Rotational and Tunneling Dependence of Vibrational Predissociation in the HF Dimer," J. Chem. Phys. (in press).

Richter, L. J., Buntin, S. A., Cavanagh, R. R., and King, D. S., "Non-Boltzmann Rotational and Inverted Spin-Orbit State Distributions for Laser-induced Desorption of NO from Pt(111)," J. Chem. Phys. (in press).

Schneider, M., Maki, A. G., Vanek, M. D., and Wells, J. S., "Heterodyne Measurements on OCS near 1372 cm^{-1}," J. Mol. Spectrosc. (submitted).

Suenram, R. D., Lovas, F. J., Fraser, G. T., and Marfey, P. S., "Microwave Spectrum and ^{14}N Quadrupole Coupling Constants of Carbazole," J. Mol. Struct. (in press).

Suenram, R. D., Fraser, G. T., Lovas, F. J., Zozom, J., and Gillies, C. W., "Microwave Spectrum, Structure and Electric Dipole Moment of the Ar-Formamide van der Waals Complex," J. Chem. Phys. (in press).

Vanek, M. D., Schneider, M., Wells, J. S., and Maki, A. G., "Heterodyne Measurements on N_2O near 1635 cm^{-1}," J. Mol. Spectrosc. (in press).

Wells, J. W., Schneider, M., and Maki, A. G., "Calibration Tables Covering the 1460 to 1550 cm^{-1} Region from Heterodyne Frequency Measurements on the ν_3 Bands of $^{12}CS_2$ and $^{13}CS_2$," J. Mol. Spectrosc. (in press).

Wofford, B. A., Ram, R. S., Quinonez, A., Bevan, J. W., Olson, W. B., and Lafferty, W. J., "Rovibrational Analysis of the ν_7^1 Inter-molecular Hydrogen Bonded Bending Vibration in HCN-HF Using Far Infrared Fourier Transform Spectroscopy," Chem. Phys. Lett. (in press).

6. TALKS

Casassa, M. P., "Time- and State Resolved Measurements of Vibrational Predissociation of van der Waals Molecules," ILS-III Conference, Atlantic City, NJ, November 1987.

Fraser, G. T., "High Resolution Spectroscopy of Weakly-Bound Complexes," Harvard-MIT Physical Chemistry Seminar, Cambridge, MA, October 1987.

Fraser, G. T., "Sub-Doppler Infrared Spectra of CO_2 Complexes," 3rd Laser Science Conference, Atlantic City, NJ, November 1987.

Fraser, G. T., "Sub-Doppler Infrared Spectra of CO_2 Complexes in the Region of the $2\nu_2^0+\nu_3/\nu_1+\nu_3$ Fermi Diad of CO_2," Naval Research Laboratory, Washington, D.C., November 1987.

Fraser. G. T., "Sub-Doppler Infrared Spectra of CO_2 Complexes in the Region of the 2.7μm Fermi Diad of CO_2," Princeton University Chemical Physics Seminar, Princeton, NJ, February 1988.

Fraser, G. T., "Sub-Doppler Infrared Spectra of CO_2 Complexes," 12th Austin Symposium on Molecular Structure, Austin, TX, February 1988.

Fraser, G. T., "Optothermal-Infrared and Pulsed-Nozzle Fourier-Transform Microwave Spectroscopy of Rare Gas-CO_2 Complexes," 43rd Symposium on Molecular Spectroscopy, The Ohio State University, Columbus, OH, June 1988.

Fraser, G. T., "Optothermal Spectroscopy of HF Complexes with CO_2, OCS, and NO," 43rd Symposium on Molecular Spectroscopy, The Ohio State University, Columbus, OH, June 1988.

Fraser, G. T., "Infrared and Microwave Investigations of Interconversion Tunneling in the Acetylene Dimer," 43rd Symposium on Molecular Spectroscopy, The Ohio State University, Columbus, OH, June 1988.

Garmer, D. R., "Techniques in the Modelling of Intermolecular Interactions for Reaction Field Calculations," presented at the Molecular Mechanics and Molecular Dynamics Workshop, Florida State University, April 1988.

Heilweil, E. J., "Vibrational Relaxation Measurements of Carbon Monoxide on Metal Clusters," Sixth International Conference on Ultrafast Phenomena, Kyoto, Japan, July 1988.

Heilweil, E. J., "Picosecond Studies of Vibrational Relaxation for Molecules in Solution and on Surfaces," National American Chemical Society Fall Meeting, Los Angeles, CA, September 1988.

Hougen, J. T., "The Water Dimer: Theory and Measurement," Molecular Structure Symposium at Kanazawa University, Japan, October 1987.

Hougen, J. T., "The Use of High-speed Computers in Molecular Spectroscopy," Kanazawa University, Japan, October 1987.

Hougen, J. T., "Overview of Molecular Spectroscopy Research at NBS," Institute for Molecular Science, Okazaki, Japan, October 1987.

Hougen, J. T., "The Water Dimer," Kyushu University, Japan, November 1987.

Hougen, J. T., "The Water Dimer," Kobe University, Japan, November 1987.

Hougen, J. T., "Five Lectures on Molecular Spectroscopy," Katholieke Universiteit in Nijmegen, The Netherlands, March 1988.

Hougen, J. T., "The Water Dimer," Free University of Brussels, Belgium, March 1988.

Hougen, J. T., "The Water Dimer," University of Giessen, Germany, April 1988.

Hougen, J. T., "The Water Dimer," University of Amsterdam, The Netherlands, April 1988.

Hougen, J. T., "Spectrum of the Water Dimer: A Group-Theoretical and Multidimensional Tunneling Approach to the Data," 43rd Symposium on Molecular Spectroscopy, Columbus, OH, June 1988.

Hougen, J. T., "A Group-theoretical Approach to Certain Multidimensional Tunneling Problems," Molecular Spectroscopy Symposium, Prague, Czechoslovakia, September 1988.

Hougen, J. T., "The Water Dimer," University of California at Berkeley, Berkeley, CA, September 1988.

Hougen, J. T., "Group-theoretical Treatment of Some Small Molecule Multidimensional Tunneling Problems," ACS Symposium on Frontiers in Molecular Vibrations, September 1988.

Jacox, M. E., "Vibrational and Electronic Spectra of H_2CN," JANNAF Panel Meeting on Kinetic and Related Aspects of Propellant Combustion Chemistry, Applied Physics Laboratory, Johns Hopkins University, Laurel, MD, May 1988.

Jacox, M. E., "Vibrational and Electronic Spectra of Combustion Intermediates Trapped in Solid Argon," Department of Chemistry, Furman University, Greenville, SC, May 1988.

Jacox, M. E., "The Effect of Hydrogen Bonding on the Vibrational Spectrum of t-HOCO Trapped in Solid Ar and CO," 43rd Symposium on Molecular Spectroscopy, Columbus, OH, June 1988.

Jacox, M. E., "Electronic and Vibrational Spectral Databases," Workshop on Standard Reference Data Chemical Databases, National Bureau of Standards, Gaithersburg, MD, July 1988.

Jacox, M. E., "Vibrational and Electronic Spectra of Intermediates in the Decomposition and Combustion of Nitramines Trapped in Solid Argon," Symposium on the Characterization and Diagnostics of Energetic Materials, Mount St. Mary's College, Los Angeles, CA, August 1988.

Jacox, M. E., "Vibrational and Electronic Spectra of Combustion Intermediates Trapped in Solid Argon," Aerospace Corporation, Los Angeles, CA, August 1988.

Julienne, P. S., "Theory of Collision-Induced Optical Trap Loss," 3rd International Laser Science Symposium, Atlantic City, NJ, November 1987.

Julienne, P. S., "The Strange World of Ultracold Atomic Collisions," NBS Laser Lunch Bunch, February 1988.

Julienne, P. S., "Ultracold Atom Collisions in Optical Traps," American Physical Society Division of Atomic, Molecular, and Optical Physics Meeting, Baltimore, MD, April 1988.

Julienne, P. S., "Calculation of Collision-Induced Emission Loss Rate Coefficient," American Physical Society Division of Atomic, Molecular, and Optical Physics, Baltimore, MD, April 1988.

Julienne, P. S., "Nonlorentzian Line Shapes in O_2 Schumann-Runge Predissociation," American Physical Society Division of Atomic, Molecular, and Optical Physics, Baltimore, MD, April 1988.

Julienne, P. S., "Theory of Atomic Collisions at Ultracold Temperatures," Observatory of Paris Seminar, Meudon, France, June 1988.

Julienne, P. S., "Theory of Atomic Collisions at Ultracold Temperatures," 11th International Conference on Atomic Physics, Paris, July 1988.

Julienne, P. S., "Collision-Induced Spectral Phenomena at Ultracold Temperatures," 9th International Conference on Spectral Line Shapes, Torun, Poland, July 1988.

Julienne, P. S., "Na Resonance Line Broadening in Ultracold Collision," 9th International Conference on Spectral Line Shapes, Torun, Poland, July 1988.

Julienne, P. S., "The Strange World of Ultracold Atomic Collisions," Laser Science and Engineering Seminar, University of Iowa, Iowa, September 1988.

Julienne, P. S., "Close Coupled Theory of Alignment Effects in Atomic Collisions," Laser Science and Engineering Seminar, University of Iowa, Iowa City, Iowa, September 1988.

King, D. S., "Energy Flow and Decomposition of Energetic Molecules from Metastable Vibrational States," High Energy Density Matter Conference, Newport Beach, CA, March 1988.

King, D. S., "Dynamics of Highly Excited Molecules," Department of Chemistry, University of Pennsylvania, Philadelphia, PA, May 1988.

King, D. S., "Unimolecular Dynamics Following Vibrational Overtone Excitation of HN_3, ν_1=5, and ν_1=6: $HN_3(X; \nu,J,K) \rightarrow HN\ (X^3\Sigma^-; \nu,J,\Omega) + N_2(X\ 1^{\Sigma+}_g)$," Gordon Conference on Atomic and Molecular Interactions, Plymouth, NH, August 1988.

King, D. S., "Dynamics of Overtone Excited Molecules," Gordon Research Conference on Atomic and Molecular Interactions, Plymouth, NH, August 1988.

Krauss, M., "Use of Pseudo Potentials in Quantum Chemistry," University of New Orleans, Department of Chemistry, New Orleans, IL, October 1987.

Krauss, M., "Calculations of Metal Binding of Biomolecules," University of New Orleans, New Orleans, IL, October 1987.

Krauss, M., "Enthalpies of Metal Transfer Reactions," CARB, NBS, February, 1988.

Krauss, M., "Theoretical Model of Metal Binding Sites in Proteins," OHOLO Conference, Eilat, Israel, May 1988.

Lafferty, W. J., "IR Spectra of Loosely Bound Molecules," University de Paris, Paris, France, June 1988.

Lafferty, W. J., "Infrared and Microwave Investigations of Interconversion Tunneling in the Acetylene Dimer," 43rd Symposium on Molecular Spectroscopy, The Ohio State University, Columbus, OH, June 1988.

Lovas, F. J., "Structures of Molecular Complexes Containing Water," Physical Chemistry Seminar, Department of Chemistry, University of Arizona, February 1988.

Lovas, F. J., "Rotational Spectra and Structures of the Molecular Complexes $(H_2O)_2$, H_2S-H_2O and $(H_2S)_2$," 12th Austin Symposium on Molecular Structure, University of Texas, Austin, TX, March 1988.

Lovas, F. J., "Rotational Spectra and Structures of the H_2S-H_2O and $(H_2S)_2$ Complexes," 43rd Symposium on Molecular Spectroscopy, The Ohio State University, Columbus, OH, June 1988.

Maki, A. G., "The Infrared Spectrum of the Four Lowest Fundamental Bands of Nitric Acid," 43rd Molecular Symposium, The Ohio State University, Columbus, OH, June 1988.

Mies, F. H., "Unified Analysis of Atomic Scattering and Diatomic Spectroscopy," Laboratoire de Photohysique Moleculaire, Paris, France, March 1988.

Mies, F. H., "A Half Collision Analysis of Photodissociation," Laboratoire de Photohysique Moleculaire, Paris, France, March 1988.

Mies, F. H., "O_2 Predissociation," American Physical Society Meeting, Baltimore, MD, April 1988.

Mies, F. H., "Ultracold Collisions in Strong Laser Fields," Institute of Physics, Academia Sinica, Beijing, Peoples Republic of China, August 1988.

Olson, W. B., "Optical Design of Efficient Absorption Sampling Systems for FTIR Spectrometer," 43rd Symposium on Molecular Spectroscopy, The Ohio State University, Columbus, OH, June 1988.

Pine, A. S., "Vibrational Predissociation in the CO_2 Dimer and Trimer and Rare Gas-CO_2 Complexes," 43rd Symposium on Molecular Spectroscopy, The Ohio State University, Columbus, OH, June 1988.

Pine, A. S., "Vibrational, Rotational, and Tunneling Dependence of Vibrational Predissociation in the HF Dimer," 43rd Symposium on Molecular Spectroscopy, The Ohio State University, Columbus, OH, June 1988.

Pine, A. S., "Difference-Frequency and Color-Center Laser Spectroscopy of van der Waals Complexes," Adriatico Research Conference on "Coherent Sources for Frontier Spectroscopy," International Center for Theoretical Physics, Trieste, Italy, August 1988.

Stephenson, J. C., "Picosecond Studies of Molecular Energy Transfer," Chemistry Department, Columbia University, New York, NY, February 1988.

Stephenson, J. C., "Picosecond Studies of Molecular Energy Transfer," Gordon Reserach Conference on Atom and Molecular Interactions, Plymouth, MA, July 1988.

Suenram, R. D., "Structure Studies of Hydrogen Bonded Water Complexes using Pulsed-Molecular Beam Microwave Spectroscopy," Penn State University, State College, PA, February 1988.

Suenram, R. D., "Structure Study of $H_2O\cdots H_2O\cdots CO_2$ Trimer," 12th Austin Symposium on Molecular Structure, Austin, TX, March 1988.

Suenram, R. D., "Microwave Spectrum of Carbazole," 12th Austin Symposium on Molecular Structure, Austin, TX, March 1988.

Suenram, R. D., "Microwave Spectrum Structure, and Dipole Moment of the $H_2CO\cdots CO_2$ Complex," 12th Austin Symposium of Molecular Structure, Austin, TX, March 1988.

Suenram, R. D., "Structural Studies of CO_2-H_2O Hydrogen Bonded Complexes," University of Kansas, Lawrence, Kansas, April 1988.

Suenram, R. D., "Microwave Spectrum of the Ozone-Water Complex," 43rd Molecular Spectroscopy Symposium, The Ohio State University, Columbus, OH, June 1988.

Suenram, R. D., "Studies of Isotopically Enriched Water Dimer Species," 43rd Molecular Symposium, The Ohio State University, Columbus, OH, June 1988.

Weber, A., "High Resolution Spectroscopy of van der Waals and Hydrogen Bonded Complexes at NBS-Gaithersburg," University of California - Berkeley, Berkeley, CA, January 1988.

Weber, A., "High Resolution Spectroscopy of van der Waals and Hydrogen Bonded Complexes at NBS-Gaithersburg," Jet Propulsion Laboratory, Pasadena, CA, January 1988.

Weber, A., "High Resolution Spectroscopy of van der Waals and Hydrogen Bonded Complexes at NBS-Gaithersburg," UCLA, Los Angeles, CA, January 1988.

Weber, A., "Gas Phase Fourier Transform Raman Spectroscopy," Pittsburgh Conference, New Orleans, LA, February 1988.

Weber, A., "Electric Dipole Moments of HCl- and HCN-Hydrocarbon Complexes," 43rd Molecular Spectroscopy Symposium, The Ohio State University, Columbus, OH, June 1988.

7. MOLECULAR SPECTROSCOPY DIVISION SEMINARS

Brocks, G. Phillips Research Laboratories, Eindhoven, The Netherlands, "Large Amplitude Motions and Calculated Spectra of Molecular Dimers" May 1988.

Butcher, R. J. Cavendish Laboratory, Cambridge University, England, "CO_2 Laser Saturation Spectroscopy of SF_6 and CH_3I at kHz Linewidths" March 1988.

Coalson, R., Department of Chemistry, University of Pittsburgh, Pittsburgh, PA, "Time Domain Approaches to Excited State Spectroscopy" January 1988.

Dykstra, C. E., Chemistry Department, University of Illinois, Urbana, IL, "Theoretical Studies of Hydrogen Bonding" May 1988.

Field, R. W., Department of Chemistry, MIT, Cambridge, MA, "Acetylene: Isomerization, Dissociation, and Chaos" December 1987.

Hovde, D. C., Department of Chemistry, University of California - Berkeley, Berkeley, CA, "Laser Magnetic Resonance Studies of Ions" January 1988.

Janda, K., University of Pittsburgh, Pittsburgh, PA, "Rotational Rainbows, Quantum Diffraction and Intermolecular Vibrational Relaxation, All in a Triatomic Molecule" December 1987.

Kleiner, I., Laboratoire de Chimie Physique Moleculaire, Universite Libre de Bruxelles, Belgium, "Work at the University of Brussels: HNO_3, CH_3CHO, etc." July 1988.

Meerts, W. L., Physics Department, University of Nijmegen, The Netherlands, "Order and Chaos in the S_1 State of Pyrazine ($C_4N_2H_4$)" June 1988.

Miller, R. E., Department of Chemistry, University of North Carolina, Chapel Hill, NC, "Infrared Spectroscopy and Vibrational Predissociation of Several Binary and Tertiary Complexes" October 1987.

Muenter, J., University of Rochester, Rochester, NY, "Microwave and Infrared Spectroscopy of Acetylene Containing Complexes" April 1988.

O'Brien, S., Department of Chemistry, Rice University, Houston, TX, "The Photophysics of Buckminsterfullerene" January 1988.

Pascale, J., Service de Physique des Atomes et des Surfaces, Saclay, France, "Quantum Mechanical Study of Non-reactive Collisions Between Rb(5p) and H_2 or D_2" October 1987.

Phillips, L., Department of Chemistry, Cornell University, Ithaca, NY, "High Resolution Spectroscopy of Tryptophan and Tryptophan Analogs in a Supersonic Jet" October 1987.

Povilly, B., University of Lille, Lille, France, "Theoretical Study of Energy Transfer in Collisions of Aligned Calcium 4s5p ^1P Atoms with Noble Gases" October 1987.

Pulay, P., Department of Chemistry and Biochemistry, University of Arkansas, Favetteville, AR, "Local Treatment of Electron Correlation in Large Molecules" November 1987.

Rice, J., Naval Research Laboratory, Washington, D.C., "The Study of Oriented Biomolecular Reactions Using van der Waals Pre-cursors" April 1988.

Rothberg, L., AT&T Bell Laboratories, Murray Hill, NJ, "Charged Solition Dynamics in Trans-Polyacetylene" February 1988.

Stahl, W., Institute for Physical Chemistry, Kiel University, Germany, "Current MW Experiments at Kiel University" July 1988.

Synder, L. E., Department of Astronomy, University of Illinois, Urbana-Champaign, IL, "Molecular Radio Spectroscopy of Comets" April 1988.

Tyuterev, V. G., Institute of Atmospheric Optics, USSR Academy of Science, Tomsk, USSR, "Processing and Extrapolation of Vibration-Rotation Energies of Non-Rigid Molecules Based on Non-Polynomical Rotational Hamiltonians" June 1988.

Weinstein, H., Department of Biophysics, Mt. Sinai Medical School, New York City, NY, "Theoretical Analysis of Biological Specificity and Activity: Recognition of Neurotransmitters and Calcium Binding Structures" November 1987.

Whetten, R. L., Department of Chemistry, University of California, Los Angeles, CA, "Optical Spectroscopy of Large Clusters" April 1988.

Williams, C., Department of Chemistry, North Western University, Evanston, IL, "Vibrational Predissociation of the Hydrogen-bonded HCN Dimers" May 1988.

Wilson, T., Max Planck Institute, Bonn, Germany, "Hot NH_3 and CH_3OH in the Galaxy" March 1988.

Zimmerman, G., Department of Chemistry, Bryn Mawr College, Bryn Mawr, PA, "Spectroscopy and Photochemistry of Ruthenum Oxides" October 1987.

8. VISITING SCIENTISTS

The Molecular Spectroscopy Division has been host to the following scientists who have worked with NIST scientists on problems of mutual interest.

Basch, Harold, Bar Ilan University, Israel, is engaged in research on metal interactions with biomolecules. He works with M. Krauss and W. J. Stevens.

Blake, Thomas, Department of Chemistry, Wesleyan University, CT, works with F. J. Lovas and R. D. Suenram on pulsed beam Fourier transform microwave spectroscopy of weakly bound complexes of CO_2 and formaldhyde.

Chipman, Daniel, Chemistry Division, National Science Foundation, works with W. Stevens on accurate prediction of molecular properties using quantum chemistry.

Craig, N., Oberlin College, works with W. J. Lafferty on the Fourier transform infrared spectrum of 1,2-difluorethylene.

Gillies, C. W., Chemistry Department, Rensselaer Polytechnic Institute, works with F. J. Lovas and R. D. Suenram on pulsed beam Fourier transform microwave spectroscopy of hydrogen bonded molecules containing ozone.

Jennings, Donald E., NASA/Goddard Space Flight Center, works with A. Weber on a project to do Raman spectroscopy of gases with the Fourier transform spectrometer of the National Solar Observatory (Kitt Peak).

Kleiner, Isabelle, Universite Libre de Bruxelles, Belgium, worked with J. T. Hougen on the theory of internal rotation in molecules.

Konowalow, Daniel D., Professor at SUNY-Binghamton, New York, works with M. Krauss on studies of electronic structure of alkali and alkaline earth molecules.

Lengsfield, Byron H., Ballistic Research Laboratory, works with M. Krauss and W. J. Stevens on electronic structure codes for the chemistry and spectroscopy of large molecules.

Leung, Helen O., Department of Chemistry, Harvard University, works with R. D. Suenram and F. J. Lovas on the rotational study of N_2-H_2O.

Marfey, Peter S., Department of Biological Services, State University of New York, Albany, works with R. D. Suenram and F. J. Lovas on rotational spectra of large organic species, e.g., carbazole.

Marshall, Mark D., Department of Chemistry, Amherst College, MA, works with R. D. Suenram and F. J. Lovas on rotational studies of N_2-H_2O and CCl_3F.

Matsumura, Keiji, Department of Liberal Arts, Seinan Gakuin University, works with F. J. Lovas and R. D. Suenram on pulsed beam microwave studies of weakly bound complexes of H_2O and SO_2.

Novick, Stewart E., Department of Chemistry, Wesleyan University, CT, works with F. J. Lovas and R. D. Suenram on pulsed beam Fourier transform microwave spectroscopy of weakly bound complexes of CO_2 and formaldhyde.

Ohashi, Nobukimi, Kanazawa University, Physics Department, Japan, works with J. T. Hougen, W. J. Lafferty, and W. B. Olson on high resolution infrared spectroscopy and theory of methylamine.

Onda, Musao, Department of Chemistry, Sophia University, Japan, worked with F. J. Lovas and R. D. Suenram on several weakly bound complexes to learn the method of operation of the Fourier transform microwave spectrometer.

Osman, R., Mt. Sinai School of Medicine, New York, works with W. J. Stevens on the application of ab initio quantum chemistry to biochemical modeling.

Rice, Jane, Naval Research Laboratory, Bethesda, Maryland, works with F. J. Lovas and R. D. Suenram on the pulsed beam microwave spectrum and structure of CO_2-H_2S.

Sattler, Joseph L., Harry Diamond Laboratories, U. S. Army, works with W. J. Lafferty and A. Maki on precise line frequency measurements in the infrared.

Stahl, Wolfgang, Institute of Physical Chemistry, University of Kiel, West Germany, works with F. J. Lovas and R. D. Suenram on pulsed beam microwave studies of the weakly bound complex CO_2-H_2S.

Vahala, Linda L., Physics Department, Old Dominion University, Norfolk, VA, works with P. S. Julienne on the theory of molecular line broadening and final state branching ratios for the resonance transitions of alkali atoms perturbed by rare gas collision partnes.

Zozom, Jennifer, Chemistry Department, Rensselaer Polytechnic Institute works with F. J. Lovas and R. D. Suenram on pulsed beam Fourier transform microwave spectroscopy of hydrogen bonded molecules containing ozone.

NBS-114A (REV. 2-8C)

U.S. DEPT. OF COMM. BIBLIOGRAPHIC DATA SHEET (See instructions)	1. PUBLICATION OR REPORT NO. NISTIR 89-4051	2. Performing Organ. Report No.	3. Publication Date MARCH 1989

4. TITLE AND SUBTITLE

Technical Activities 1986-1988 - Molecular Spectroscopy Division

5. AUTHOR(S)

A. Weber

6. PERFORMING ORGANIZATION (If joint or other than NBS, see instructions)

NATIONAL BUREAU OF STANDARDS
U.S. DEPARTMENT OF COMMERCE
GAITHERSBURG, MD 20899

7. Contract/Grant No.

8. Type of Report & Period Covered

9. SPONSORING ORGANIZATION NAME AND COMPLETE ADDRESS (Street, City, State, ZIP)

10. SUPPLEMENTARY NOTES

☐ Document describes a computer program; SF-185, FIPS Software Summary, is attached.

11. ABSTRACT (A 200-word or less factual summary of most significant information. If document includes a significant bibliography or literature survey, mention it here)

This report summarizes the technical activities of the NIST Molecular Spectroscopy Division for the Fiscal Year 1987 and 1988. The activities span experimental and theoretical research in high resolution molecular spectroscopy, quantum chemistry, and laser photochemistry, and include the development of frequency standards, critically evaluated spectral data, applications of spectroscopy to important scientific and technological problems, and the advancement of spectroscopy measurement methods and techniques. A listing is given of publications and talks by the Division staff.

12. KEY WORDS (Six to twelve entries; alphabetical order; capitalize only proper names; and separate key words by semicolons)

molecular spectroscopy; molecular dynamics; quantum chemistry; atmospheric spectroscopy; molecular surface interactions; van der Waals molecules.

13. AVAILABILITY

☒ Unlimited

☐ For Official Distribution. Do Not Release to NTIS

☐ Order From Superintendent of Documents, U.S. Government Printing Office, Washington, D.C. 20402.

☒ Order From National Technical Information Service (NTIS), Springfield, VA. 22161

14. NO. OF PRINTED PAGES

133

15. Price

$19.95

USCOMM-DC 6043-P80